

CHALMERS



Design of slabs-on-ground regarding shrinkage cracking

Master of Science Thesis in the Master's Programme Structural Engineering and Building Performance Design

FABIAN NARIN

OLLE WIKLUND

Department of Civil and Environmental Engineering
Division of Structural Engineering
Concrete Structures
CHALMERS UNIVERSITY OF TECHNOLOGY
Göteborg, Sweden 2012
Master's Thesis 2012:59

MASTER'S THESIS 2012:59

Design of slabs-on-ground regarding shrinkage cracking

*Master of Science Thesis in the Master's Programme Structural Engineering and
Building Performance Design*

FABIAN NARIN

OLLE WIKLUND

Department of Civil and Environmental Engineering
Division of Structural Engineering
Concrete Structures

CHALMERS UNIVERSITY OF TECHNOLOGY

Göteborg, Sweden 2012

Design of slabs-on-ground regarding shrinkage cracking

Master of Science Thesis in the Master's Programme Structural Engineering and Building Performance Design

FABIAN NARIN & OLLE WIKLUND

© FABIAN NARIN & OLLE WIKLUND, 2012

Examensarbete / Institutionen för bygg- och miljöteknik,
Chalmers tekniska högskola 2012:59

Department of Civil and Environmental Engineering
Division of Structural Engineering
Concrete Structures
Chalmers University of Technology
SE-412 96 Göteborg
Sweden
Telephone: + 46 (0)31-772 1000

Cover:

The cover is a photograph taken by the authors, illustrating a crack in a slab-on-ground. The photo was captured 2012-02-17 while observing the response of a floor.

Chalmers Reproservice / Department of Civil and Environmental Engineering
Göteborg, Sweden 2012

Design of slabs-on-ground regarding shrinkage cracking

Master of Science Thesis in the Master's Programme Structural Engineering and Building Performance Design

FABIAN NARIN

OLLE WIKLUND

Department of Civil and Environmental Engineering

Division of Structural Engineering

Concrete Structures

Chalmers University of Technology

ABSTRACT

Shrinkage cracking constitutes a common reason for damages to concrete floors, having large economical effects. The knowledge of how to design slabs-on-ground with regard to shrinkage cracking is limited and shrinkage cracking is often overlooked in design situations. This project aimed at improving the prediction of how a chosen design affects the risk of shrinkage cracking. For this reason, two different calculation models for slabs-on-ground were developed, complemented by measurements from four studied reference objects.

The first model considers external restraints for a pile-supported slab-on-ground using the direct stiffness method. In order to evaluate the model it was implemented on two of the reference objects. When adapting the model to studied slab sections, the cracked areas matched the calculated stress distributions from the model. Despite that the stress values were based on several assumptions, the model demonstrated potential of evaluating crack prone regions in slabs. It also illustrated that restraints from perimeter strips are likely to have a large influence on shrinkage cracking, while piles seem to constitute a smaller restraint.

The second model studies the friction between slab and sub-base using non-linear data adapted from full-scale testing. The results indicated that the general approach, assuming a fully developed friction, is conservative. By implementing this more precise procedure, larger slab portions can be designed and fewer joints need to be incorporated in the design.

Both developed models indicated improved possibilities of understanding and modelling shrinkage behaviour of slabs-on-ground. Recommendations for further research include combining the models and to include crack response in the analysis.

Key words: concrete design, crack risk evaluation, cracking process, design methods, direct stiffness method, friction, industrial floor, non-linear friction model, pile-supported slab-on-ground, restraint, shrinkage, shrinkage cracking, slab-on-ground.

Dimensionering av plattor på mark med hänsyn till krymsprickor

Examensarbete inom Structural Engineering and Building Performance Design

FABIAN NARIN & OLLE WIKLUND

Institutionen för bygg- och miljöteknik

Avdelningen för Konstruktionsteknik

Betongbyggnad

Chalmers tekniska högskola

SAMMANFATTNING

Krymsprickor i betonggolv är ett vanligt förekommande fenomen som har stora ekonomiska konsekvenser. Kunskapen om hur man skall dimensionera plattor på mark med hänsyn till krymsprickor är begränsad och ofta försummas risken för krymsprickor i dimensioneringsprocessen.

Målet med det här examensarbetet var att förbättra förståelsen för hur en vald utformning påverkar risken för krymsprickor. Föranlett av det här har två olika beräkningsmetoder för platta på mark utvecklats, vilka även kompletterats med undersökningar av fyra referensobjekt.

Den första modellen belyser, med hjälp av förskjutningsmetoden, inverkan av yttre tvång för pålunderstödda plattor på mark. För att utvärdera modellen implementerades den på två av referensobjekten. När modellen anpassades till de studerade sektionerna överensstämde de spruckna områdena med spänningsfördelningen från modellen. De beräknade spänningarna var baserade på en rad antaganden, men trots det här visade modellen goda möjligheter att utvärdera sprickkänsliga områden i en platta på mark. Vidare visade modellen att tvånget från kantförstyvningar sannolikt har en stor inverkan på bildandet av krymsprickor samtidigt som pålar har mindre inverkan.

Den andra modellen beaktar friktionen mellan platta på mark och bärlager med hjälp av icke-linjära friktionskurvor från fullskaletest. Resultaten indikerade att den vanligt förekommande beräkningsmetoden där fullt utvecklade friktion antas är konservativ. Med hjälp av den utvecklade metoden kan större gjutetapper och färre fogar tillåtas.

Båda metoderna påvisade förbättrade möjligheter för förståelse och dimensionering av plattor på mark med hänsyn till krymsprickor. Att kombinera de två modellerna samt att inkludera sprickbildningsprocessen utgör rekommendation för fortsatta studier.

Nyckelord: industrigolv, betongdesign, tvång, friktion, krympning, krymsprickor, designmetoder, förskjutningsmetoden, icke-linjär friktionsmodell, platta på mark, pålunderstödd platta på mark, sprickbildning, sprickriskbedömning.

Contents

ABSTRACT	I
SAMMANFATTNING	II
CONTENTS	III
PREFACE	VII
1 INTRODUCTION	1
1.1 Background and problem description	1
1.2 Aim	1
1.3 Scope	1
1.4 Method	2
1.5 Outline	3
2 INDUSTRIAL FLOORS	4
2.1 Design concepts of slabs-on-ground	5
2.2 Detailing	8
2.2.1 Perimeter strips and local thickenings	8
2.2.2 Columns	9
2.2.3 Joints	9
2.2.4 Reinforcement details	12
2.2.5 Surface finishing	12
2.3 Restraints	13
2.3.1 Restraint degree	13
2.3.2 Internal restraints	14
2.3.3 External restraints	14
2.4 Friction	15
2.5 Construction methods	17
3 RESPONSE OF MATERIALS AND COMPONENTS	21
3.1 Concrete	21
3.2 Shrinkage of concrete	23
3.2.1 Drying shrinkage	24
3.2.2 Chemical shrinkage	28
3.2.3 Autogenous shrinkage	28
3.2.4 Plastic shrinkage	29
3.2.5 Carbonation shrinkage	30
3.2.6 The effect of shrinkage reducing additives	30
3.3 Thermal behaviour of concrete	31
3.4 Reinforcing steel	31
3.4.1 Ordinary reinforcement	32
3.4.2 Steel fibre reinforcement	33

3.5	Cracking process	34
3.6	Effects of cracking	37
4	DESIGN METHODS	39
4.1	Choosing concrete class	40
4.2	Prediction of shrinkage strain	40
4.3	Design with regard to restraint cracking	44
4.3.1	Joint spacing according to Petersons (1992)	44
4.3.2	Minimum reinforcement according to EC2 7.3.2-7.3.3	47
4.3.3	Minimum reinforcement according to BBK04	49
4.3.4	Minimum reinforcement according to DS 411	49
4.3.5	Minimum reinforcement according to ACI	50
4.3.6	Crack risk evaluation according to Engström (2011)	52
4.3.7	Crack evaluation according to Engström (2011)	54
5	OBSERVED RESPONSE OF FLOORS	56
5.1	Method	56
5.2	Overview of studied objects	58
5.3	Object 1	59
5.3.1	Object specific data	60
5.3.2	Observations	62
5.3.3	Evaluation	64
5.4	Object 2	65
5.4.1	Object specific data	65
5.4.2	Observations	67
5.4.3	Evaluation	69
5.5	Object 3	71
5.5.1	Object specific data	71
5.5.2	Observations	74
5.5.3	Evaluation	76
5.6	Object 4	77
5.6.1	Object specific data	77
5.6.2	Observations	80
5.6.3	Evaluation	82
5.7	Evaluation	83
6	ANALYSIS USING THE DIRECT STIFFNESS METHOD	86
6.1	Model concept	86
6.2	General calculation procedure	87
6.2.1	Stiffness of slab elements	87
6.2.2	Stiffness of perimeter strips and slab thickenings	88
6.2.3	Stiffness of piles	90
	Global stiffness matrix	92
6.2.4	Centre of movement	93

6.2.5	Load definition	93
6.2.6	Solution	95
6.3	Program structure	95
6.4	Application of method	96
6.4.1	Calculation for generic model	98
6.4.2	Object 1	99
6.4.3	Object 2	101
6.5	Evaluation	103
6.5.1	Evaluation of assumptions	103
6.5.2	Evaluation of design measures	105
7	NON-LINEAR ANALYTICAL FRICTION MODEL	107
7.1	Friction tests performed by Pettersson (1998)	107
7.2	Calculation procedure	110
7.3	Results	112
7.4	Evaluation	113
8	FINAL REMARKS	117
8.1	Conclusions	117
8.1.1	Observed response of floors	117
8.1.2	Analysis using the direct stiffness method	118
8.1.3	Non-linear analytical friction model	119
8.2	Design recommendations	120
8.3	Further investigations	121
9	REFERENCES	122
APPENDIX A	SHRINKAGE AND CREEP CALCULATION	A-1
APPENDIX B	DATA AND DRAWINGS, OBJECT 1	B-1
APPENDIX C	DATA AND DRAWINGS, OBJECT 2	C-1
APPENDIX D	DATA AND DRAWINGS, OBJECT 3	D-1
APPENDIX E	DATA AND DRAWINGS, OBJECT 4	E-1
APPENDIX F	STIFFNESS CALCULATIONS FOR PILES	F-1
APPENDIX G	MATLAB CODE FOR DIRECT STIFFNESS METHOD	G-1
APPENDIX H	ANALYTICAL FRICTION MODEL	H-1

Preface

In this master's project, methodology on how to design industrial floors in order to avoid shrinkage cracking is investigated. The project was carried out from January 2012 to June 2012 and was a co-operation between Skanska Teknik and the Division of Structural Engineering, Concrete Structures, at Chalmers University of Technology. This master's thesis is a part of completing our master's degree at the master's program Structural Engineering and Building Performance Design at Chalmers University of Technology.

We, the authors, have carried out the project in close cooperation with each other. Both of us have been involved in each part of the project, critically reviewing each other's work. The cooperation has been very rewarding and we are certain that neither of us would have been capable of performing this project as successfully by himself.

We would like to thank our supervisor at the Division of Structural Engineering, Professor Björn Engström for his excellent guidance throughout the work of this thesis. We would also like to thank Jim Brouzoulis at the Department of Applied Mechanics for his support and advisory opinions.

Our supervisor at Skanska Teknik, Robert Drotz, and his colleagues have provided a good working climate and support on a daily basis, which we would like to thank them for.

Furthermore, our opponents, Simon Carlsson and Erik Holmbom have given us helpful feedback and support which we would like to thank them for.

Finally we would like to show our gratitude to friends and family who have supported and encouraged us during the work.

Göteborg June 2012



Fabian Narin



Olle Wiklund

Notations

Roman upper case letters

A_I	Area in state 1
A_{ef}	Effective area
A_c	Gross concrete area
A_{ct}	Concrete area within tensile zone
A_s	Steel area
$A_{s,min}$	Minimum steel area / Minimum reinforcement area
E	Modulus of elasticity
E_c	Concrete modulus of elasticity
$E_{c,ef}$	Concrete effective modulus of elasticity
E_s	Modulus of elasticity for steel
F	Force
F_{cs}	Shrinkage force
F_x	Force in x-direction
H	Height
\mathbf{K}	Stiffness matrix
\mathbf{K}_{el}	Element stiffness matrix
\mathbf{K}_{restr}	Restraint stiffness matrix
L	Member length / Joint spacing
L_g	Characteristic pile length
N	Normal force
N_{cr}	Cracking load
N_y	Normal force when steel yields
R	Restraint degree
$S_{el,i}$	Stiffness of element i
S_i	Stiffness of member i
S_{pile}	Stiffness of pile
S_{strip}	Stiffness of perimeter strip

Roman lower case letters

b	Influence width
b_p	Pile width
c_u	Undrained shear strength
c	Concrete cover
d	Effective height
f_{ct}	Concrete tensile strength
f_{ctk}	Characteristic concrete tensile strength
$f_{ctk0.05}$	Concrete tensile strength, lower characteristic value
$f_{ctk,sus}$	Concrete tensile strength for sustained loading
f_s	Steel strength
f_t	Tensile strength
f_y	Yield strength
g	Self weight
h	Member height

h_{cr}	Height of tensile zone just before cracking
k_h	Shape coefficient
n	End displacement
n_{cr}	Number of cracks
p	Vapour pressure
p_0	Vapour pressure at saturation
q	Variable load
r	Meniscus radius
s	Slip / spacing
s_0	Transmission length
$s_{r,max}$	Maximum crack spacing
u_x	Displacement in x-direction
w_k	Characteristic crack width
w_{lim}	Crack width limit
w_m	Mean crack width
$w_{m,all}$	Allowable mean crack width
w_{max}	Maximum crack width
$w_{m,sus}$	Mean crack width at sustained loading
x_o	Centre of movement
z	Depth

Greek upper case letters

\emptyset	Reinforcement bar diameter
-------------	----------------------------

Greek lower case letters

α	Angle / constant
α_c	Thermal expansion coefficient of concrete
β_{as}	Time function for drying shrinkage
β_{ds}	Time function for autogenous shrinkage
ε	Strain
ε_{cd}	Drying shrinkage strain
$\varepsilon_{cd,0}$	Nominal drying shrinkage strain
ε_{cs}	Total shrinkage strain
ε_{ca}	Autogenous shrinkage strain
κ_1	Coefficient depending on type of reinforcement
κ_2	Coefficient depending on tensile strain distribution
ρ_r	Reinforcement ratio
σ	Stress
σ_c	Concrete stress
σ_s	Steel stress
$\sigma_{s,all}$	Maximum allowable steel stress
τ	Shear stress
τ_b	Bond stress
μ	Friction coefficient
φ	Creep coefficient

Abbreviations

ACI	American Concrete Institute
Bwd	Backward
CEB	Euro international concrete comitée
DS	Danish concrete design code
EC	Eurocode
EC2	Eurocode 2
Fwd	Forward
HCP	Hardened cement paste
RH	Relative humidity
SFRC	Steel fibre reinforced concrete
SW	Self weight
w/c	Water/cement ratio

1 Introduction

1.1 Background and problem description

Concrete shrinks when it ages, mainly due to the emission of water from the pores, called drying shrinkage, but also at early age due to the ongoing hydration process, called autogenous shrinkage. For a reinforced concrete member, this induces tensile forces in the concrete due the steel partly preventing the need for movement.

For a slab-on-ground there are several other restraints that also prevent the concrete from shrinking freely. These include for example friction to the sub-base and the influence of piles, columns, perimeter strips and local slab thickenings.

As the restraints prevent free movements and induce tensile stresses, cracking can occur if the stresses reach the tensile strength of the concrete. Cracks in floors are undesired since they precipitate degradation as well as being aesthetically unappealing.

Damages to concrete floors account for 20% of all reported damages to concrete structures in Sweden. Out of these, 35% are related to cracks, where concrete shrinkage is the most common reason for cracking (Swedish Concrete Association, 2008). These damages can result in large economical consequences if buildings have to be closed because of repair works.

Risk can be defined as the product of likelihood and consequence. Due to the large likelihood and economical consequences related to shrinkage cracks, the economical risk is high. Studies regarding how the number of damages caused by shrinkage cracking can be reduced are consequently of high relevance and there is a need for a better design approach when designing concrete floors with regard to shrinkage cracking.

1.2 Aim

The aim of the project was to develop recommendations for future design situations, resulting in a better understanding and prediction of how a chosen slab-on-ground design affects the quality of the product in terms of shrinkage cracking.

Furthermore, the project aimed at developing new design methods to study shrinkage cracking of slabs-on-ground.

1.3 Scope

There are several ways of designing slabs-on-ground in order to minimise cracks. The following four structural floor systems are common solutions (Hedebratt, 2005).

- Plain concrete with closely spaced joints
- Reinforced concrete
- Post-tensioned concrete
- Steel fibre reinforced concrete, SFRC

Due to the limited scope of this project they could not all be covered. Consequently, the project was restricted to only study slabs-on-ground reinforced with ordinary reinforcement and/or steel fibre reinforcement. These methods are common construction methods for Skanska and therefore highly relevant for the project.

Furthermore, when designing the structural system of a building, the slab-on-ground can be incorporated in the load bearing system of the structure by joining the walls to the slab. However, this prevents the movement of the slab, resulting in a restraint which can lead to cracking (Hedebratt, 2005). Consequently, since this method should be avoided, the project only considered slabs-on-ground separated from the load bearing system of the structure.

Slabs-on-ground can be found in several different floor constructions, e.g. basements, lift shafts etc. This project was however limited to only study industrial floors at ground level. Furthermore, external restraints caused by concentrated loads from walls and columns have not been considered in the project.

Depending on the bearing capacity of the underlying soil, piles might be needed and attached to the slab to provide adequate capacity against settlements. This type of pile-supported slabs were also included in the study, since it is a common construction method when ground bearing capacity is poor, as often is the case in regions with strata consisting of thick layers of soft clay, e.g. in Göteborg.

1.4 Method

In order to provide adequate knowledge regarding the subject a literature study was initially to be undertaken. Shrinkage behaviour should be studied both on a material level and on a structural level in order to investigate the possibilities of influencing the sources of shrinkage and how to deal with shrinkage in a practical way.

In order to determine possible improvements when designing a slab-on-ground, available methods were to be studied and evaluated. Wherever possible the European technical standards Eurocode, for design of concrete structures, EC2, should be adapted. However, for situations where EC2 was found inadequate, methods following other design codes should also be considered. The study of other methods should allow for a comparison with EC2.

With the purpose of further investigating the shrinkage behaviour of slabs-on-ground it was decided to study the response of floors from reference objects. The selected objects were four warehouse buildings with industrial floors designed as slabs-on-ground, completed between 4-6 years ago. The study should allow for a comparison between measurements from the objects with theories and calculations.

In order to improve today's design procedures, new design approaches should be developed and analysed.

1.5 Outline

The following chapter, Chapter 2, gives an overview of industrial floors as a concept including design components and detailing. Furthermore, it explains the effects from restraints and friction. It also covers how the choice of construction methods can influence shrinkage cracking.

Chapter 3 presents a theoretical description of the response of materials and their components in a reinforced slab-on-ground. The interaction between steel and concrete is also covered together with information regarding the cracking process and the effects of cracking.

In Chapter 4 the general slab-on-ground design procedure is covered along with explanations and evaluations of existing calculation methods. The calculations consider maximum joint spacing, shrinkage strain, minimum reinforcement for crack control and crack risk evaluation.

Chapter 5 covers observed response of floors from four different reference objects. Collected data from each object is evaluated and the likely causes of the observations are discussed.

Chapter 6 presents a model to evaluate the normal stress distribution due to shrinkage strain in a slab-on-ground using the direct stiffness method, considering the external restraints as additional stiffness along the slab. In contrast to available design procedures, the method aims at studying slabs-on-ground from a global perspective, taking into account project specific restraints and geometries. The method predicts where the largest stresses would be located and consequently where the first shrinkage crack can be expected, information that is not found using the available design procedures. The chapter also describes the evaluation of the model, using data from the reference objects.

Chapter 7 presents a model to evaluate the non-linear friction relationship between a slab-on-ground and the sub-base. The solution is analytical and based on non-linear friction-slip relationships in combination with formulations adapted from calculations regarding the bond-slip relationship between concrete and steel reinforcement. This method was developed to get a more precise prediction of the friction effects in comparison with the general method based on coefficients of friction.

Finally, in Chapter 8, conclusions from the project, design recommendations and suggestions of further research are presented.

2 Industrial floors

There exist several types and varieties of floor designs. Each design has different advantages and is based on specific demands. Since requirements and site conditions are individual for each project, there is no given optimal design.

The key task for a designer is to balance the resistance of the floor to the actions. A schematic illustration of this balance is shown in Figure 2.1. It is of high importance to, in an early stage, set up relevant demands and to fulfil these throughout the different processes of design, construction and operation.

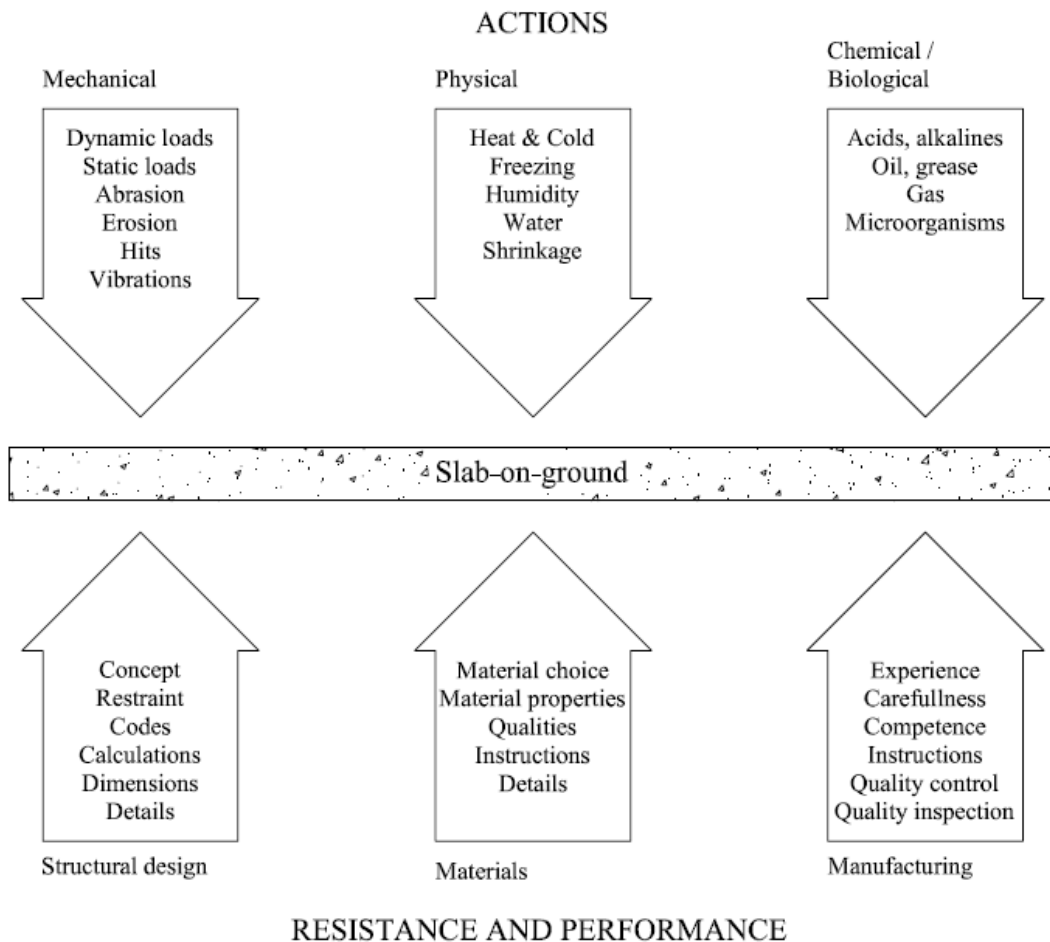


Figure 2.1 Illustration of balance between action and resistance and performance, adopted from AB Jacobson & Widmark (2005).

This project focused on studying the shrinkage behaviour of slabs. As a result, some of the phenomena in Figure 2.1 were disregarded, but should of course be considered when performing a complete design of a floor.

2.1 Design concepts of slabs-on-ground

One of the first demands from a client to fulfil is to plan and dispose the requested building/floor area. The area must be disposed to work with the site specific topology and adjacent buildings, roads, landscape and other relevant parameters. For industrial buildings there is often a need to optimise the logistics in and around the building, which sets demands regarding where loading bays and doors should be located. The specific activity that a building is designed for sets additional demands regarding what features should be included; for example if there should be a workshop area there could be a need of adding foundations for heavy machinery. A generic floor plan of a typical slab-on-ground for an industrial building is shown in Figure 2.2 below. The building area is about 430 m² and includes material storage area, offices, toilets and a kitchen.

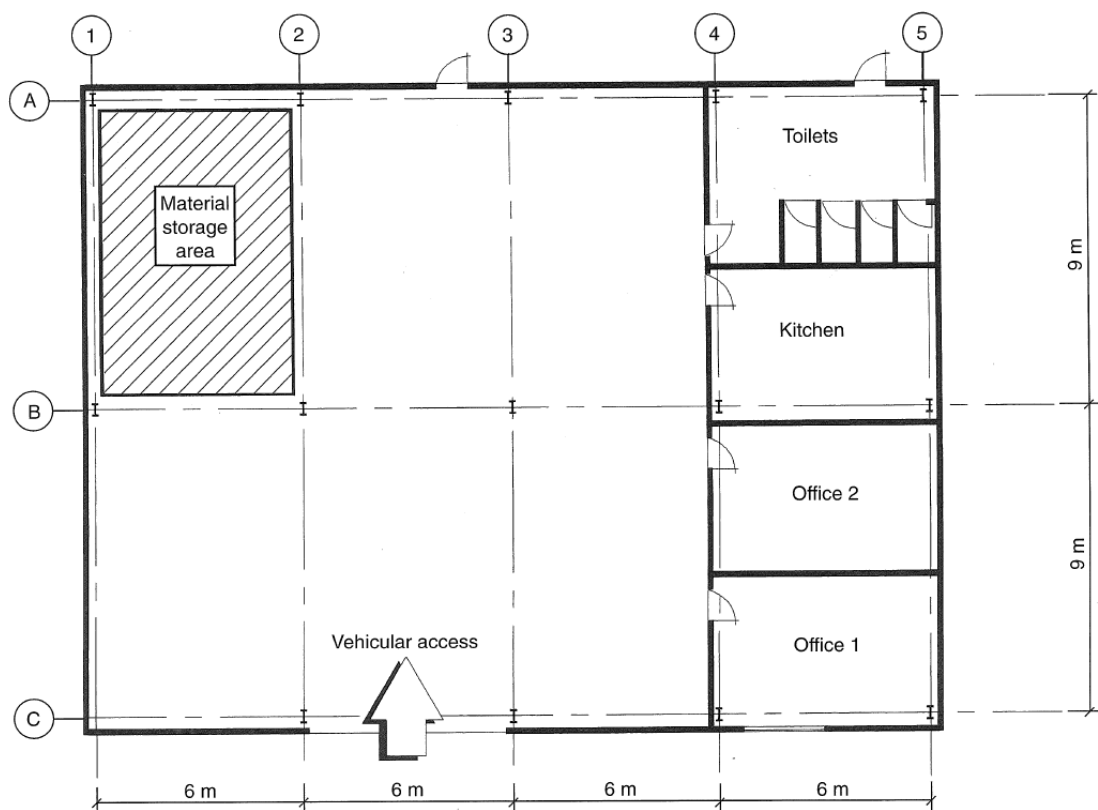


Figure 2.2 Typical floor plan of an industrial building (Knapton, 2003).

Further detailing regarding material properties, reinforcement arrangement, joints and more accurate geometries will follow the demands on the floor, in order to compose a structure that will resist the actions and have sufficient performance during its entire service life.

As previously discussed, this project focused on slabs-on-ground with and without support from piles. Figure 2.3 illustrates a typical section of a pile-supported slab.

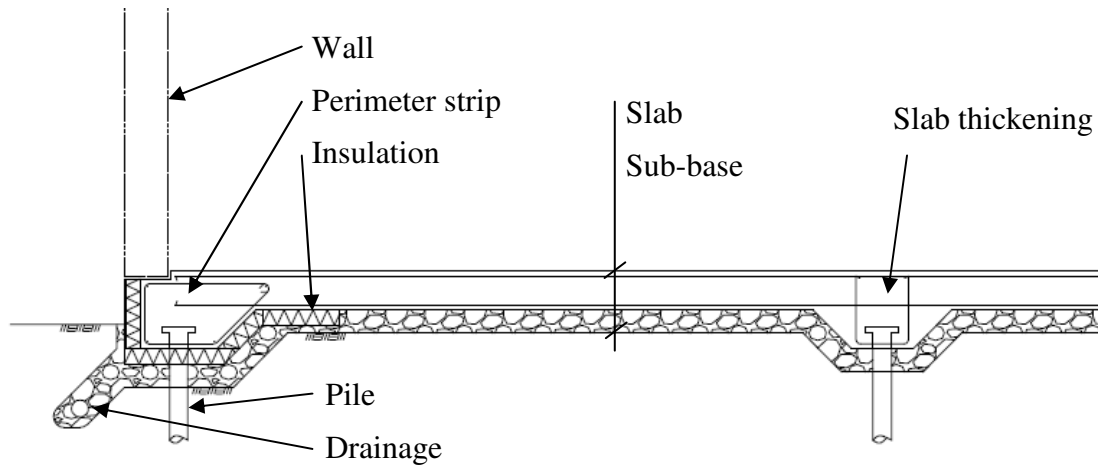


Figure 2.3 Typical section of a pile-supported slab-on-ground.

If the ground conditions are sufficient, piles will not be necessary and the design will instead be more similar to the one shown in Figure 2.4. The slab thickening can here be removed, unless additional capacity is needed locally in order to transfer load from internal columns or walls.

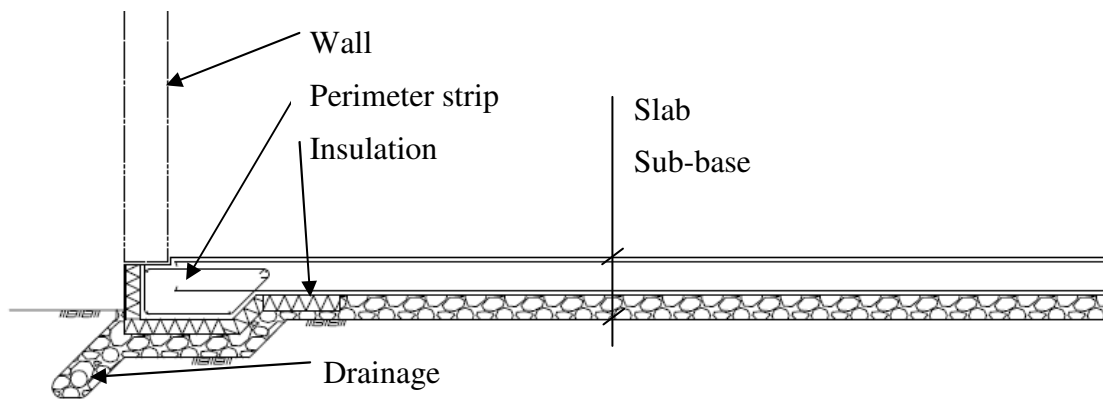


Figure 2.4 Typical section of a slab-on-ground without pile-support.

If the external slab thickening, the perimeter strip, also can be removed, the design can instead be according to Figure 2.5. This design is beneficial with regard to shrinkage effects, since the external restraint of the perimeter strip is removed by isolating the slab-on-ground. The slab is now more free to move, which reduces the restraint forces.

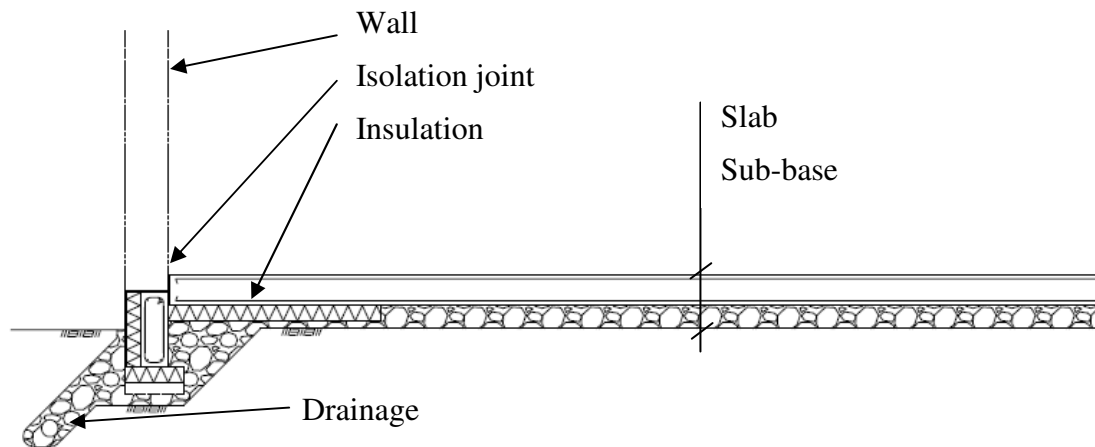


Figure 2.5 Typical section of a slab-on-ground without pile-support and perimeter strip.

In order to control cracking of concrete, the amount and layout of reinforcement is essential. In general it is important that the reinforcement amount is sufficient in order for the concrete section to have a lower tensile capacity than the yield capacity of the reinforcement. Large single cracks can then be avoided, since a new crack will be formed before the steel yields in the initial crack.

Based on this, the choice of concrete strength is also important with respect to cracking behaviour. The concrete needs to have an adequate compressive and abrasive strength to resist the impact on the floor, but at the same time a lower tensile capacity than the reinforcement.

The reinforcement which is aimed at controlling the crack development in a slab-on-ground can consist of ordinary reinforcement, steel fibre reinforcement or a combination of the two. A benefit of using steel fibres is that the heavy work procedure of positioning the reinforcement is avoided, reducing the workload (Knapton, 2003). Furthermore, it also creates a more homogenous material compared to concrete with ordinary reinforcement and thereby distributes cracks in a more efficient way. Often a better result of controlling cracks is achieved when combining steel fibres with ordinary reinforcing bars, instead of using only steel fibres (Swedish Concrete Association, 2008).

The use of fibre reinforcement in concrete is increasing, especially for slabs-on-ground. There is no design method described in EC, which complicates the design procedure. There is however a method described in MC2010 which can be adopted (International Federation for Structural Concrete, 2012).

Good measures and instructions regarding detailing of slabs-on-ground are available in literature, but fundamental knowledge of how structures behave during the shrinkage process when influenced by external restrains is not as well documented. Understanding this behaviour is however deemed highly important in order to be able to minimise problems caused by shrinkage cracking. As a result, a large portion of the work carried out for this project considers the global behaviour of slabs-on-ground subjected to restrained shrinkage.

2.2 Detailing

In order to take the concept further and finalise a design, there are several specific details that have to be regarded and given detailed specifications on how to be carried out. Each choice is important and to avoid shrinkage cracking, detailing that creates restraints should of course be avoided whenever possible.

2.2.1 Perimeter strips and local thickenings

When a slab-on-ground is provided with perimeter strips and/or local thickenings the slab will gain increased horizontal stiffness in these local regions (Swedish Concrete Association, 2008). The actual dimensions of the perimeter strips and local thickenings will vary from case to case and follow the project specific demands. A generic perimeter strip is found in Figure 2.3. There are some general advantages and disadvantages when incorporating perimeter strips and local thickenings in a slab, which are outlined in Table 2.1 below.

Table 2.1 Advantages and disadvantages of incorporating perimeter strips and/or local thickenings in a slab-on-ground, modified from the Swedish Concrete Association (2008).

Effects of incorporating perimeter strips and/or local thickenings	
Advantages	Disadvantages
<p>The edge lifting will be reduced. The larger weight reduces the edge lifting along the thicker edge.</p> <p>The slab will have a stiff edge with a large effective depth that is able to transfer and carry concentrated loads.</p> <p>The deformations will be less.</p> <p>There is a possibility to make excavations underneath the slab-on-ground even after the construction is finished.</p>	<p>There is a risk of cracking perpendicular to the perimeter strip in case of shrinkage and thermal strain, due to the larger horizontal stiffness in the perimeter strip in relation to the slab.</p> <p>There will be restraints in one or two directions that often lead to severe through cracking.</p> <p>The loading of the perimeter strip leads to forces in the same direction as the shrinkage forces.</p> <p>The joint openings will be larger with the risk of crushed joint edges, due to increased restraints.</p> <p>There will be a local increase in drying time that reduces the rate of drying. This creates a moisture gradient and a length difference between the inner parts of the slab-on-ground and the perimeter strip. This can lead to cracking.</p> <p>There can be a “stationary” moisture condition in the core of the perimeter strip that can emit moisture at cracking.</p>

If it is chosen not to incorporate perimeter strips in the slab, the advantage is that the restraints from these details are eliminated. However, in order to prevent edge lifting, the slab-on-ground must still provide enough stiffness. A common solution in these cases is to transfer line loads and concentrated loads from walls to a standalone socket or foundation, see Figure 2.5.

2.2.2 Columns

Where columns are positioned onto a slab-on-ground there will be concentrated support reactions. In general these loads are instead preferred to be transferred to foundations that in its turn transfer the loads to the ground (Swedish Concrete Association, 2008). If the foundations are connected to the slab-on-ground, there will be a change in stiffness and in geometry, similar to adding perimeter strips. This deviation creates restraints that are unfavourable with regard to shrinkage cracking.

The design detailing of column connections are thus important, as restraint forces can develop if the detailing is not carefully carried out. To minimise the restraint the column and its foundation should be isolated from the rest of the slab to allow for movement and to maintain a uniform stiffness over the slab. The joints used to isolate the columns are isolation joints, see Section 2.2.3. Figure 2.6 below illustrates an example of good detailing.

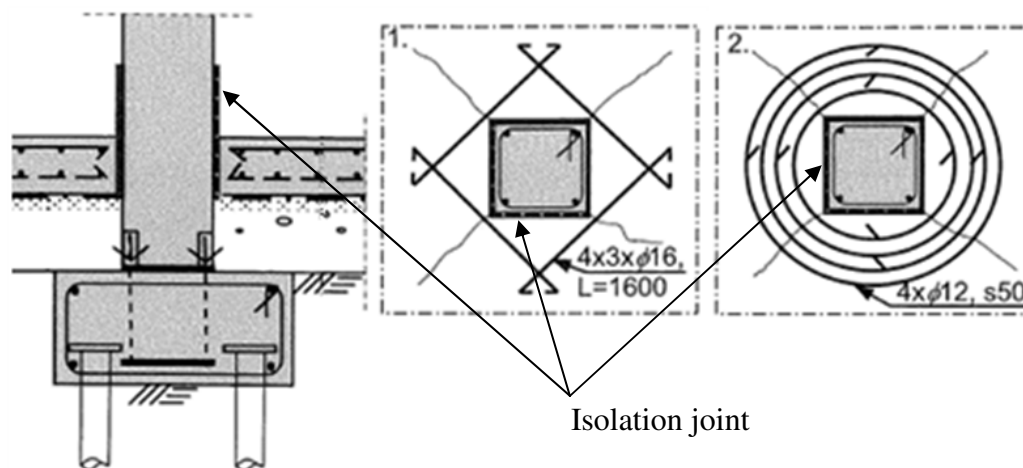


Figure 2.6 Joint and reinforcement detailing around columns, modified from the Swedish Concrete Association (2008).

2.2.3 Joints

When possible it is often preferred to design floors without any joints (Swedish Concrete Association, 2008). However, joints are often necessary and it is then preferable to keep the total length of joints as low as possible to optimise the performance of the floor. In order to do this, it is often beneficial to incorporate several different joint functions into one joint where possible, see Table 2.2. One example can be to finish a cast step at the location where movement joints are provided to avoid creating a construction joints within the slab portion. Construction joints are interfaces between two successive casting steps of concrete (National Ready Mixed Concrete Association, 1998).

Table 2.2 Advantages and disadvantages of incorporating several joint types into one joint, adapted from Swedish Concrete Association (2008).

Effects of incorporating several joint types into one joint	
Advantages	Disadvantages
<p>Damages often occur at joints and due to this the number of joints should be limited.</p> <p>The number of cases with edge lifting is lowered, if the number of joints is limited.</p> <p>A well designed and constructed dilatation joint will transfer shear forces to the adjacent slab with little force loss.</p> <p>The movement due to thermal and shrinkage strain is relatively free to develop at the edges as the restraint in the slab plane is reduced to a minimum.</p>	<p>At large joint spacing the shrinkage and shear forces can grow larger and be concentrated due to restraints and uneven loading. When the slab movement in other parts is free to develop and the friction is low, the risk for these large and concentrated loads increases.</p> <p>High demands lie at the function of the dilatation joint.</p>

As mentioned, it is preferable to isolate the slab-on-ground from the main structure and not create restraints at column connections. By incorporating isolation joints, movement is allowed and the risk of shrinkage cracking is reduced. The isolation joint is not able to transfer any load, but allows for a certain amount of movement (Williamson, 2003), see Figure 2.6 above for a typical isolation joint around an internal column. The joint should allow for a movement of 10-20 mm in most cases, but the need for movement could be larger if the joint spacing is large (Swedish Concrete Association, 2008). It is also of importance that the isolation material is sufficiently compressible. In order to achieve this it is recommended to use cellular rubber in the isolation joints (Williamson, 2003).

To lower the shrinkage forces in a slab-on-ground there is an option of including contraction joints in the design (Swedish Concrete Association, 2008). The contraction joint is preferably formed by saw cutting the surface of the slab, commonly in a square pattern with joint spacing of 5-10 m. In industrial floors there are often strict tolerances on the surface finish and evenness, which makes saw cutting the preferred method to make grooves in the surface, instead of using plastic inserts or similar methods that disturbs the surface (Williamson, 2003). As the joint section will be weakened by the groove, a crack inducement is created, which allows for control of where possible cracks will occur (Knapton, 2003). The contraction joint will however still create restraints and transfers forces perpendicular to the joint and in plane of the slab due to reinforcement across the joint section (Swedish Concrete Association, 2008). The restraint can be lowered by allowing a gap in the main reinforcement where the contraction joint is formed and instead provide a dowel in that section. The dowel should then be detached from the concrete at one end, to allow for dilatation movement. See Figure 2.7 for examples of contraction joints.

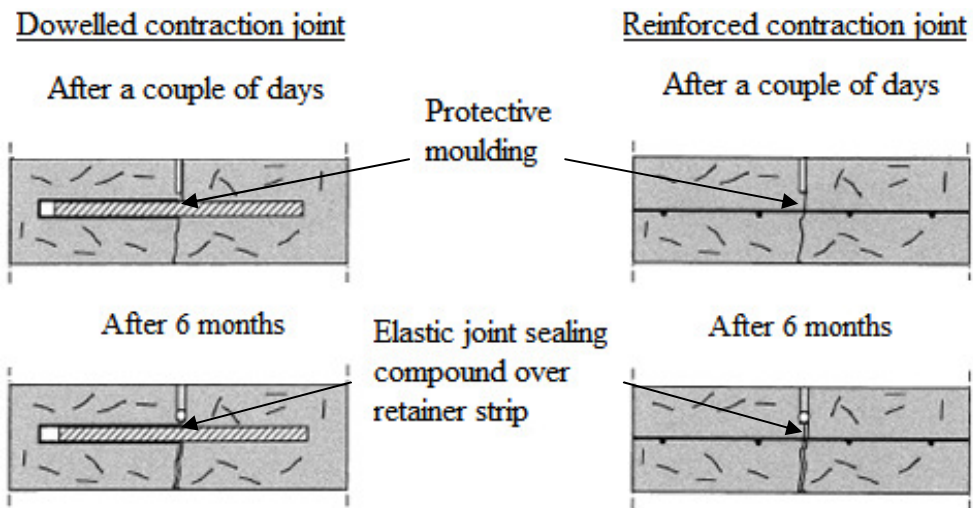


Figure 2.7 Example of solutions for contraction joints and isolation joints, modified from Swedish Concrete Association (2008).

The best way to allow for movement in the plane of the slab, both perpendicular to (dilatation) and along the joint, is to use a well designed and constructed dilatation joint. Preferably the dilatation joint should be the only joint in an industrial floor in combination with sufficient isolation joints (Swedish Concrete Association, 2008). Figure 2.8 shows a prefabricated dilatation joint with cartridge dowels, alpha type. A prefabricated dilatation joint like this also works as formwork at casting.

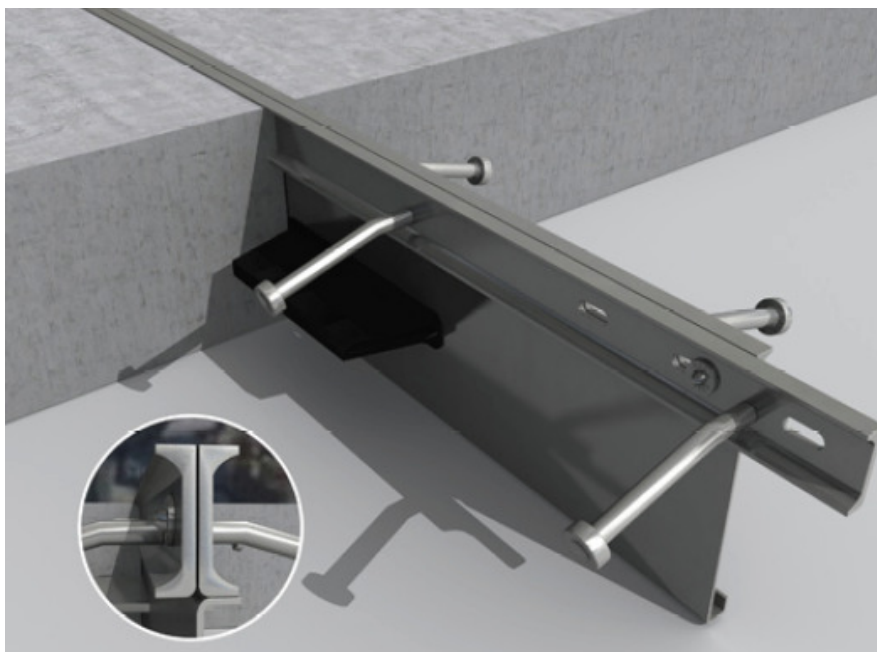


Figure 2.8 Example of prefabricated dilatation joint (Permaban, n.d.).

2.2.4 Reinforcement details

At locations that by experience are known to be critical with regard to cracking it can be justified to provide additional reinforcement. The locations can be at weakened regions like holes or drains where stresses are known to build up or at locations where there are known restraints like non-isolated columns. Figure 2.9 shows some examples of how additional reinforcement can be arranged in some specific situations. The reinforcement should be arranged as close to the adjacent parts as possible, but the required nominal cover thickness should not be violated.

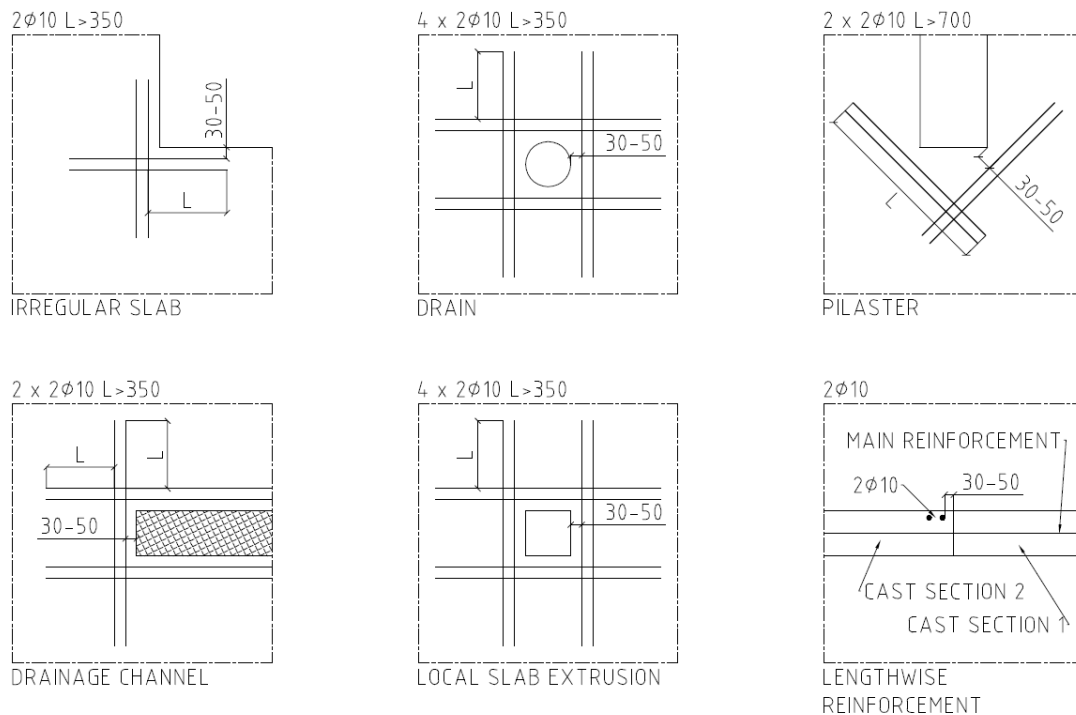


Figure 2.9 Examples of additional reinforcement for details known to induce cracks, modified from AB Jacobson & Widmark (2001).

2.2.5 Surface finishing

The specific factors that influence the choice of surface and surface finish of a floor include traffic type, storage principle, abrasion, impact, chemical resistance and aesthetics (Knapton, 2003). There are several ways of how to treat the plain concrete surface in a mechanical way before it sets and besides this there is also a range of commercial materials that by different methods change the properties of the surface.

The surface of a concrete floor can look very different depending on which method was used to treat the surface. For example the options can be to just finishing the surface with a wooden board or plank, using a float or trowelling it by hand and/or with machines. The resulting surface can have a rather distinct texture, but the choice for industrial floors is generally a smooth, hard and even surface (Swedish Concrete Association, 2008).

Commercial materials range from dry shake floor hardeners and chemical hardeners to a wide range of sealers and coatings. The dry shake floor hardeners are sprinkled

over the cast section and then trowelled into the fresh wet surface of the floor. When executed correctly this creates a dense, toughened and wear resistant surface. This hardener can also provide improved smoothness and dust reduction (Knapton, 2003). Most of the chemical hardeners improve the wear resistance and prevent dusting. For a more specific description of these products it is recommended to consult the manufacturer for updated information. The sealers and coatings can significantly improve the abrasion and chemical resistance of floors and they can also colour floors to improve their appearance (Knapton, 2003).

After the chosen measures have been executed it is of high importance to let the concrete and the surface set and harden under the right controlled conditions. Some important factors that are influenced by the curing procedure are the risk of plastic shrinkage cracks, the surface abrasion and the drying shrinkage with its consequences (Swedish Concrete Association, 2008). The most important factor is to not let the surface dry out as the cement hydration stops if there is an insufficient source of water. The drying of the surface is influenced by the ambient relative humidity, the sun and the wind. To prevent the drying of the surface it should be covered and protected until sufficient strength has developed (Swedish Concrete Association, 2008).

2.3 Restraints

Cracks in concrete structures can appear for a number of reasons. This project has however focused on cracking due to prevention of concrete to move freely when it shrinks. The prevention is caused by restraints and when this results in a tensile strain equal to the, relatively low, ultimate tensile strain of the concrete, cracking occurs. The restraint forces are different from external forces, such as imposed loads, and can be a result of either internal or external restraints (Petersons, 1994). As illustrated in Figure 2.1, piles, perimeter strips, slab thickenings, friction to sub-base and cast-in connections all constitute external restraints and will influence the risk of cracking.

2.3.1 Restraint degree

In order to understand the behaviour of a restrained structural member, the degree to which the member is prevented to move, the restraint degree, R , can be formulated. Three different cases can be identified; no restraint, full restraint and partial restraint.

A general formulation for restraint degree can be expressed as the ratio of actual restraint force and the restraint force in case of full restraint, according to equation (2.1). The expression is valid for both reinforced and plain concrete members, if the restraint forces are regarded as external restraint forces only. As follows from the equation; no restraint gives $R = 0$, full restraint gives $R = 1$ and for partial restraint $0 < R < 1$.

$$R = \frac{\text{actual restraint force}}{\text{restraint force in case of full restraint}} [-] \quad (2.1)$$

A structural member can be restrained both by internal restraints and external restraints, which are further explained in the two following sections.

2.3.2 Internal restraints

Internal restraints in concrete are caused by aggregates and reinforcement, acting on different levels. The aggregates prevent the hardened cement paste, HCP, from shrinking. There reinforcement prevents the concrete, where the aggregates are included, from shrinking.

Since aggregates and reinforcement compose a vital part of most concrete structures, these restraints cannot be removed. Instead, the cracks associated with them must be evenly distributed using appropriate placement of reinforcement and well graded aggregates. Through this method, large crack widths should be avoided in favour of several smaller cracks.

2.3.3 External restraints

For a slab-on-ground the external restraints are caused by partial prevention of movement by e.g. piles, perimeter strips, frictional resistance or by unintended interlocking in the joints between the slab and walls or columns. A good design measure is to allow for movement of the slab when possible, in order to reduce the restraints.

A concrete member cast against a surface creating a longitudinal edge restraint is shown in Figure 2.10. The restraint occurs due to friction, bond or roughness at the joint interface. Depending on the specific geometry the upper edge is however more or less unrestrained in its longitudinal direction which results in a gradient of the restraint degree throughout the cross section of the member. The figure also illustrates how the restraint degree varies in y-direction depending on length, L , and height, H .

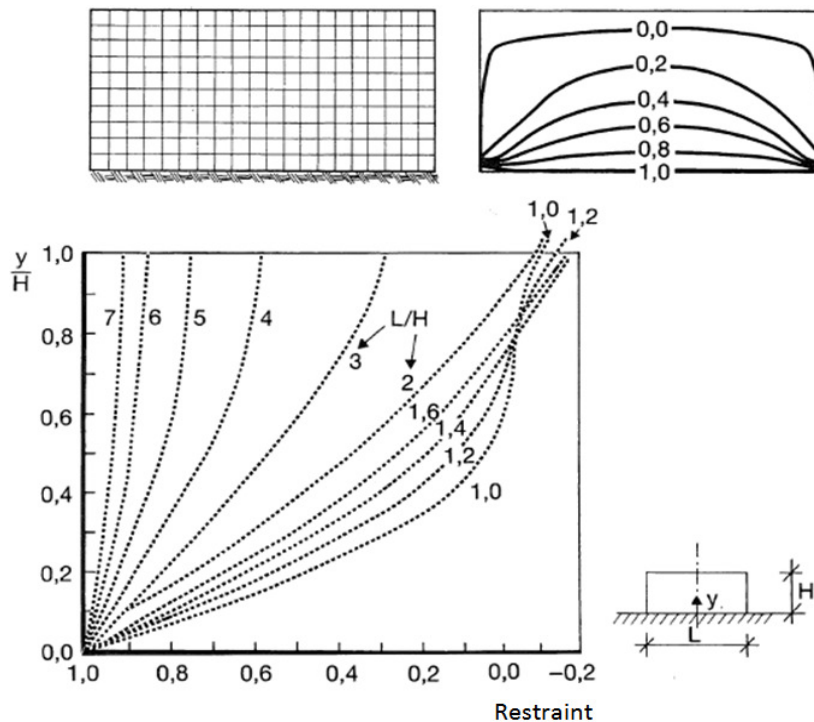


Figure 2.10 Variation of restraint degree with depth in a wall that is fully fixed at the bottom edge (Bernander, et al., 1994).

Assuming that this model would also be valid when studying the restraint in one direction for a slab-on-ground, the following observation can be made. If a worst-case scenario is studied with $H = 0.5\text{m}$ and $L = 5\text{m}$, i.e. a very thick slab with a small length, the ratio L/H equals 10. This results in that the quota y/H is close to 1, which implies that the restraint variation over the slab is very small and most likely negligible. The restraint situation present in the bottom of the slab will therefore be representative throughout the thickness of the slab.

This reasoning is based on a fully fixed bottom, which is not the case for a slab-on-ground. However, it suggests that the low thickness of a slab results in a relatively uniform restraint degree as a result of friction to the sub-base.

2.4 Friction

Friction is the resistance against slip in the contact boundary between two materials. The frictional resistance results in a frictional force along the slip plane opposite the direction of the movement. When considering the friction between two materials, the coefficient of friction, μ , is normally used. This can be expressed according to Equation (2.2) below (Ljungkrantz, et al., 1994). The use of this coefficient assumes fully developed frictional force, despite the actual displacement between the slab-on-ground and the material below it.

$$\mu = \frac{\text{maximum frictional force}}{\text{normal force}} \quad (2.2)$$

The previous model in Figure 2.10 described a member with a fully fixed edge. However, as mentioned above, for a slab-on-ground the restraint is not fully fixed and instead depends on the interface between the slab and sub-surface. Table 2.3 below illustrates how the coefficient of friction varies for the interface depending on which type of material that is used.

Table 2.3 Examples of coefficients of friction for a slab-on-ground (Petersons, 1992).

Material under slab-on-ground	μ
Crushed aggregate – uncompacted and uneven	> 2.0
Crushed aggregate – compacted and smooth	1.5
Insulating material	1.0
Sand layer - even	0.75
Plastic Sheeting – one layer	0.75

Figure 2.11 below illustrates a slab-on-ground subjected to shrinkage strain. As can be seen the resulting normal force in the slab, here N , is dependent on the coefficient of friction, member length, self weight and variable load. This definition is also used in a design method by Petersons (1992) to calculate the maximum allowable slab length, further explained in Section 4.3.1.

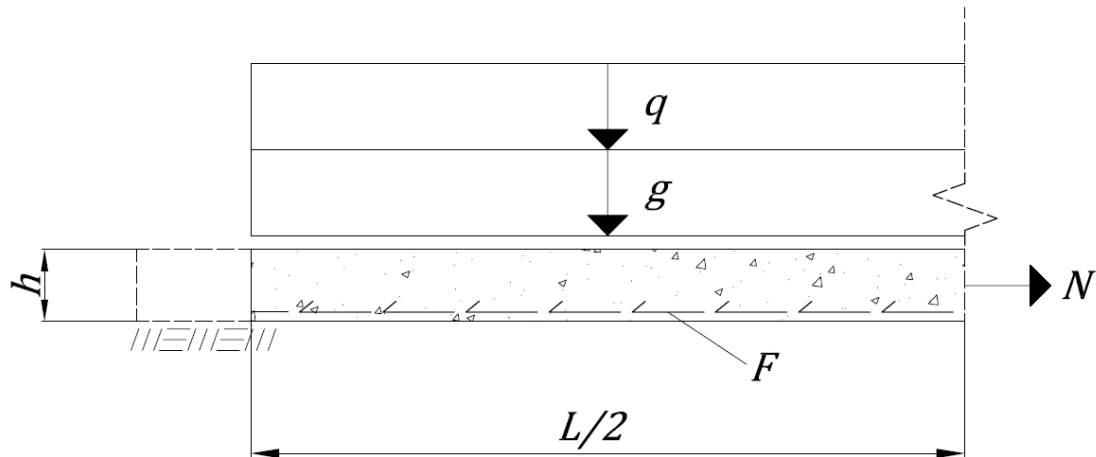


Figure 2.11 Schematic illustration of normal force in a slab-on-ground affected by shrinkage, modified from Petersons (1992).

Through horizontal equilibrium between the friction along the slab and the resulting frictional force the following expression can be derived.

$$N = \mu \cdot (q + g) \cdot \frac{L}{2} \text{ [N/m]} \quad (2.3)$$

where

- μ = coefficient of friction [-]
- g = uniformly distributed self weight [N/m²]
- q = uniformly distributed variable load [N/m²]
- L = length of slab [m]

There have been suggested approaches and tests to describe the friction in a more sophisticated way, as the method using coefficient of friction neglects the actual non-linear relationship between displacement and coefficient of friction. A test curve from a shear test is shown in Figure 2.12. The test specimen used was a 1.2 m by 0.8 m slab with a thickness of 200 mm, which was pushed forwards, then backwards and at last forwards again (Pettersson, 2000).

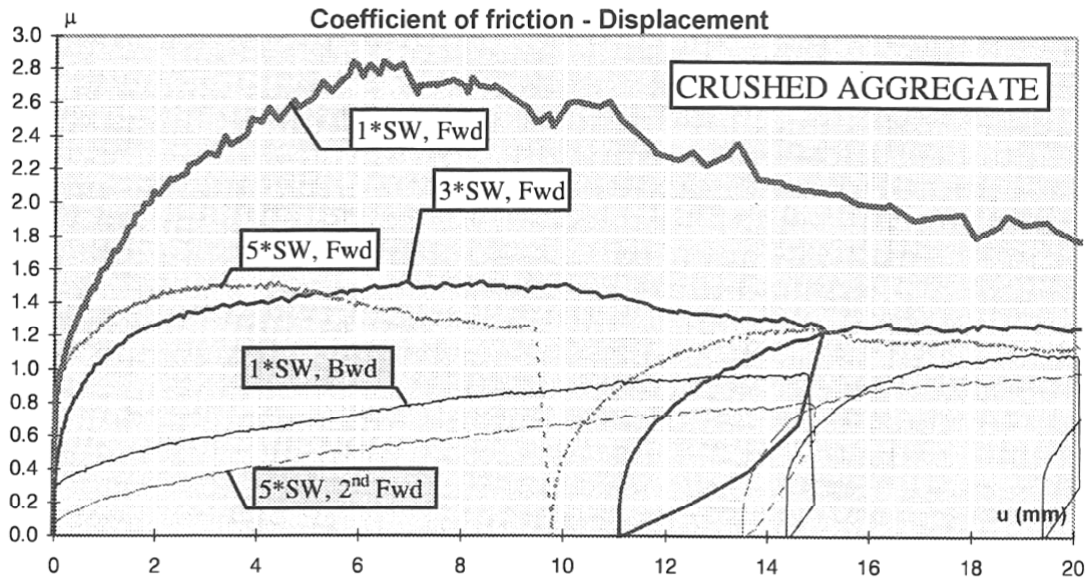


Figure 2.12 Friction curves for test specimens on crushed aggregate, where SW=Self weight, Fwd=Forward, Bwd=Backward (Pettersson, 2000).

From Figure 2.12 it can be concluded that the reality is deviating from the generally used simplification. For slabs-on-ground there are several possibilities of where the actual sliding surface will develop when the slab is moving, for instance due to shrinkage. It can either develop directly under the concrete or at a small distance into the adjacent material, depending on its properties and on the bond between slab and ground. When casting the slab against a coarser material, like crushed aggregate, there will be a transition zone where the aggregate is mixed with the concrete, thus creating a more complex situation for determining the sliding surface (Pettersson, 2000).

It is important to note that friction is unlikely to be uniform along a large slab. As the ground material likely will develop uneven settlements there will be local deviations of the frictional force.

The effect of friction for an uncracked slab can be regarded as unfavourable. The friction will then act as a distributed restraint along the lower bound region of the slab-on-ground. However, when the first crack develops in the slab, positive effects from the friction can be taken into consideration. The friction phenomena will then act in analogy with the reinforcement, reducing the crack widths and distributing the cracks over the total length of the slab, creating a system of distributed cracks rather than a set of few large cracks.

2.5 Construction methods

The choice of construction method and the execution are influencing the cracking behaviour of industrial floors, both in a short and long time perspective. There are several suggestions of how to optimise the procedure to minimise cracking and to achieve a good performance when constructing an industrial floor. The optimisation is however often limited by a budget and time plan.

The construction process for an industrial floor is illustrated on a timeline in Figure 2.13. The measures that can be conducted to construct a good industrial floor are linked to the different activities on the timeline.

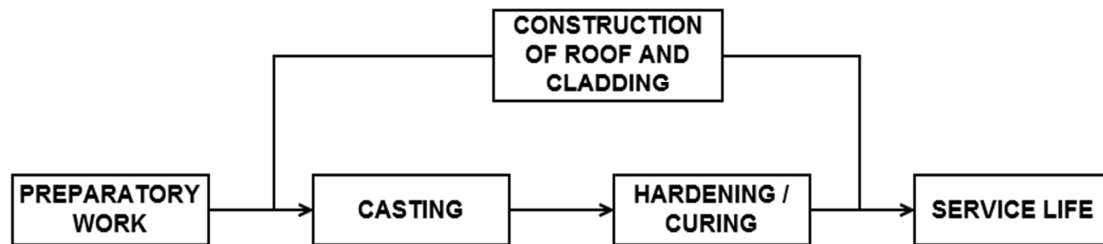


Figure 2.13 Timeline over the construction process for an industrial floor.

Before the work at site is initiated it is crucial to plan the project in detail so that the involved organisation knows what should be accomplished, how and when. The purpose of the planning is to ensure that the client's expectations and demands can be fulfilled in a satisfying way and that there is enough manpower with adequate competence to complete the project within the time limit (Swedish Concrete Association, 2008). It is also important to plan what checks and inspections that are to be carried out during the construction process, who executes them and to whom the results are reported (Williamson, 2003). Some of the checks will be for the contractor to examine his own work and to ensure that each feature is constructed correctly.

The parameters in Table 2.4 should be checked during the construction process following the recommendation of the Swedish Concrete Association (2008). The parameters are not all directly linked to the shrinkage behaviour and resulting shrinkage cracking, but should still not be neglected in the construction process.

Table 2.4 Recommended checks during the construction process of an industrial floor, modified from Swedish Concrete Association (2008).

Parameters to check before casting of industrial floors
<ul style="list-style-type: none"> • Compaction properties of the ground • Evenness of the sub-grade and sub-base • Quality of sub-base • Reinforcement amount and arrangement • Location of drains and other installations • Levelling of formwork, joints and laser against a reference height • The finished floor height • That sufficient mechanical equipment and workers to handle them are available • Coordinate concrete quality, amount and delivery schedule with the concrete supplier.

Parameters to check during casting of industrial floors
<ul style="list-style-type: none">• Evenness of the sub-base• Evenness of casting surface• That the downfalls to drains are correctly executed• Deviations in consistency of concrete
Parameters to check after casting of industrial floors
<ul style="list-style-type: none">• Evenness of slab surface against the specific demand• That the downfalls to drains are correct• That the curing is sufficient and that covering of the surface is present• Avoid temperature drops during curing• That the sun does not heat up unprotected areas of the slab

The current relative humidity, wind, sun and temperature at casting will influence the mitigation of moisture from the slab. As stated before, it is of importance to prevent a fast mitigation of moisture from the slab and its surface. Whether the casting takes place in an inside or outside environment or if it is summer or winter, the drying of the concrete surface must be controlled. It should always be sought for to have an even moisture and temperature gradient so the surface does not dry out and the hardening process will be uniform throughout the concrete section (Swedish Concrete Association, 2008). Sufficient weather covering and curing under moist conditions will prevent the concrete from drying out too quickly.

The actual method to place the concrete is of minor importance when regarding shrinkage effects, if the different methods give an equally compacted concrete and the same evenness. The construction method should be chosen with regard to the actual circumstances and is for example affected by the number of obstacles in the floor and the need for construction capacity (Knapton, 2003). There are several common methods for placing the concrete; examples are the laser screed method, the manual laser screed method and the traditional long and wide strip method.

When not casting the whole floor area in one step and parts of the floor are chosen to be cast against each other it is important to still limit the restraints that will occur. A solution of how to minimise the restraints when sections are cast against each other is shown in Figure 2.14. Not more than two perpendicular edges are fixed during cooling of each element.

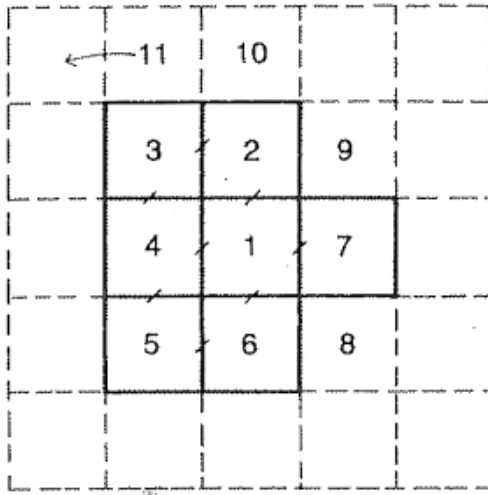


Figure 2.14 Acceptable arrangement of casting sequence (Bernander, et al., 1994).

Vacuum treatment is an interesting technology that recently has gained new attention in Sweden (Swedish Concrete Association, 2008). The technology is based upon that large sheets are placed over the concrete floor and linked to pumping equipment that creates a negative pressure, which forces the water to leave the concrete. Naturally the effect takes place only in the surface layers of the concrete, depending on the transportation properties, but can ultimately reduce the shrinkage with 50% (Swedish Concrete Association, 2008). A direct effect of reducing the water content of the concrete is that the w/c ratio is lowered and the strength of the concrete will therefore be higher (Swedish Concrete Association, 2008). The disadvantages are problems with getting the desired effect at edge zones and that not all concrete mixes are adaptable for this treatment. Figure 2.15 shows a concrete road slab which is being vacuum treated.



Figure 2.15 Vacuum treated concrete road slab (Balvac inc., 2007).

3 Response of materials and components

Reinforced concrete is a composite material, consisting of steel and concrete. However, concrete is in its turn also a composite material and can simply be seen as a composite of cement paste and aggregates. In order to understand and interpret the overall behaviour of reinforced concrete, it is important to first understand the behaviour and characteristics of each component.

Furthermore, the conditions and mechanisms ultimately forming a crack in the concrete are also fundamental to understand, in order to prevent and/or limit the cracks. The reasons for preventing or limiting cracks in a slab-on-ground floor can be both aesthetic and technical. A randomly cracked floor does not look good and open cracks can precipitate further degradation of the concrete and reinforcement. It is therefore of importance for the designer and contractor to fulfil the established requirements.

3.1 Concrete

Concrete can simply be considered as a composition of cement, water and aggregates where the cement and water reacts and creates a hardened cement paste, HCP. The aggregates consist of a graded rock material, which is contained inside the HCP and together they form the concrete material.

These two materials behave differently when exposed to stresses, which can be illustrated by the simplified stress-strain relationship in Figure 3.1. The aggregates will have a much higher E-modulus than the HCP and, as illustrated, the concrete will have an intermediate value. Furthermore, even though both the aggregate and the HCP behave mainly linearly until failure, the concrete will to a greater extent behave non-linearly. This is due to the relative weaknesses in the transition zone between HCP and aggregates where microcracks are induced. The number and size of microcracks increase with increased stress, resulting in the non-linear behaviour.

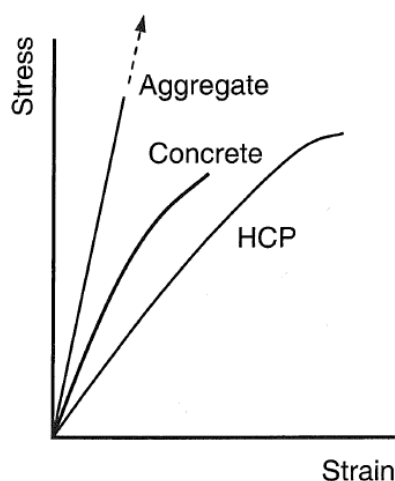


Figure 3.1 Stress-strain relationship of aggregate, HCP and concrete (Domone & Illston, 2010).

As mentioned above, HCP consists of cement and water. The proportion of how these are mixed is defined by the water/cement ratio, also called w/c ratio. Typical values of the w/c ratio are in the interval 0.3-1.0. Several important characteristics of a concrete are highly influenced by this ratio. However, a more accurate way of categorising modern concrete is on its water/binder ratio, where binder includes both cement and additions such as fly ash or condensed silica fume (Domone & Illston, 2010).

Figure 3.2 below illustrates the relationship between w/c ratio and compressive strength. In addition to this, the influence of age on compressive strength is also illustrated.

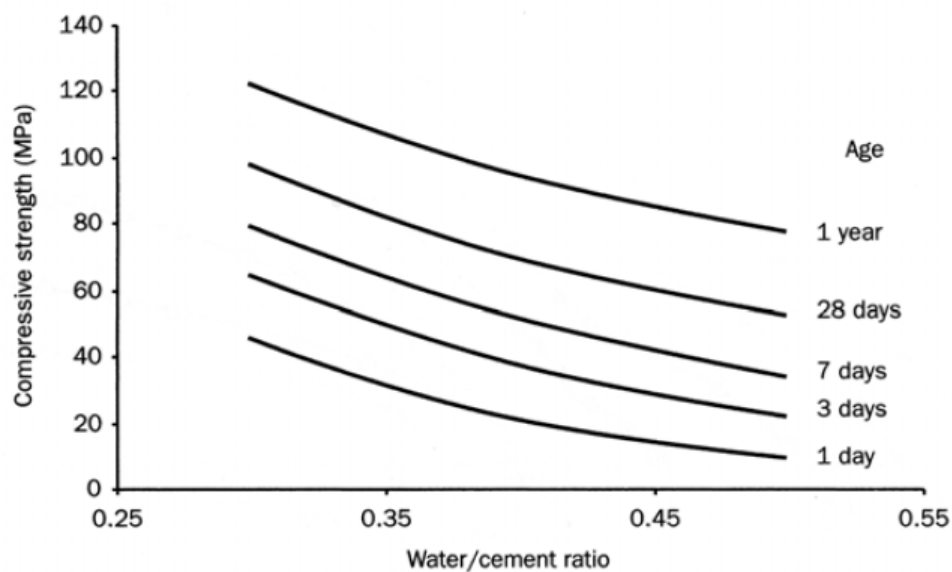


Figure 3.2 Relationship between w/c ratio, concrete age and compressive strength for a Portland cement paste sample stored in water at 20°C (Domone & Illston, 2010).

The volume of the HCP in concrete is highly water-sensitive. As a result, when water leaves the concrete pores and evaporates to the external environment, the volume of the HCP decreases, which results in concrete shrinkage and potential shrinkage cracking. It is therefore important to understand how water is contained in concrete. Figure 3.3 below illustrates a gel structure and different locations where water can be found within the HCP structure.

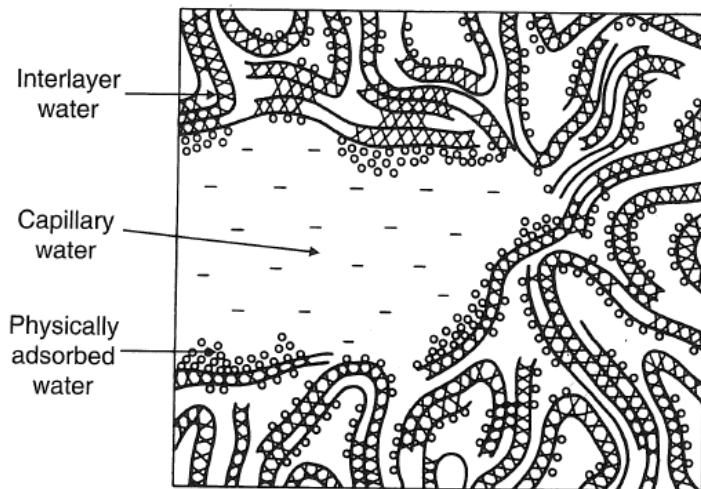


Figure 3.3 Location of water in a HCP gel structure (Domone & Illston, 2010).

In total, water is contained in five different ways, which are explained below. The further down in the list, the more strongly bound the water is to the material. It should however be noted that there is no strict boundary between the different types of water (Domone & Illston, 2010).

- *Water vapour.* This can be found in larger voids that will not be completely water-filled.
- *Capillary water.* This is contained in the capillary and gel pores of 5-50 nm width. Water in larger voids is considered as free water.
- *Adsorbed water.* This is located next to the solid surfaces and subjected to surface attractive forces.
- *Interlayer water.* This water exists in pores smaller than 2.6 nm and is strongly connected to the pores through tension forces from two surfaces due to the narrowness of the pore.
- *Chemically combined water.* This water is involved in the hydration process and cannot be removed unless heated to temperatures above 1000°C.

3.2 Shrinkage of concrete

Shrinkage of concrete depends on of several known phenomena acting during different time-spans of the concrete life cycle. The general factor affecting the shrinkage is volume reduction due to loss of water. Shrinkage leads to cracking if it is restrained and if the stresses from the restrained situation reach values equal to the tensile capacity of the concrete in any section. In Table 3.1 typical defects of concrete are explained and it is stated approximately at what age they normally appear.

Table 3.1 Typical concrete ages for appearance of various defects, adapted from Day & Clarke (2003).

Type of defect	Typical age of appearance
Plastic settlement crack	Ten minutes to three hours
Plastic shrinkage cracks	Thirty minutes to six hours
Early thermal contraction cracks	One day to two or three weeks
Long-term drying shrinkage cracks	Several weeks or months

Chemical reactions in the concrete cause water movement inside the structure and as the hydration processes continues over time, this is a complex situation. Chemical and autogenous shrinkage are fundamentally based and defined by these chemical reactions. They are both internal phenomena, occurring without moisture exchange with the external environment.

The water departing from concrete to the outside environment causes drying shrinkage due to water loss from the internal structure. Figure 3.4 illustrates how water loss correlates with shrinkage strain for a concrete with w/c ratio of 0.5.

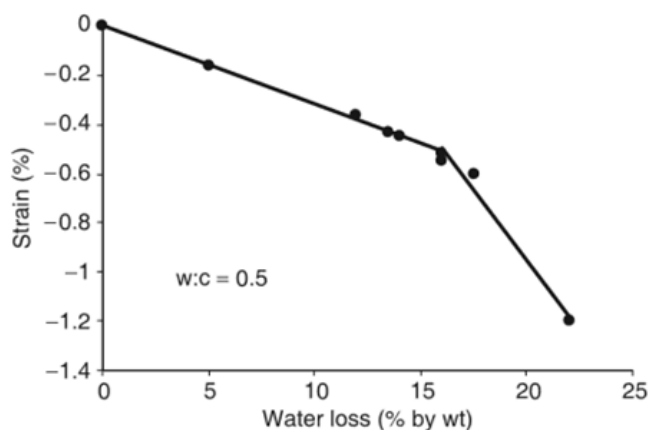


Figure 3.4 Relationship between water loss and strain (Domone & Illston, 2010).

Another defined shrinkage phenomena is plastic shrinkage which occurs when water evaporates from the surface of early age concrete under certain conditions.

3.2.1 Drying shrinkage

As concluded above, water loss from the HCP causes shrinkage. Water loss can however occur through several mechanisms. This is illustrated in Figure 3.4 through the change of slope of the graph at about 17% of water loss. Other research results propose that up to three changes of slope can occur, resulting in four different proposed mechanisms (Domone & Illston, 2010). These will be explained below. The

first three mechanisms concern free and adsorbed water, while the fourth concerns the interlayer water. Opinions regarding in which ranges of RH and to which extent the different mechanisms contribute to shrinkage are divided.

- *Capillary action.* This phenomenon can be visualised through lowering a small tube, such as a straw, into a glass of water. Due to the combined action of cohesive and adhesive forces the water will rise up a small distance into the tube. The smaller the radius of the tube, the larger the forces will be and the higher the water will rise. This effect is also present in HCP where the tubes in this case are the capillaries and larger pores. The capillary action causes tension at the water surface, which is dependent on the radius of the water surface (also called meniscus), r , and on the vapour pressure, p . This relationship is illustrated below in Figure 3.5. Here p_0 is the saturation vapour pressure and corresponds to the vapour pressure resulting in a flat water surface. When the vapour pressure decreases, condensation of the water begins and the meniscus radius decreases until it reaches its minimum value of half the capillary diameter. As the radius decreases, tensile forces are introduced. The shrinkage effects from this phenomenon are generally considered to appear for values of RH down to 50% (Domone & Illston, 2010).

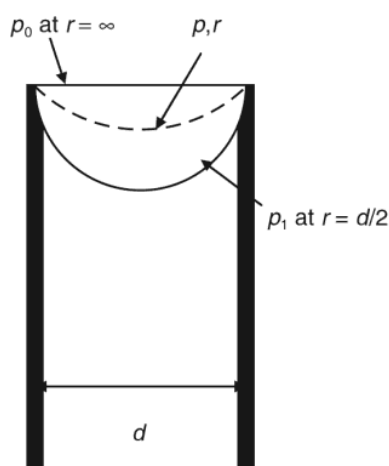


Figure 3.5 The relation between radius of water surface and vapour pressure in a pore structure (Domone & Illston, 2010).

- *Surface tension.* When water in the HCP comes in contact with the solid particles, cohesive and adhesive forces will act on it. The cohesive forces are attractive forces within the water molecules, pulling them tightly together. This is for example the reason why water lumps together, creating droplets. The adhesive forces are the forces acting between two different types of molecules, for example through letting a drop of water rest on a vertical glass surface. The way in which a certain liquid behaves when in contact with a surface depends on the net attractive forces between cohesive and adhesive forces. The surface tension is a measure of the energy required to increase the surface area of a liquid, in this case water, by a unit of area. When water molecules are lost from the particle surfaces, the surface energy is increased which then leads to an increase of internal stresses in the HCP and to a decrease in volume, i.e. shrinkage (Domone & Illston, 2010).

- *Disjoining pressure.* In narrow pores, the adsorbed water will cause a swelling pressure. Figure 3.6 illustrates a gel pore where the wider section contains a 1.3 nm thick water layer at saturation, which is subjected to capillary tension. As the pore narrows, a thicker water layer will be cumulated due to surface tension from two surfaces. This water causes a disjoining (swelling) pressure which, when water is reduced from the pore, decreases and as a result causes shrinkage (Domone & Illston, 2010).

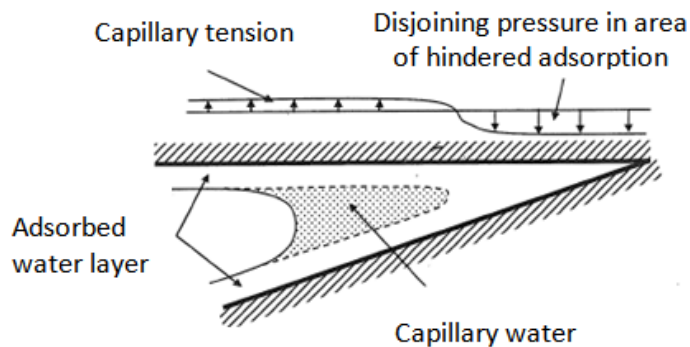


Figure 3.6 Capillary tension and disjoining pressure in HCP (Domone & Illston, 2010).

- *Movement of interlayer water.* The interlayer water is strongly bound to the HCP through its long paths and connection to the solid surfaces. As a result, removal of the interlayer water demands a lot of energy, but its removal also leads to a large shrinkage. This is therefore likely to describe the steeper slope at the end of the graph in Figure 3.4. As the particle surfaces move closer, due to shrinkage caused by the movement of interlayer water, new inter-particle bonds are created. The HCP thereby becomes denser and the shrinkage becomes partly irreversible. If concrete is subjected to high temperatures or RH lower than 10%, this phenomenon can highly contribute to shrinkage of the HCP (Domone & Illston, 2010).

Since a concrete member dries out from its surfaces, there is a strong link between the outside environment and the drying process. After setting, a slab-on-ground regularly develops a relatively stable moisture gradient over its section. The bottom will be colder and the relative humidity will here approach 100%. The top layers will approach the value of relative humidity of the indoor environment, which is often warmer and dryer. The moisture profile is non-linear and dependant on the permeability and moisture transportation properties of the concrete. This non-linearity will over time result in a non-linear drying shrinkage strain over the section, where the top will shrink to a larger extent than bottom, see Figure 3.7 below.



Figure 3.7 Distribution of RH and drying shrinkage strain in a slab section.

The actual ambient relative humidity of the environment also affects the final drying shrinkage. Drier environments with low relative humidity result in more shrinkage than more humid environments. There is a strong link between the relative humidity in the pore structure and the final shrinkage, and the ambient relative humidity is the driving factor determining the actual state in the pore structure (Fjällberg, 2002).

In order to reduce drying shrinkage it is important to avoid using a lower concrete strength class than necessary. As was described in Figure 3.2, the higher the strength class, the lower is the w/c ratio. Furthermore, there is also a proved relationship between the w/c ratio and drying shrinkage; this is illustrated in Figure 3.8 below. The higher the water content and w/c ratio, the more shrinkage will occur. As the figure shows, high cement content will also result in less shrinkage strain.

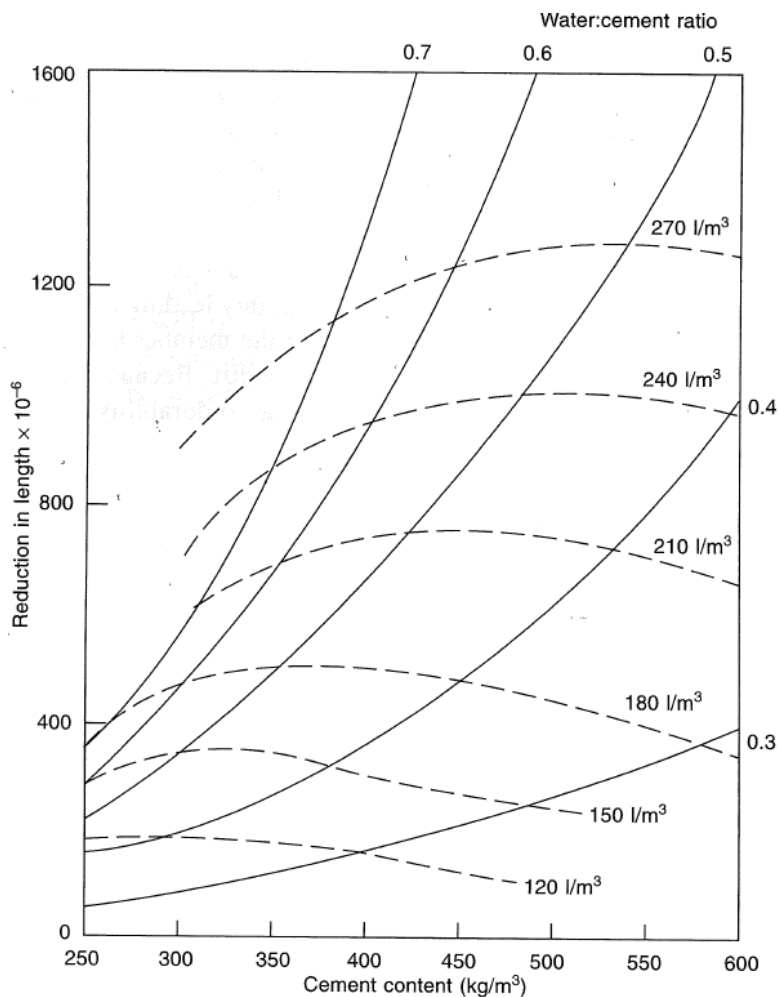


Figure 3.8 Relationship between drying shrinkage and concrete composition (Day & Clarke, 2003).

3.2.2 Chemical shrinkage

The volume change called chemical shrinkage occurs when the absolute volume of hydration products is less than the total volume of unhydrated cement and water before hydration starts. As the net volume will be less than before hydration starts, shrinkage will occur. This shrinkage is caused by chemical reactions taking place in the early age concrete in liquid phase, and due to this it does not result in any shrinkage strain. As the concrete sets and the cement paste hardens, the chemical reactions will instead tend to create new pores/voids and this is when autogenous shrinkage starts (Khairallah, 2009). The different stages are illustrated below in Figure 3.9. The proportions of various types of shrinkage in the figure are however only schematically illustrated.

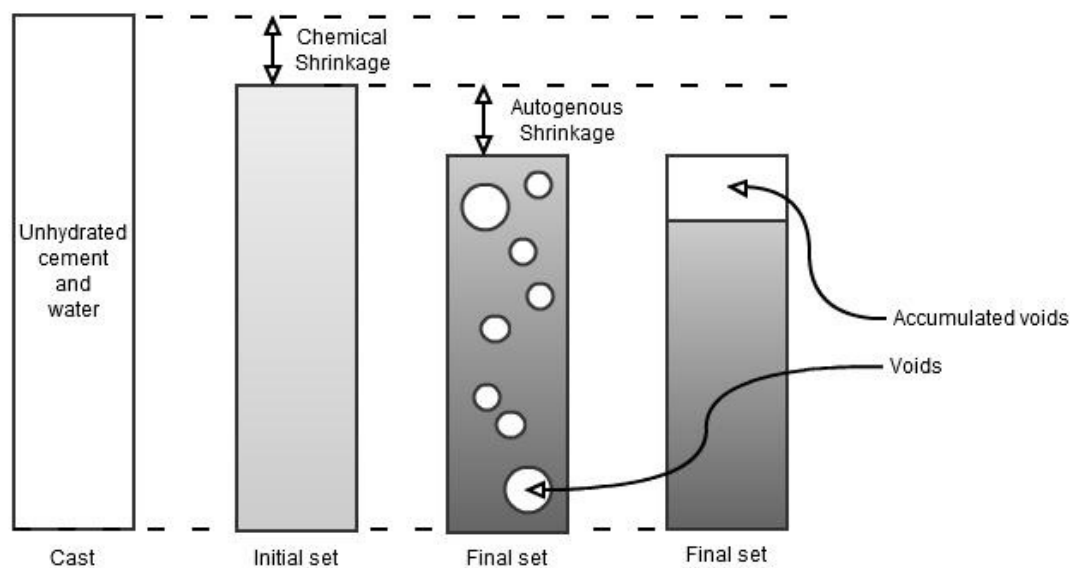


Figure 3.9 Illustration of shrinkage of HCP without ambient moisture exchange, modified from Portland Cement Association (n.d).

When the concrete sets the autogenous shrinkage starts, but it should be noted that there is no strict boundary between chemical and autogenous shrinkage and opinions of where this boundary should be drawn deviates (Fjällberg, 2002).

3.2.3 Autogenous shrinkage

When hydration of the concrete continues, under the condition that there is no moisture exchange with the outside environment, self-desiccation will lead to removal of water from the capillary pore structure. This will lead to a lowering of the relative humidity and cause the autogenous shrinkage. The general part of the autogenous shrinkage takes place during the first days after casting, when the hydration reactions have its highest rate (Domone & Illston, 2010). Attention to this type of shrinkage was drawn when usage of high strength normal density concrete became more regular. The significantly higher autogenous shrinkage in high strength concrete is due to its large cement content. The autogenous shrinkage is often one order less than for drying shrinkage and was not originally accounted for in EC (European Concrete Platform ASBL, 2008).

3.2.4 Plastic shrinkage

Plastic shrinkage is a short term response phenomena. This shrinkage effect takes place in the upper layer of the concrete specimen, close to the drying surface. The effect is mainly due to water evaporation from the surface but should be distinguished from drying shrinkage which is a long term effect (Day & Clarke, 2003).

The problems of plastic shrinkage will in general be most critical when constructing slabs, due to the large horizontal surfaces. The shallow cracks will usually form between 1 and 6 hours after casting, although they are often not noticed until the next day (Day & Clarke, 2003).

Directly after casting, the concrete is still in its liquid state and the water is free to move. During compaction the water will move upwards through the specimen, while heavier particles move downwards. This phenomenon is called bleeding. If there is a high rate of water evaporating from the surface, this might exceed the rate at which new water from bleeding is being transported to the surface. This causes the surface layer to dry out and meniscuses are formed between the larger particles just below the surface. The meniscus creates tensile stresses that can lead to cracking, if the stresses reach the tensile capacity of the fresh concrete, this is called plastic shrinkage cracking (Day & Clarke, 2003). The crack pattern from plastic shrinkage is a relatively fine crazing of evenly distributed cracks, see Figure 3.10 below.

During the concrete's fresh state the surface can also settle. Horizontal reinforcing bars can then prevent this movement locally and cause a crack to be formed along and above the bars. This is called plastic settlement and will result in straight cracks at even spacing over the bars, see Figure 3.10 below.

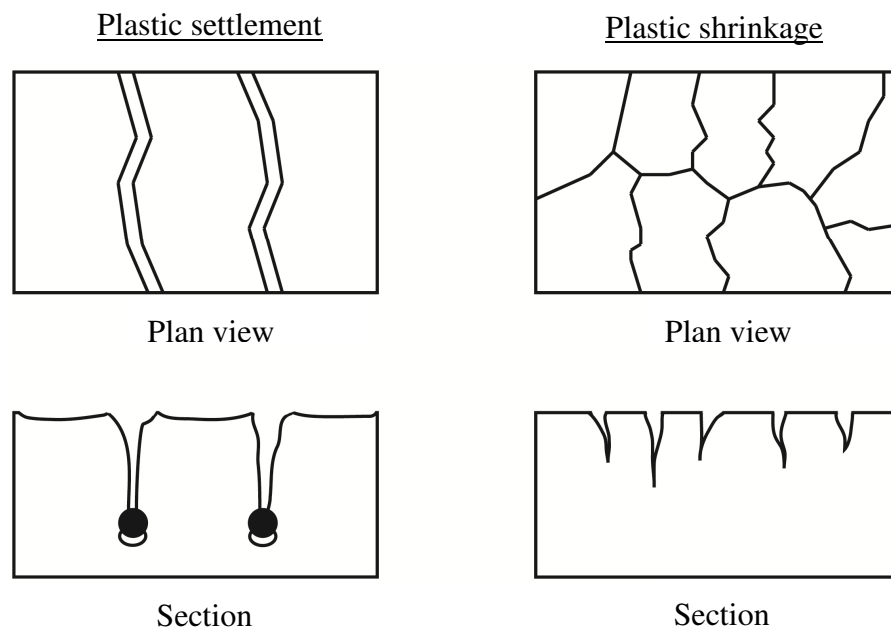


Figure 3.10 Schematic illustration of cracking due to tensile stresses caused by plastic settlement and plastic shrinkage, adapted from Domone & Illston (2010).

3.2.5 Carbonation shrinkage

Carbonation shrinkage is defined and distinguished from drying shrinkage and plastic shrinkage from that it is chemical in hardened concrete and is not a result from movement and/or loss of water. Carbon dioxide when combined with water as carbonic acid reacts with the hardened cement paste. The main reaction is between carbonic acid and calcium hydroxide. The reaction creates calcium carbonate and releases water, resulting in shrinkage. From this the cement paste increases in weight, gains strength and gets a lower permeability. Consequently the carbonation is highly dependent on the relative humidity in and around the concrete. If the pore system is fully saturated, the carbon dioxide cannot penetrate the surface of the concrete and no carbonation occurs. At the same time a completely dry pore system cannot develop any carbonic acid, which also results in a concrete without carbonation shrinkage (Domone & Illston, 2010). In Figure 3.11 the carbonation shrinkage strain is shown in relation to relative humidity.

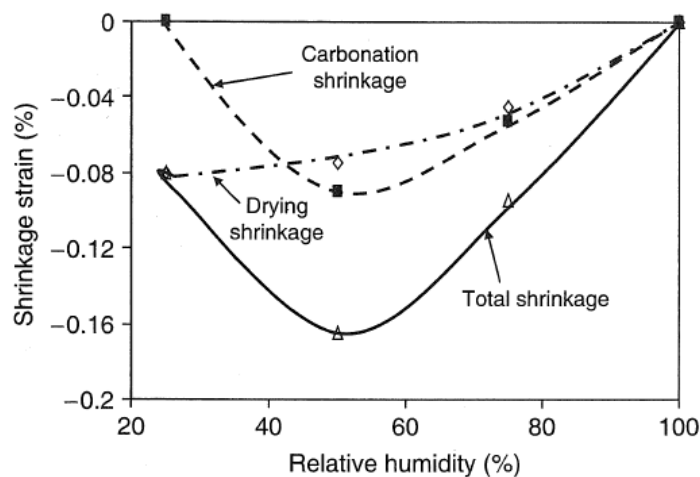


Figure 3.11 Effects of RH on shrinkage (Domone & Illston, 2010).

Carbonation shrinkage is mainly occurring in the concrete surface and is greatest at RH levels around 50%. The results are patterns of thin cracks, crazing, occurring after a long time (Fjällberg, 2002).

3.2.6 The effect of shrinkage reducing additives

The shrinkage effects in concrete can be controlled by several measures. One of them is to incorporate shrinkage reducers in the concrete mix. The shrinkage reducers are fabricated in several forms with the similarity that they are all composed of alcohol. The effect is visible both in short- and long-term perspectives. The main mechanism creating a reduction of shrinkage is explained by means of that the surface energy of the water in the pore system is lowered in presence of alcohol, ultimately lowering the internal stresses and therefore the shrinkage (Fjällberg, 2002).

The actual effect of the shrinkage reducers is highly dependent on the concrete mix, especially w/c ratio, water amount and type of cement. Some research indicates that the shrinkage after 28 days can be reduced by 50-80% and the final shrinkage by 25-50% (Fjällberg, 2002).

When incorporating shrinkage reducers and other additives, carefulness is necessary as other properties may gain unwanted effects. Problems have for example been reported when trying to trowel concrete floors with shrinkage reducing additives incorporated in the concrete mix, likely as a result of the lowered surface energy of the water.

3.3 Thermal behaviour of concrete

Concrete expands under heating and contracts during cooling like most other materials. The thermal coefficient varies during curing when the heat of hydration changes the temperature in the concrete. This must be regarded when analysing the contraction/expansion effects in early age and curing concrete.

In a long-term perspective the thermal coefficient will be more stable and thereby easier to define. Usually the thermal coefficient is considered for this long-term perspective, even when calculating thermal effects in a more short-term perspective, disregarding the precise behaviour during curing (Domone & Illston, 2010).

Furthermore, as concrete is a complex material, consisting of a composition of different materials, it will inherit properties from each part in the concrete mix (Domone & Illston, 2010). According to EC the thermal expansion coefficient of concrete can be taken as $\alpha_c = 10 \cdot 10^{-6} [K^{-1}]$ if no explicit data exists. However, in reality the coefficient depends on the mix composition and on the moisture conditions at the time when the thermal conditions change (Brooks, 2003).

3.4 Reinforcing steel

Steel is the most commonly used material for reinforcement of structural concrete. A general stress-strain relation for steel is shown in Figure 3.12. Normally the steel is regarded as linear until it reaches its yield capacity, where the material starts to behave non-linearly due to plastification.

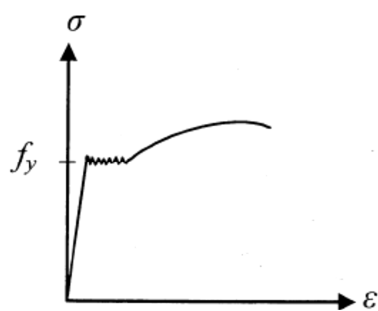


Figure 3.12 General stress strain relation for steel.

The fundamental reason for incorporating reinforcement in structural members is to compensate for the low tensile capacity of concrete. Another important and useful feature is that crack development can be controlled through an efficient incorporation of reinforcement (Engström, 2011).

Steel reinforcement can for example be ordinary reinforcement placed at even spacings, or in fibre form, distributed in the fresh concrete.

3.4.1 Ordinary reinforcement

Ordinary reinforcement can consist of either traditional bars or meshes. For a slab-on-ground the most common method is to use meshes. This is appropriate due to the large areas and the relative simplicity of the reinforcement layout.

A common problem when using meshes is when these need to be overlapped. If the meshes are simply positioned on top of one another, this will become very thick where several meshes meet and thereby the accuracy of the concrete cover is jeopardised, see Figure 3.13 below.

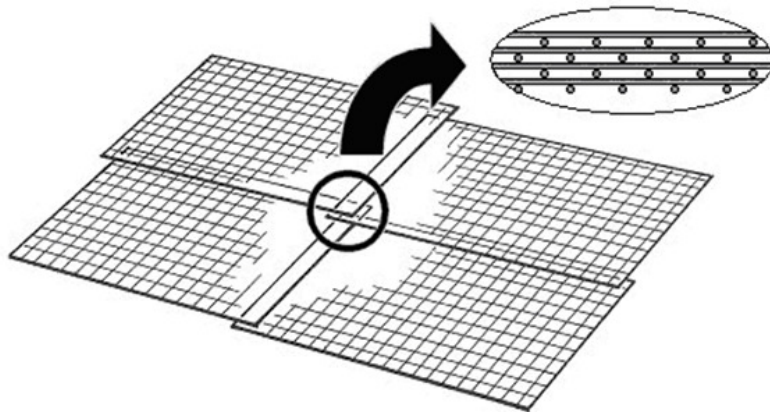


Figure 3.13 Problems with poorly detailed overlap of reinforcement mesh (Celsa Steel Service, n.d).

One solution of this problem is to use meshes with finger joints, see Figure 3.14 (Celsa Steel Service, n.d).

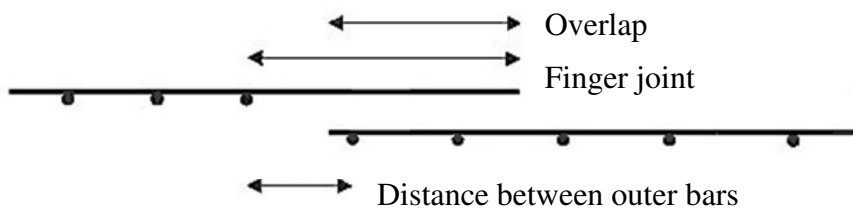


Figure 3.14 Finger joint of reinforcement mesh (Celsa Steel Service, n.d).

The surface of reinforcement bars can be smooth or intentionally deformed, where the latter has properties to improve the bond to the surrounding concrete. The mechanism and force transmission between concrete and steel can be thought of as bond stresses which are acting along the surface of the reinforcement bar (Engström, 2008). At small stress levels the interaction depends on adhesion, however as the stress levels increase, the adhesion breaks and the shear-key effect becomes the general factor. The surface unevenness of the reinforcement bar is the source to the shear-key effect, see Figure 3.15.

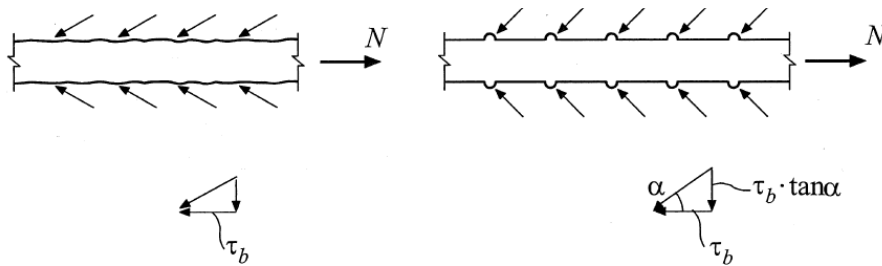


Figure 3.15 Contact forces due to shear-key effect between reinforcement bar and concrete (Engström, 2008).

3.4.2 Steel fibre reinforcement

An alternative, or complement, to using ordinary reinforcement is steel fibres. This construction method is in several countries already the dominating method. In Sweden approximately 50 % of newly built industrial floors are constructed using steel fibres and this is likely to increase further in the years to come (Swedish Concrete Association, 2008).

For industrial slabs-on-ground the size of steel fibres are normally in the range of 45-50 mm with a thickness of 1 mm. Figure 3.16 below illustrates an example of steel fibres. The steel fibres are produced using steel of higher tensile strength than ordinary reinforcement, approximately 1000 MPa compared with 500 MPa. The amount of fibres used in an industrial floor varies depending on loading conditions and type of fibres but an approximate value is 35-50 kg/m³ (Swedish Concrete Association, 2008).



Figure 3.16 Example of steel fibre (New Construction Group, n.d).

Several benefits of using SFRC are mentioned from manufacturers. BASF (n.d) for example emphasis the increase of tensile strength and also claim the fibres will have the ability to remove all crack tendencies. Furthermore, BASF (n.d) also mentions an increase in compressive strength, abrasion resistance and a more homogeneous material compared with ordinary reinforcement. However, even though an increased tensile strength is a documented effect of fibres, it should be noted that cracks are not fully prevented. The Swedish Concrete Association (2008) concludes that the fibres will prevent cracks to increase freely, but that cracks larger than 0.2 mm can still occur. In order for the steel fibres to successfully divide the cracks over the entire surface, amounts of 80 kg/m³ or more could be needed. Figure 3.17 below illustrates how the steel fibres can reduce the cracks width by transmitting tension across the crack.

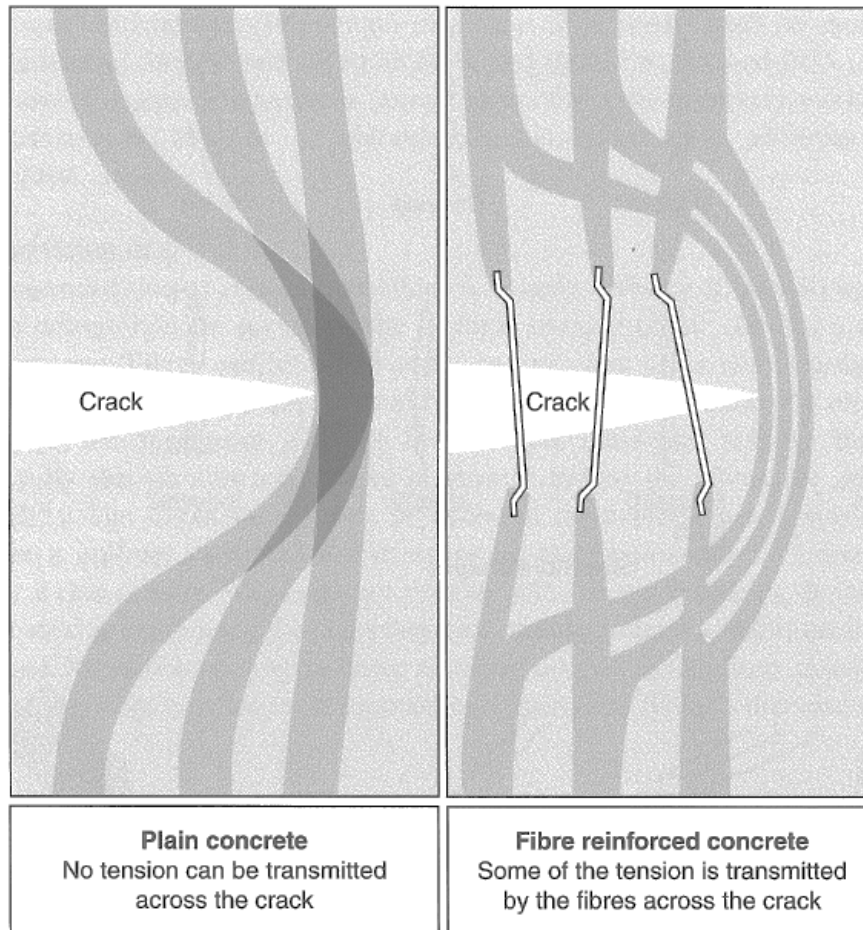


Figure 3.17 Illustration of how steel fibres transmit tension across a crack. Lines indicate stress paths (Knapton, 2003).

Problems with the surface finish of slabs cast with SFRC are known to occur. Fibres close to the surface can be dragged along the surface during surface treatment, resulting in small craters and round patterns with fibres sticking up (Swedish Concrete Association, 2008). Furthermore, SFRC is not considered in EC and this report therefore has its focus on ordinary reinforced concrete.

3.5 Cracking process

When a crack is formed in a specimen of ordinary concrete it starts and propagates from the transition zone between aggregate and hardened cement paste. The paste in the transition zone is more porous than the bulk paste and therefore makes this zone weaker, thus cracking starts and propagates along this zone. Figure 3.18 illustrates this behaviour. As the propagation continues and forms a continuous crack path through the entire concrete section, tensile stresses will be induced on the reinforcement.

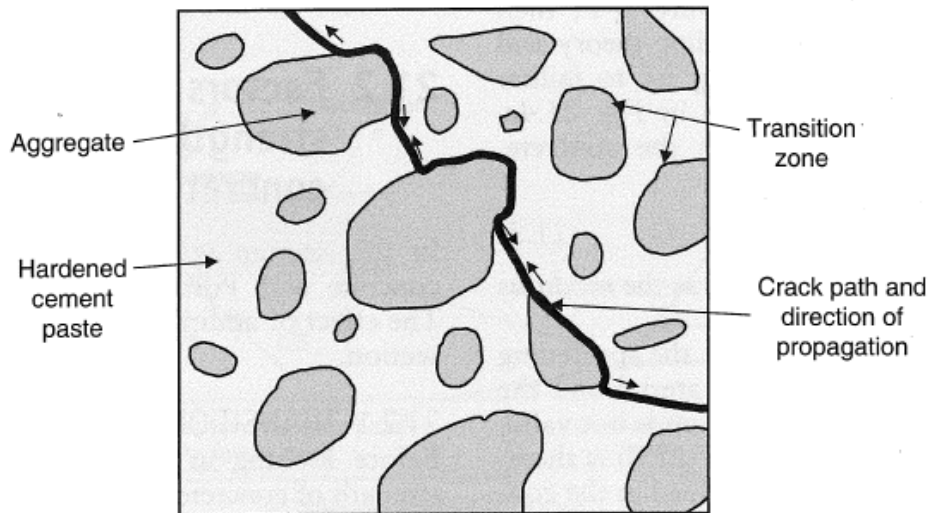


Figure 3.18 Crack initiation along the interface of aggregates (Domone & Illston, 2010).

Studying a cracking process in a more macroscopic view a specimen of reinforced concrete in tension is analysed. Figure 3.19 demonstrates the relationships. As the first crack is formed the concrete stress will be zero in this section. The tension stress in the concrete will grow within a certain distance s_0 from the crack until the tension stress no longer is affected by the discontinuity at the crack. A second crack can form anywhere outside the region $\pm s_0$ where the concrete section remains unaffected by the formed crack. As two or more cracks are formed a new crack can only form between two cracks if the distance between them is larger than $2 \cdot s_0$. A fully cracked specimen has crack spacings that vary between s_0 and $2 \cdot s_0$.

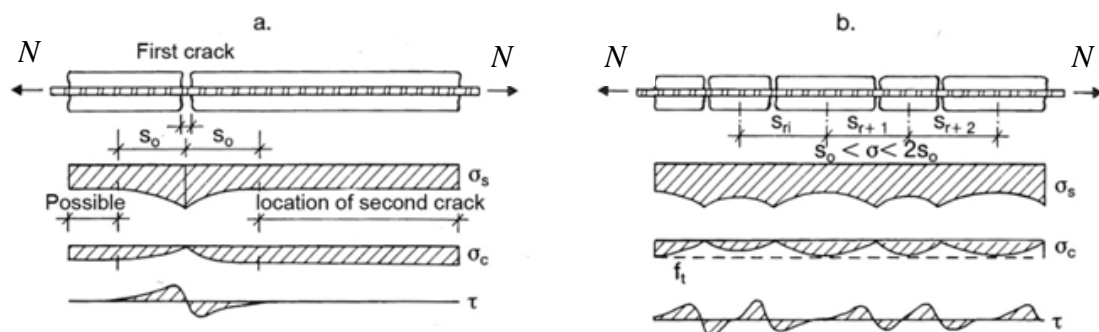


Figure 3.19 Mechanism for crack development of a reinforced concrete member, subjected to tension. At the section where the first crack is formed the steel carries all the stress. After the transmission length, s_0 , stress has been built up in the concrete. If this stress reaches the concrete tensile capacity, here f_t , a new crack can be formed. Figure a. illustrates the formation of the first crack and Figure b. illustrates when cracking is stabilised and the crack distances do not allow for the concrete stress to reach the tensile capacity between the cracks (Petersons, 1994).

The cracking process of a concrete specimen is often described in three stages: uncracked, crack formation and stabilised cracking. In Figure 3.19 a, the crack formation begins and in b the stabilised cracking is formed. Figure 3.20 illustrates the different stages for a concrete specimen when going from the uncracked stage to the stabilised cracking stage. In the state of stabilised cracking no new cracks occur, when the load increases, the crack width of already existing cracks increases.

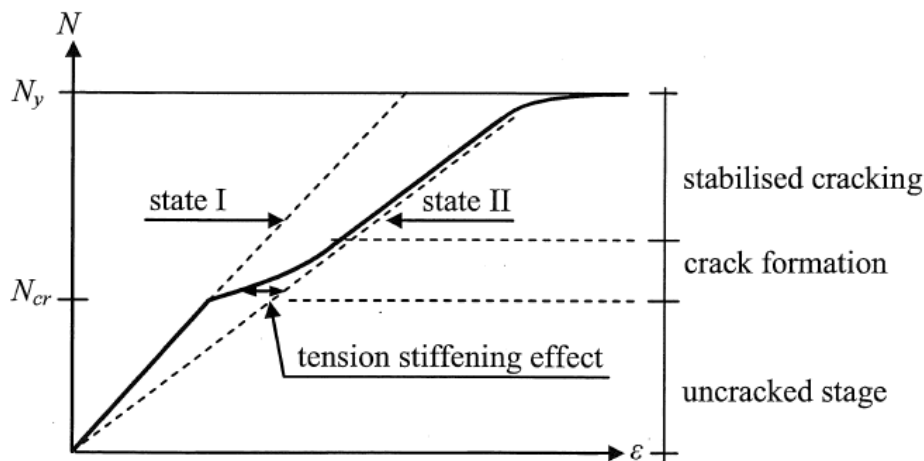


Figure 3.20 Response of a reinforced concrete specimen at three cracking stages.

The concrete specimen remains uncracked as long as the stresses do not reach the tensile strength, f_{ct} , in any section. As long as this capacity is not reached a sectional analysis can be carried out in state I. As the crack formation starts and propagates, the sectional analysis is carried out under the assumption that the section is in state II. There is a contribution to the global stiffness of the specimen from the uncracked concrete portions between formed cracks, which makes the actual stiffness higher than the one assumed in state II analysis. This phenomenon is called tension stiffening.

It is preferable to have a concrete member that, when subjected to load, forms several smaller cracks compared to a few wide cracks. In order to allow for the formation of more cracks it is important that an adequate amount and arrangement of steel reinforcement is used. A basic requirement is that the reinforcement amount should be large enough to ensure that the yield capacity of the steel is higher than the tensile capacity of the concrete section.

The first crack is formed for the cracking load, N_{cr} , defining the boundary between uncracked stage and the cracking stage. The cracking load is defined according to the following equations (Engström, 2011). The formulas are valid for the first formed crack, despite sectional geometries.

$$N_{cr} = f_{ctk} \cdot A_I \text{ [N]} \quad (\text{short term response}) \quad (3.1)$$

$$N_{cr} = f_{ctk,sus} \cdot A_{I,ef} \text{ [N]} \quad (\text{long term response}) \quad (3.2)$$

where f_{ctk} = tensile concrete strength [Pa]
 $f_{ctk,sus}$ = tensile concrete strength sustained loading [Pa]
 A_I = transformed concrete area in state I [m²]
 $A_{I,ef}$ = transformed concrete area in state I, with regard to concrete creep [m²]

Since the concrete strength decreases under sustained loading, the value for tensile capacity for sustained loading should be reduced to get a more reliable comparison. MC2010 presents a formulation to describe the concrete tensile strength under sustained loading according to Equation (3.3).

$$f_{ctk,sus} = \alpha \cdot f_{ctk} \text{ [Pa]} \quad (3.3)$$

where α = 0.6 for normal strength concrete [–]
= 0.7 for high strength concrete [–]

When the yield capacity of the steel is larger than the cracking load, a new crack can be formed before the steel in the initial crack yields. Following this reasoning, a minimum amount of reinforcement needed to create new cracks can be calculated. Section 4.3.2 explains how this method can be used according to EC in order to find minimum reinforcement.

In addition to allowing for the formation of cracks, as described above, it is also important to limit the widths of the cracks. This is done by defining a maximum allowable steel stress in the reinforcement, $\sigma_{s,all}$. EC has presented a simplified method, using tabulated values, which is further explained in Section 4.3.2.

3.6 Effects of cracking

The reason why cracks should be avoided in an industrial floor can be divided into three aspects; aesthetics, functionality and degradation of the slab. With respect to aesthetics, extensive cracking can be found ill-looking and can also give the impression of an un-safe and poorly constructed building. Considering functionality, cracks can be a problem for forklifts passing over the cracks repeatedly, further damaging the concrete surface next to the cracks and also causing an inconvenience for the forklift drivers. Further aspects concerning functionality, for example in factories or hospitals, can be with regard to cleaning. Often the gathering of chemical or microbiological waste in cracks must be avoided and cracks are therefore unwanted.

In addition to these problems, cracks can also lead to problems with degradation of the concrete. When steel reinforcement is embedded in concrete, it is effectively protected against corrosion. However, when a crack has been formed the steel can be

exposed to the outside environments and water can reach the steel, leading to corrosion. When the steel corrodes its volume increases considerably. The resulting expansion leads to tensile stresses in the concrete, further cracking the concrete, see Figure 3.21 (Domone & Illston, 2010).

For cracks in industrial floors where trucks travel between inside and outside environment there is also a risk of de-icing agents to penetrate existing cracks. These contain corrosion accelerating chlorides, which rapidly increases the corrosion process and for these situations it is highly important to limit crack widths considerably.

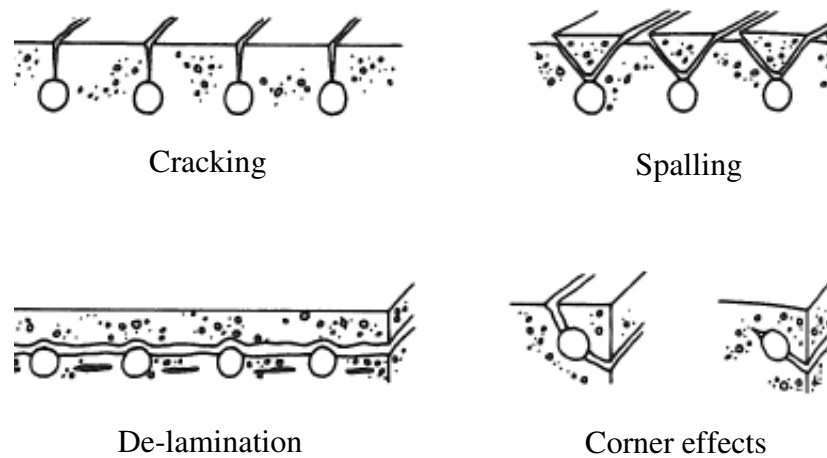


Figure 3.21 Possible damages caused by corrosion of steel reinforcement (Domone & Illston, 2010).

4 Design methods

This chapter considers how the design of a slab-on-ground can be approached with regard to shrinkage cracking. The levels at which the design is considered can be divided according to Figure 4.1. The concept design is at the most macroscopic level and the material design is at microscopic level. The concepts, design components and detailing are covered in Chapter 2.

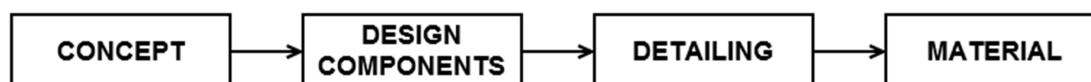


Figure 4.1 Design levels.

All of the incorporated features for the floor must follow the demands that the situation yields, see Chapter 2. As well as following the regulations, the designer must also follow the demands and expectations from the client regarding how the floor should perform.

The governing regulation in Sweden, EC, has a classification system to ensure a durable construction. The system defines 6 groups of exposure classes based on degradation mechanisms. The environmental conditions for each part of a structure determine which exposure classes that should be used in order to result in a durable structure. The exposure classes chosen to govern the design are then used to specify critical details such as nominal cover thickness and limits for calculated crack widths, w_{max} . The specified values of w_{max} are presented in Table 4.1 below.

Table 4.1 Specified values of w_{max} [mm], modified from EC2. Note that the table values are not valid in Sweden according to the national annex.

Exposure class	Reinforced members and prestressed members with unbonded tendons
	Quasi-permanent load combination
X0, XC1	0.4 ¹
XC2, XC3, XC4	0.3
XD1, XD2, XS1, XS2, XS3	
Note 1: For X0, XC1 exposure classes, crack width has no influence on durability and this limit is set to guarantee acceptable appearance. In the absence of appearance conditions this limit may be relaxed.	

During the design process of a slab-on-ground the concrete strength class must be chosen. This is in general chosen dependent on required strength. However, Section

4.1 outlines why resistance is non-critical for an industrial floor and why focus instead should be on performance.

Section 4.2 evaluates a set of known calculation method that on a macroscopic level focus on member geometries and reinforcement amounts. Since EC2 does not provide adequate information for this purpose other methods have also been conducted. The methods are described and evaluated in order to make a result comparison.

4.1 Choosing concrete class

When choosing type of concrete for a structural member, focus is often on strength in order to achieve an adequate load bearing capacity. However, for a slab-on-ground the load capacity is often not critical and it is important that focus shifts from resistance to performance. When designing against shrinkage cracks, it is important to choose a concrete that results in less shrinkage and whose strength is in proportion to the chosen amount of reinforcement (Swedish Concrete Association, 2008).

The choice of w/c ratio has several aspects that affect each other. As previously shown in Figure 3.2, there is a strong link between w/c ratio and compressive strength; the lower the w/c ratio of the concrete, the higher the compressive strength. As a result, when a low w/c ratio is chosen, more reinforcement will be needed to compensate for the increased tensile strength of the concrete to prevent single large cracks. In addition to this, high strength concrete is also more expensive.

However, a reduced w/c ratio can also be beneficial, since a lower amount of water in the HCP leads to a reduced drying shrinkage. In addition to this a low w/c ratio leads to an increased abrasive resistance, which is important for industrial floors. A low w/c ratio also leads to a concrete with increased density which is beneficial regarding durability. However, on the other hand, a lowering of w/c ratio also leads to a fast hardening and a more brittle concrete, which is why very low numbers of w/c ratio should be avoided.

Determining the best suited w/c ratio is therefore not obvious and depends on each project's specific demands. The Swedish Concrete Association (2008) recommends that a w/c ratio of approximately 0.55 is chosen for industrial floors. This would result in a concrete strength class of C30/37 and would result in an abrasive resistance adequate for most industrial floors. The abrasive resistance is of high importance, since this, to a great extent, determines the service life of a floor. If a higher abrasive resistance is required, they recommend that this is reached through surface treatment instead of reducing the w/c ratio. They further claim that research has shown that a w/c ratio of 0.55 is optimal with regard to reducing plastic shrinkage cracking.

4.2 Prediction of shrinkage strain

In literature there are several methods that deal with predicting the shrinkage strain of concrete. This section describes the procedure according to EC.

The calculation of shrinkage strain according to EC is limited to only consider autogenous and drying shrinkage. These are added in order to find the variation of the total shrinkage strain over time according to Equation (4.1).

Total shrinkage strain

$$\varepsilon_{cs}(t) = \varepsilon_{ca}(t) + \varepsilon_{cd}(t) [-] \quad (4.1)$$

where

autogenous shrinkage strain

$$\varepsilon_{ca}(t) = \beta_{as}(t) \cdot \varepsilon_{ca}(\infty) [-] \quad (4.2)$$

where $\beta_{as}(t)$ = time function [-]

$\varepsilon_{ca}(\infty)$ = autogenous shrinkage, final value [-]

drying shrinkage strain

$$\varepsilon_{cd}(t) = \beta_{ds}(t) \cdot k_h \cdot \varepsilon_{cd,0} [-] \quad (4.3)$$

where $\beta_{ds}(t)$ = time function [-]

k_h = shape coefficient [-]

$\varepsilon_{cd,0}$ = nominal drying shrinkage strain,
final value [-]

In order to illustrate how shrinkage strain varies over time according to EC2, an example for a slab-on-ground was calculated. The following assumptions were made: cement class N, ambient relative humidity 40%, slab thickness 250 mm and curing during seven days. It should be noted that the notional size is calculated based on one-sided drying as a slab-on-ground only is allowed to dry out from its upper surface.

Figure 4.2 illustrates how the final shrinkage strain varies depending on concrete strength class. As can be seen, the final shrinkage is lowered when a higher concrete strength is used, mainly due to a lower amount of water. Furthermore, it can also be seen that for normal strength concrete the autogenous shrinkage is much less than the drying shrinkage. However, in accordance with what was stated in Section 3.2.3, for high strength concrete the autogenous shrinkage constitutes a much larger proportion of the total shrinkage. This phenomena is a result of the large cement content in high strength concrete.

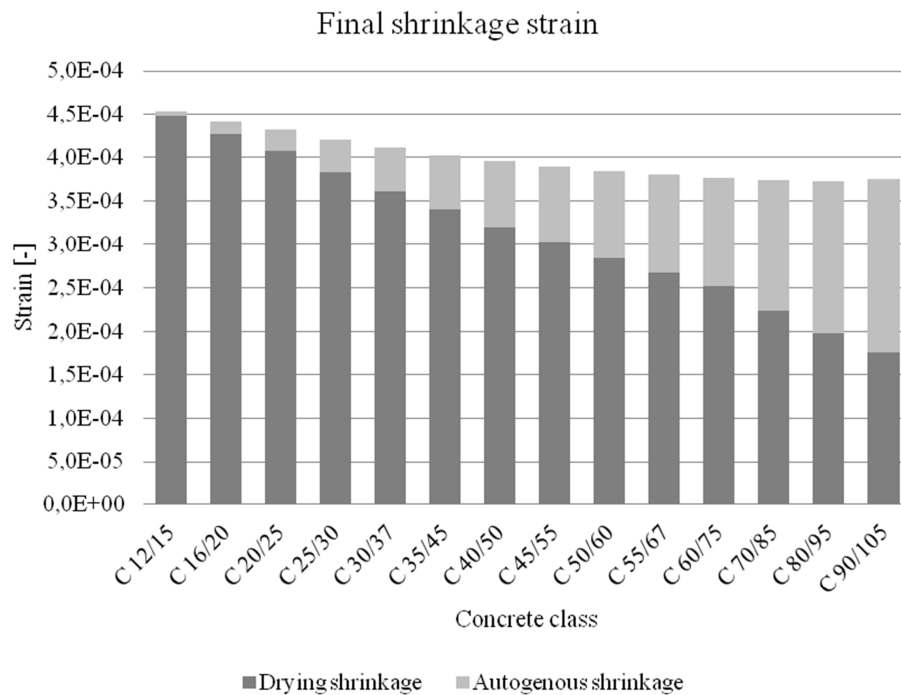


Figure 4.2 Final shrinkage strain for different concrete strength classes according to EC2. The calculation is carried out for a specimen of 250mm thickness and cement class N. The member is exposed to an ambient RH of 40 % after 7 days curing and the drying is regarded as one sided.

In order to illustrate how the shrinkage process develops over time, the shrinkage at a given time was compared to the final shrinkage as shown in Figure 4.3. In accordance with the recommendation for slabs-on-ground given by the Swedish Concrete Association (2008) explained in Section 4.1, the concrete strength class was chosen as C30/37. As can be seen in the figure, the total shrinkage converges over time. Using a too short time perspective therefore risks future cracks to occur during the building's service life.

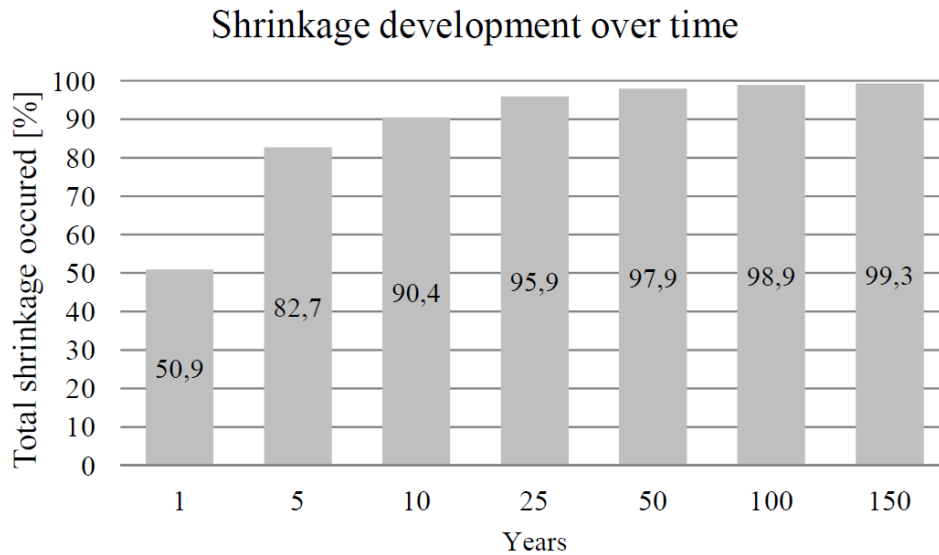


Figure 4.3 Shrinkage development over time according to EC for a 250 mm thick concrete member of C30/37 using cement class N. The member is exposed to an ambient RH of 40 % after 7 days curing. Each bar illustrates the percentage of total strain that has occurred at the given time.

Since a building is usually designed for a service life of 50 years and since approximately 98 percent of the total shrinkage has occurred at this time, this is deemed to be an appropriate time perspective to apply in the design of a slab-on-ground. Calculating total shrinkage after 50 years for the described example the following result was found.

$$\varepsilon_{cs,50years} = 4.025 \cdot 10^{-4} [-] \quad (4.4)$$

To further illustrate the shrinkage development during the first 50 years, autogenous, drying and total shrinkage was plotted over time in Figure 4.4.

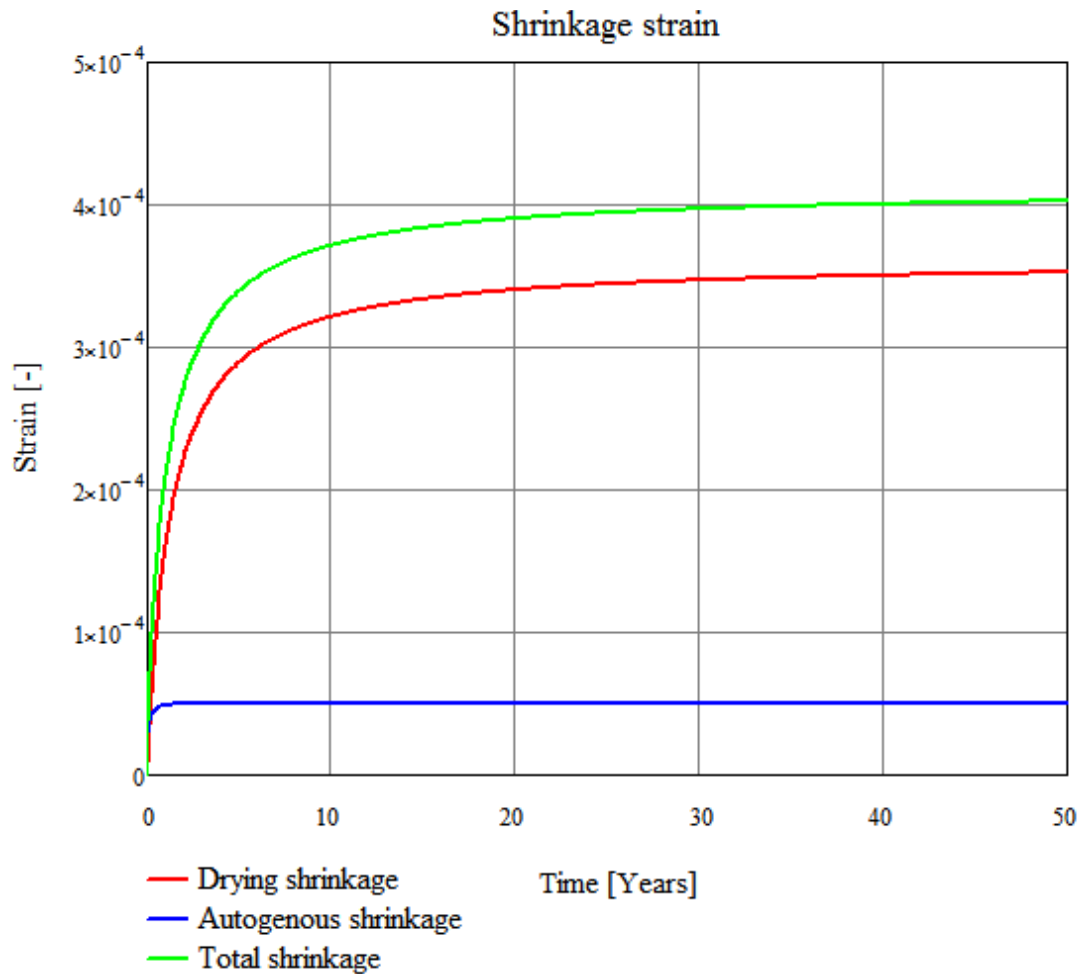


Figure 4.4 Variation of shrinkage strain over 50 years according to EC for a 250mm thick concrete member of C30/37 using cement class N. The member is exposed to an ambient RH of 40 % after 7 days curing.

4.3 Design with regard to restraint cracking

In order to evaluate the following calculation methods several input parameters were assumed. For many of the methods a concrete class was needed. Based on the motivation given in Section 4.1, when a concrete strength class was needed to be determined, the concrete strength class C30/37, which corresponds to a w/c ratio of 0.55, was used. This concrete class has been deemed to be an appropriate choice for most industrial floors. Other assumptions are explained for each method in the respective sections.

4.3.1 Joint spacing according to Petersons (1992)

Since restraint cracking due to concrete shrinkage is highly dependent on the member length, designing the spacing of joints in slabs-on-ground is important in order to reduce the normal force that may result in shrinkage cracks. The normal force is a result of the shrinkage strain and frictional resistance and the normal force increases for increased slab lengths. As a result, the length of the slab, i.e. the joint spacing, needs to be taken into account in the design.

The following section considers how to determine the needed joint spacing, based on the methodology described by Petersons (1992). The method only takes friction against the sub-base into account and does not consider other external restraints. Equation (4.6) below describes how the normal force is expressed according to the method, assuming full friction to have been developed. Also see Figure 2.11, which illustrates the variables used in the model.

$$N = \mu \cdot q \cdot \frac{L}{2} \text{ [N/m]} \quad (4.5)$$

where μ = coefficient of friction [–]
 q = uniformly distributed load [N/m²]
 L = joint spacing [m]

As long as the normal force is lower than the concrete tensile resistance, the slab will remain uncracked. This can be expressed in the following way:

$$N \leq h \cdot f_{ctk} \text{ [N/m]} \quad (4.6)$$

where h = slab thickness [m]
 f_{ctk} = characteristic tensile strength [Pa]

Rearranging the equations above, the following equation can be found for the maximum joint spacing. As can be seen, increasing μ or q will decrease the joint spacing, while increasing h or f_{ctk} will increase the joint spacing.

$$L \leq 2 \cdot \frac{h \cdot f_{ctk}}{\mu \cdot q} \text{ [m]} \quad (4.7)$$

Studying this equation for a slab of 250 mm thickness and concrete strength class C30/37, carrying its own self weight and an additional load of 15 kN/m², the relation shown in Figure 4.5 below, between μ and L , can be found. For the concrete tensile strength the lower characteristic value, $f_{ctk0.05}$, was used which results in a conservative value for the maximum allowed joint spacing.

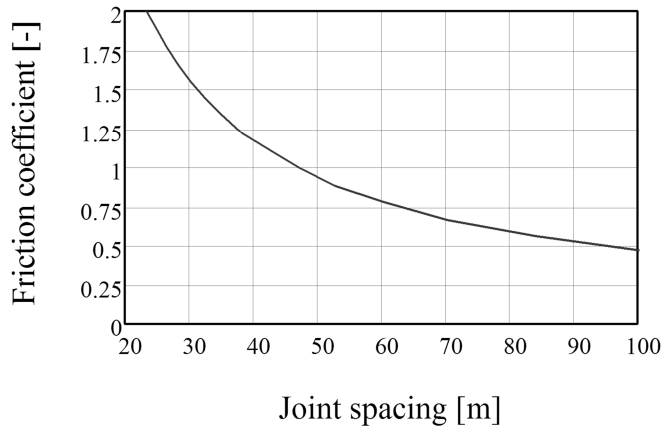


Figure 4.5 Maximum allowed joint spacing in relation to coefficient of friction for a 250 mm thick square slab of concrete strength class C30/37, based on Petersons (1992).

As the figure illustrates, the friction is considered to have a negative effect according to this model. The larger the friction, the smaller joint spacing is allowed. However, this model only considers the effect of friction before cracking occurs. It illustrates that before the member has cracked, a low friction is beneficial, since this prevents the first crack to be formed.

However, most concrete members do crack and after cracking has occurred, the friction can be seen as positive since it helps the distribution of cracks, preventing few, large cracks to be created. As a result, the model studied above is only valid if cracking can be totally prevented. This can be achieved if small joint spacing is adopted and a low friction is achieved. In addition to this, there must not be any other external restraints, e.g. perimeter strips or piles, that induce restraint cracking in the slab. Another parameter that contains uncertainties is the load. In the model the load is described as uniformly distributed but in storage and workshop areas the design load case will often include concentrated loads, creating differences in the frictional force over the area of the slab. The frictional force is the force per unit length along the interface between concrete and sub-base.

4.3.2 Minimum reinforcement according to EC2 7.3.2-7.3.3

The calculation of minimum reinforcement according to EC2 7.3.2-7.3.3 is based upon Equation (4.8) below. The minimum reinforcement area is with an allowed steel stress balanced against the effective tensile capacity of the concrete section.

$$A_{s,min} \cdot \sigma_s = k_c \cdot k \cdot f_{ct,eff} \cdot A_{ct} \text{ [N]} \quad (4.8)$$

where $A_{s,min}$ = minimum reinforcement area [m²]
 σ_s = allowable steel stress [Pa]
 k_c = coefficient that regards stress distribution [–]
 k = coefficient that compensates for eigenstresses [–]
 $f_{ct,eff}$ = concrete effective tensile strength (mean value) at the actual age when cracking is expected [Pa]
 A_{ct} = concrete area within tensile zone before cracking [m²]

The crack width is stated in EC2 to probably not be unacceptable if Equation (4.8) is used in combination with EC2 table 7.2N which limits the reinforcement bar diameter, see Table 4.2. However if crack widths exceeding the limits presented in Table 4.2 can be allowed, the allowable steel stress can be chosen disregarding the table.

Table 4.2 Maximum bar diameter for crack control according to Table 7.2N in EC2.

Steel stress [MPa]	Maximum bar size [mm]		
	w _k =0.4mm	w _k =0.3mm	w _k =0.2mm
160	40	32	25
200	32	25	16
240	20	16	12
280	16	12	8
320	12	10	6
360	10	8	5
400	8	6	4
450	6	5	

After calculating the required minimum reinforcement, the bar diameter should be modified according to Equation (4.9), which further limits the maximum allowable bar diameter. Equation (4.9), is valid if the member is subjected to tension created by centric normal force.

$$\phi_s = \phi_s^* \cdot \left(\frac{f_{ct,eff}}{2.9} \right) \cdot h_{cr} / (8 \cdot (h - d)) \text{ [mm]} \quad (4.9)$$

where ϕ_s = modified largest bar diameter [mm]
 ϕ_s^* = bar diameter according to EC2 table 7.2N [mm]
 $f_{ct,eff}$ = concrete effective tensile strength [MPa]
 h = cross – sectional height [m]
 h_{cr} = height of tensile zone just before cracking [m]
 d = effective height of outer reinforcement layer [m]

Figure 4.6 illustrates the required reinforcement ratio for a chosen bar diameter and characteristic crack width.

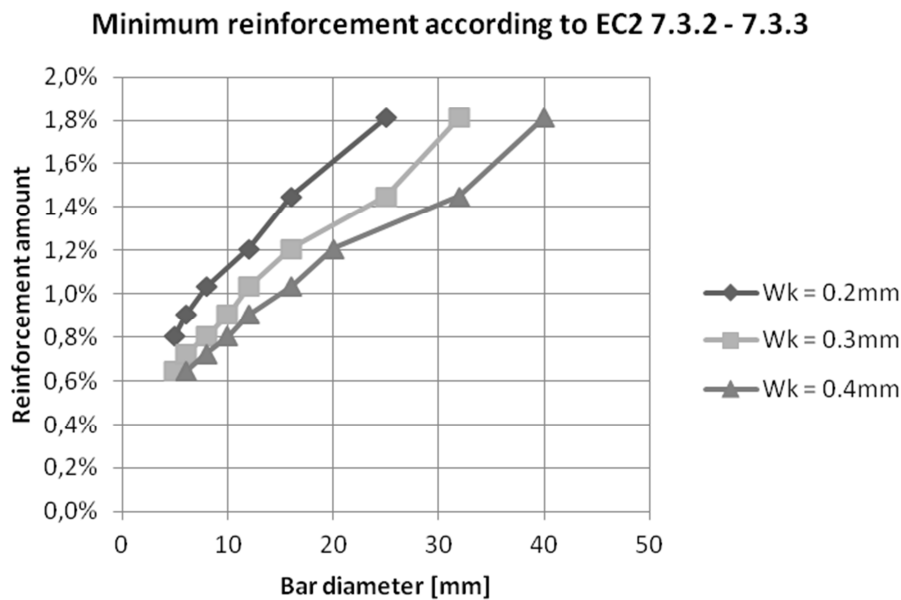


Figure 4.6 Minimum reinforcement according to EC2 7.3.2 – 7.3.3. The concrete class is C30/37 and the floor cross section is assumed to be reinforced in top and bottom. The notional size is calculated based on one sided drying of the slab.

4.3.3 Minimum reinforcement according to BBK04

In accordance with the formulation in EC2 for minimum reinforcement, see Section 4.3.2, the BBK04 formulation balances the force in the steel with the force of the concrete section, see Equation (4.10) below.

$$A_s \cdot \sigma_s \geq 1.5 \cdot f_{ctk} \cdot A_{ef} \text{ [N]} \quad (4.10)$$

where A_s = minimum reinforcement area [m²]
 σ_s = allowable steel stress [Pa]
 f_{ctk} = characteristic tensile strength
according to BBK04 [Pa]
 A_{ef} = concrete area within effective tensile zone
after cracking according to definition in
BBK04 [m²]

Equation (4.10) differs from Equation (4.8) that is used according to EC2. The concrete strength and concrete area are defined differently in the two regulations. There is also a deviation regarding which steel stress that is allowed. BBK04 allows for the minimum value of 420 MPa or f_{yk} , independently of bar diameter. Another factor separating the procedures is the reduction factor for calculated steel area, 0.7, which BBK04 allows for if the friction coefficient between the slab and the sub-base can be proven larger or equal to 1.0. However this factor does not apply for pile supported slabs-on-ground. Calculating the minimum reinforcement amount for a slab-on-ground with the same geometries and concrete strength class will result in less minimum reinforcement according to BBK04 than according to EC2 (Swedish Concrete Association, 2008), also see Figure 5.34.

4.3.4 Minimum reinforcement according to DS 411

As shown in Figure 4.6, there is a direct link between reinforcement amount and crack width. According to the Swedish Concrete Association (2008), the Danish concrete design code, DS 411, contains a simplified expression for this relationship. Even if this method cannot be used in a design situation in Sweden, it could however be interesting to investigate and use as a reference. The method consists of one simple formula to describe the minimum reinforcement amount as a function of the crack width, described in Equation (4.11).

$$\rho_{min} = \sqrt{\frac{\phi \cdot f_{tef}}{4 \cdot E_s \cdot w_k}} [-] \quad (4.11)$$

where $\rho = \frac{A_s}{A_c} [-]$

ϕ = bar diameter [m]

f_{tef} = effective tensile capacity $\approx 0.5 \cdot f_{ctm}$ [Pa]

E_s = steel modulus of elasticity [Pa]

w_k = characteristic crack width [m]

Evaluating this equation for a concrete of strength class C30/37, the relationship according to Figure 4.7 below can be derived. As can be seen, a smaller bar diameter is considered favourable. This is due to the fact that the relation between surface area and cross-sectional area of the reinforcement bars is larger for small bars. As a result, smaller bars have a relatively larger bond compared with larger bars.

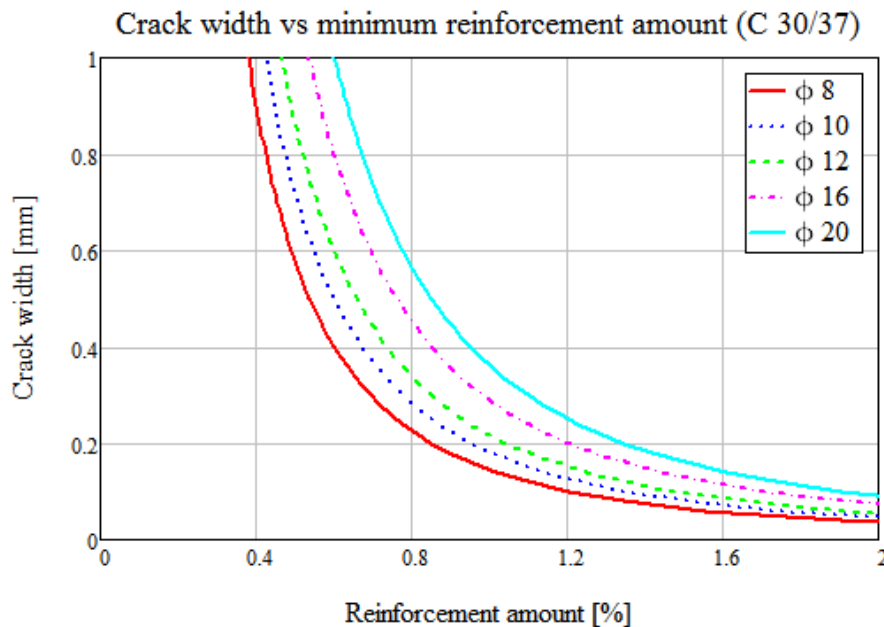


Figure 4.7 Minimum reinforcement for concrete class C30/37, based on DS 411.

4.3.5 Minimum reinforcement according to ACI

The American Concrete Institute, ACI, has presented a model to determine minimum reinforcement using what they call the "subgrade drag equation". This equation is frequently used in USA to determine the amount of non pre-stressed reinforcement to serve as crack controlling reinforcement. The required steel are is formulated according to Equation (4.12) (American Concrete Institute, 1992). The formula is very similar to the formulation by Petersons (1992) described in Section 4.3.1.

$$A_s = \mu \cdot \frac{L}{2 \cdot f_s} \cdot g \quad [\text{m}^2] \quad (4.12)$$

where

- μ = coefficient of friction [-]
- g = dead weight of the slab
[N/m² per unit thickness]
- L = distance between joints [m]
- A_s = steel area [m² per unit thickness]
- f_s = allowable steel stress [Pa]

However, a recommendation from Wire Reinforcement Institute (2003) suggests the use of Figure 4.8 to determine the maximum joint spacing relative to slab thickness. These values are then used as inputs when determining minimum reinforcement area according to the “subgrade drag equation”.



Figure 4.8 Suggested range of maximum spacing to be used together with the subgrade drag equation (Wire Reinforcement Institute, Inc., 2003).

Comparing this calculation method with the procedure described in Section 4.3.2, the minimum reinforcement amount will be less when adopting the “subgrade drag equation” combined with the recommendation in Figure 4.8.

4.3.6 Crack risk evaluation according to Engström (2011)

A method on how to estimate the tensile stress in a reinforced concrete member subjected to uniform shrinkage in the uncracked state has been presented by Engström (2011). The method utilises a concept where an equivalent shrinkage restraint force is calculated based upon the shrinkage strain. The shrinkage restraint force is then used in a compatibility condition for the specific case and the normal force for the section can be solved.

The shrinkage restraint force is calculated according to Equation (4.13) below and is illustrated in Figure 4.9. The concrete and reinforcement are regarded independently and the concrete is allowed to shrink freely. To compress the steel to the same length as the concrete the shrinkage force is applied to the steel. As the dimensions of the separated materials are now equal, they can be combined into a composite member. However, the steel has a need of elongating to its original length, which is partly prevented by the concrete, resulting in a composite member length, which is shorter than the original length. The behaviour of the composite section is the same as when applying a tensile force of the same magnitude as F_{cs} on it.

$$F_{CS} = E_s \cdot \varepsilon_{cs} \cdot A_s \text{ [N]} \quad (4.13)$$

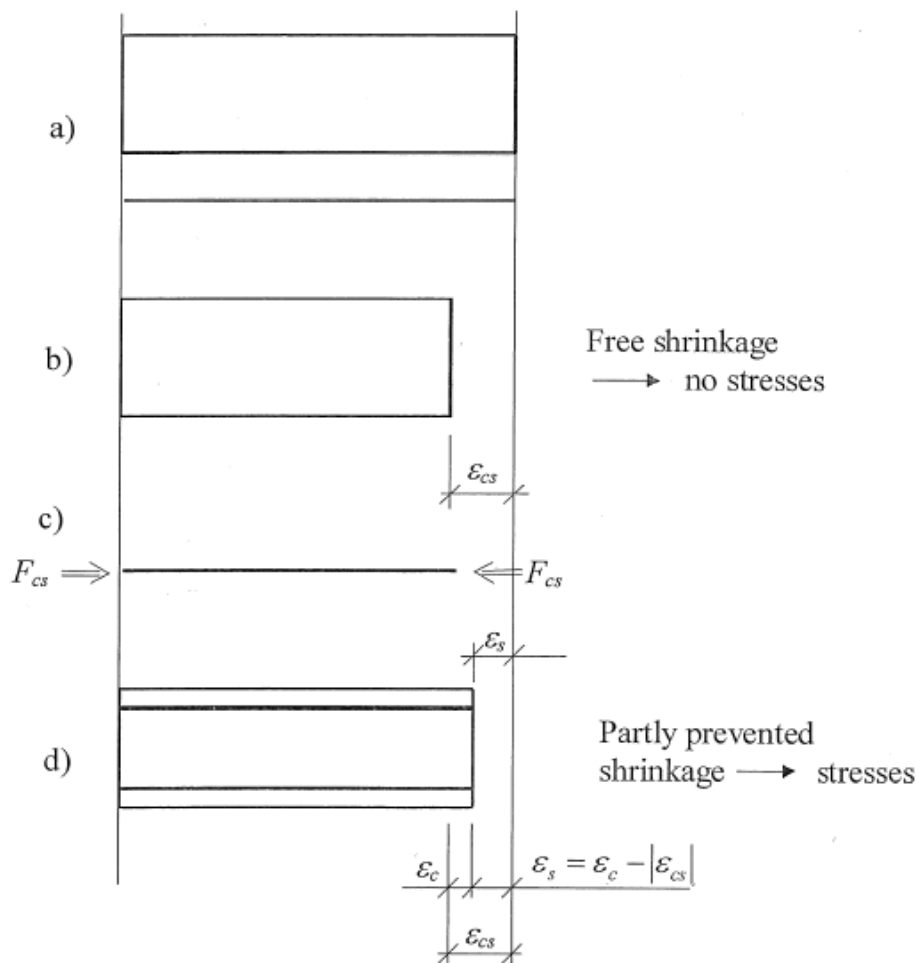


Figure 4.9 Member of reinforced concrete with symmetrically arranged reinforcement subjected to uniform shrinkage (Engström, 2011).

If a structural member according to Figure 4.10 is evaluated for risk of cracking the compatibility condition can be formulated according to Equation (4.14).

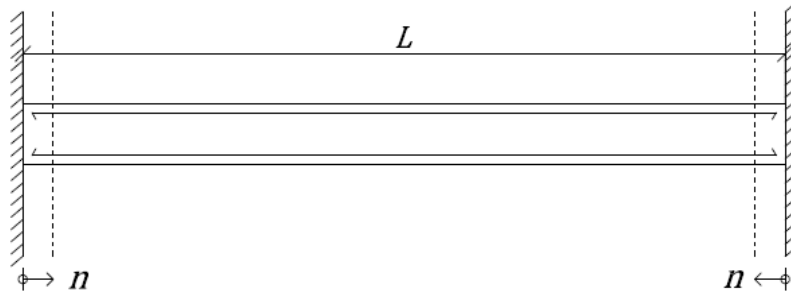


Figure 4.10 Member of reinforced concrete with partial restraints subjected to shrinkage.

$$\varepsilon_{cs} \cdot L + \varepsilon_c \cdot L + 2 \cdot n = 0 \text{ [mm]} \quad (4.14)$$

where ε_{cs} = shrinkage strain (negative) [-]
 ε_c = concrete stress dependent strain [-]
 n = end displacement [mm]
 L = member length [mm]

The formulation in Equation (4.14) can be rewritten and rearranged to solve the normal force over the section. The rewritten formulation is shown in equation (4.15) and the corresponding concrete stress is shown in equation (4.16).

$$\varepsilon_{cs} \cdot L + \frac{F_{cs} + N}{E_{c,ef} \cdot A_{I,ef}} \cdot L + 2 \cdot n = 0 \text{ [mm]} \quad (4.15)$$

where N = normal force [N]
 $E_{c,ef}$ = effective modulus of elasticity [Pa]
 $A_{I,ef}$ = effective cross – sectional area in state I [m²]

$$\sigma_c = \frac{F_{cs} + N}{A_{I,ef}} \text{ [Pa]} \quad (4.16)$$

If the calculated stress reaches the tensile strength of the considered concrete strength class, see Equation (4.17), cracking will occur. When studying long term effects it is recommended to use the concrete tensile strength under sustained loading, see Equation (3.3).

$$\sigma_c \leq f_{ctk,sus} \text{ [Pa]} \quad (4.17)$$

4.3.7 Crack evaluation according to Engström (2011)

As mentioned previously, there is no method in EC that directly takes external restraints into account, when designing against shrinkage cracks. Engström (2011) has however presented a model that considers external edge restraints. Once it has been determined according to Section (4.3.7) that the concrete member will crack, the following approach can be used to determine the number of cracks and crack widths.

In order to express the steel stress in a single crack as a function of the mean crack width, the following non-linear equation is used.

$$w_m(\sigma_s) = 0.420 \left(\frac{\phi \cdot \sigma_s^2}{0.22 \cdot f_{cm} \cdot E_s \cdot \left(1 + \frac{E_s}{E_c} \cdot \frac{A_s}{A_{ef}} \right)} \right)^{0.826} + \frac{\sigma_s}{E_s} 4 \cdot \phi \text{ [mm]} \quad (4.18)$$

where σ_s = steel stress in the cracked section [Pa]

Considering a member with partial edge restraints, the following deformations must be compatible.

- Elastic elongation of reinforced concrete
- Sum of crack widths
- Shrinkage of concrete
- End displacements

The deformation condition can be described using equations according to Equation (4.19) below (Engström, 2011).

$$\frac{\sigma_s \cdot A_s}{E_{c,ef} \cdot A_{I,ef}} \cdot L + n_{cr} \cdot w_{m,sus}(\sigma_s) + L \cdot \varepsilon_{cs} + 2 \cdot n = 0 \text{ [mm]} \quad (4.19)$$

where n_{cr} = number of cracks [–]

n = end displacements [mm]

ε_{cs} = shrinkage strain according to EC2 (negative) [–]

Combing equation (4.18) and (4.19) the only unknowns are the steel stress and the number of cracks. By iterating the number of cracks, the equation can be solved. Initially one crack is assumed, $n_{cr} = 1$, and the steel stress is determined for this case. Once this is known the corresponding steel force is determined using Equation (4.20). This steel force results in an equal normal force on the reinforced concrete that needs to be compared with the tensile force needed to form a new crack within the effective concrete area, see Equation (4.21) (Engström, 2011).

$$N_s = A_s \cdot \sigma_s \text{ [N]} \quad (4.20)$$

$$N_{cr,red} = f_{ctm} \cdot (A_{ef} + (\alpha - 1) \cdot A_s) \text{ [Pa]} \quad (4.21)$$

where A_{ef} = effective cross – sectional area calculated for a thin member

If $N_s > N_{cr,red}$ a new crack can be formed and a second iteration, stepping up the number of cracks to $n_{cr} = 2$, is required. This procedure then continues until $N_s < N_{cr,red}$ and the cracking process is finished. Once this is determined the resulting mean crack width can be calculated inserting the steel stress from the last iteration into Equation (4.18).

In order to evaluate this crack width it needs to be compared to the maximum allowable mean crack width, $w_{m,all}$. This can be found from the chosen limit value of the characteristic crack width, w_{lim} , according to Equation (4.22) for restraint loading (Engström, 2011).

$$w_{m,all} = \frac{w_{lim}}{1.3} \text{ [mm]} \quad (4.22)$$

This crack width can then be compared to the maximum allowable crack width in order to evaluate if demands are fulfilled or if additional reinforcement is required to fulfil the demands.

$$w_m(\sigma_s) < w_{m,all} \text{ [mm]} \quad (4.23)$$

5 Observed response of floors

The field studies aimed to investigate the cracking behaviour in slabs-on-ground for four different projects. The objectives were to state a likely cause of the developed cracks and to compare the collected data with theoretical estimations and calculations. All collected data is presented in Appendix B to Appendix E. These appendices contain tabulated project information, measurement data and detailed drawings.

5.1 Method

The data from the different projects was collected using several methods. Interviews were held with persons involved in the projects; drawings and building documents were studied and cracks were photographed, measured and mapped on site. In addition to this, the concrete cover was also measured for each project.

Due to the large size of the studied floor areas and due to ongoing activity with e.g. forklift traffic and storage shelves, a complete mapping of the cracks throughout the floor areas was not possible to perform. It was deemed that this task would have been very complicated without contributing a lot to the result. The adopted method was instead to identify the floor areas with the most severe cracking and to then study these in detail.

Site observations of each object, including information regarding location, orientation, spacing and lengths of cracks were recorded on plan view drawings. This was then complemented with measurements regarding crack widths and concrete cover. Instruments used in the field observations include, in addition to measurement tools and a camera, a cover meter and a crack width microscope, see Figure 5.1.



Figure 5.1 Cover meter and crack width microscope used for measurements.

Since the width of a crack varies greatly throughout its length, the chosen points of measure can to a great extent influence the result. Due to this, a mean value of the crack widths was considered to be more representative than the maximum value. As a result, the crack width was measured at even distances along each crack and an average was then calculated, which has then been displayed on the drawings in Appendix B to Appendix E . The distance between each point along the crack varied in the different measurement series, but the value was always kept the same within each series. Figure 5.2 illustrates how the measurements for a generic crack were carried out. Note that the crack width was always measured perpendicular to the crack direction for the specific measurement point.

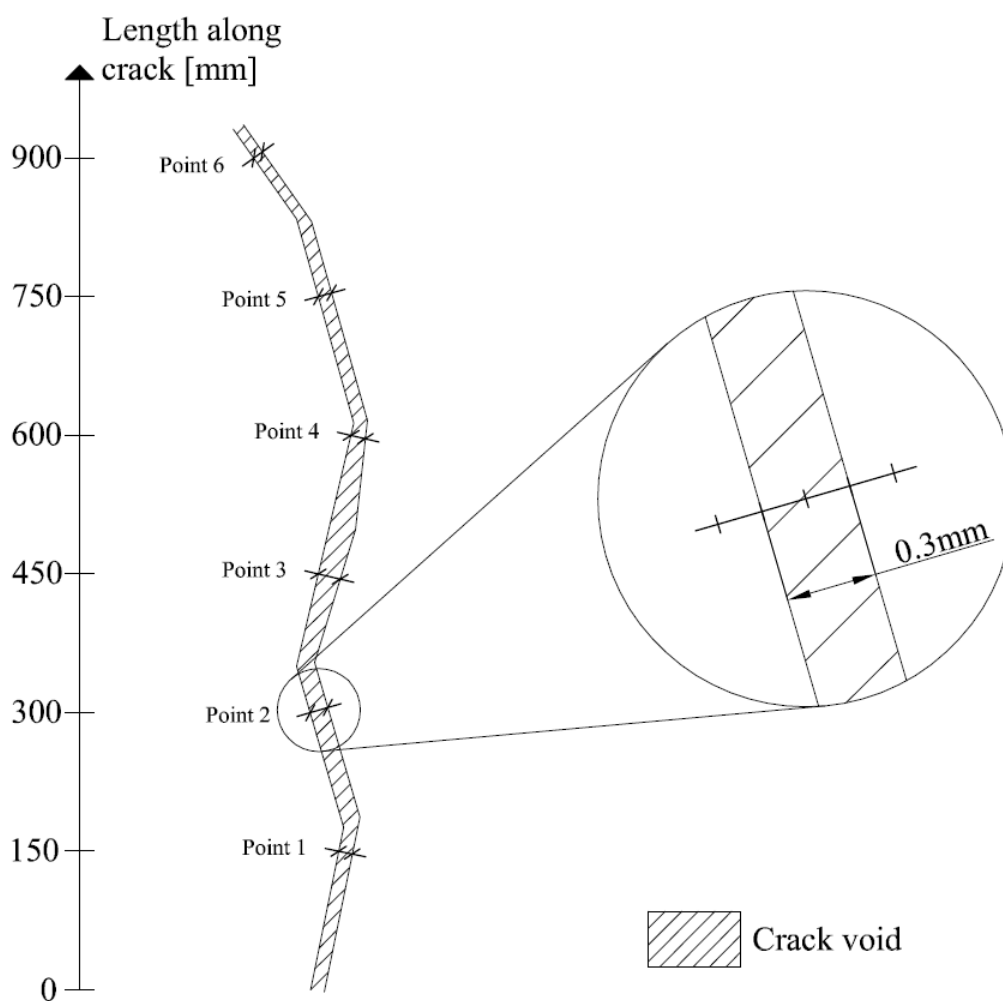


Figure 5.2 Measurement principle for measuring crack widths.

In addition to this, the concrete cover was also measured using the cover meter in the region of each crack and an average value was then calculated. Furthermore, the spacing of the reinforcement was also checked with the cover metre to confirm that the prescribed spacing had been adopted.

When evaluating the cracks, the occurrence and magnitude of shrinkage cracking was studied. The initial objective was to identify which cracks that were of the type shrinkage cracks. This was done through comparing the locations of the cracks with the geometry, reinforcement and restraint situation of the floor. Once these cracks had been identified, the results were summarised and possible reasons for cracking were evaluated.

5.2 Overview of studied objects

All of the studied objects are large space warehouse buildings with a structural system composed of steel members. The buildings have a relatively low mass in relation to the space enclosed. All of the studied objects are located in the Göteborg area in Sweden, Table 5.1 below presents and overview of the studied objects.

Table 5.1 General information of studied objects.

Object	Floor Area [m ²]	Concrete strength class	Slab thickness [mm]	Main reinforcement		Nominal concrete cover [mm]		Piled
				Top	Bottom	Top	Bottom	
1	1360	C20/25	220	φ10s125mm#	φ10s125mm#	25	30/50	Yes
2	3600	C25/30	200	φ8s150mm#	φ8s150mm#	20	30/50	Yes
3	3040	C25/30	270	φ10s150mm#	φ8s150mm#	20	30/50	Yes
4	682	C25/30	250	φ8s150mm#	φ8s150mm#	20	30/50	Yes

The design regulations in EC gives a recommended value of a maximum allowable characteristic crack width w_{max} , based upon the governing exposure class, see Chapter 4. The value w_{max} is compared to measured values from the different objects. To get an overview of the crack widths and the corresponding exposure classes for the objects, see Table 5.2. The exposure class XC1 is applicable when the degradation mechanism is chloride induced corrosion and the environment dry or permanently wet. An example of such a situation is concrete inside buildings with low air humidity.

Table 5.2 Exposure classes and corresponding w_{max} (recommended value) for studied objects

Object	Exposure class	w_{max} according to EC table 7.1N [mm]	Demands on appearance
1	XC1	0.4	Not specified
2	XC1	0.4	Not specified
3	XC1	0.4	Not specified
4	XC1	0.4	Not specified

Each project's geometry is illustrated on floor plan views below; see Figure 5.4, Figure 5.13, Figure 5.21 and Figure 5.28. The figures contain geometric information, measured crack locations and notations to specify the position of each slab portion. See Figure 5.3 for a legend intended for the floor plan views.

	BUILDING PERIMETER
	PERIMETER STRIP OR THICKENINGS
	JOINTS
	CRACKS
	COLUMN
	PILE
	MEASURED CRACK INDEX
	SLAB PORTION

Figure 5.3 Explanation of symbols used on drawings.

5.3 Object 1

Object 1 is a workshop and storage building with a total floor area of approximately 1360 m². One part is a regular office area and the rest of the building is a combined storage and workshop. The structural system is supported by columns that rest on the slab.

5.3.1 Object specific data

The whole floor was studied and the most distinct cracks were chosen to be measured. The office area of the building was covered with additional floor covering, thus the concrete surface in the area could not be studied. See Figure 5.4 for a plan view of the object. The slab is cast in four casting sections separated by dilatation joints. A photo taken before casting is shown in Figure 5.5.

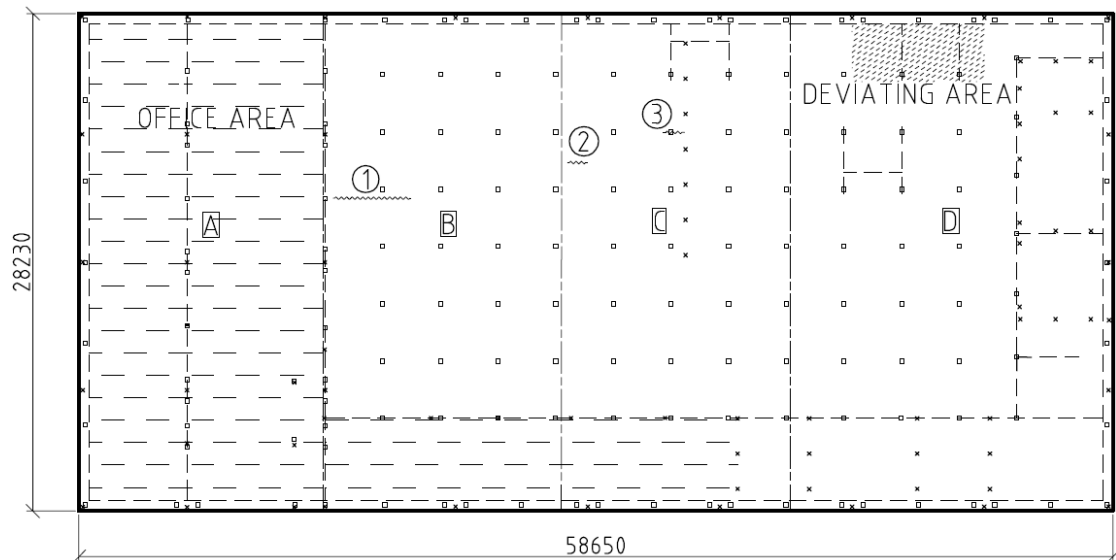


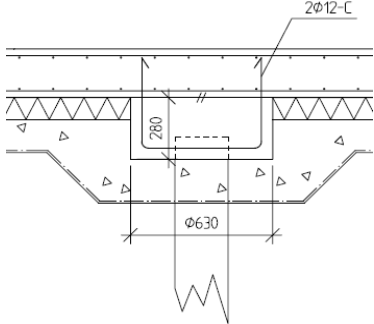
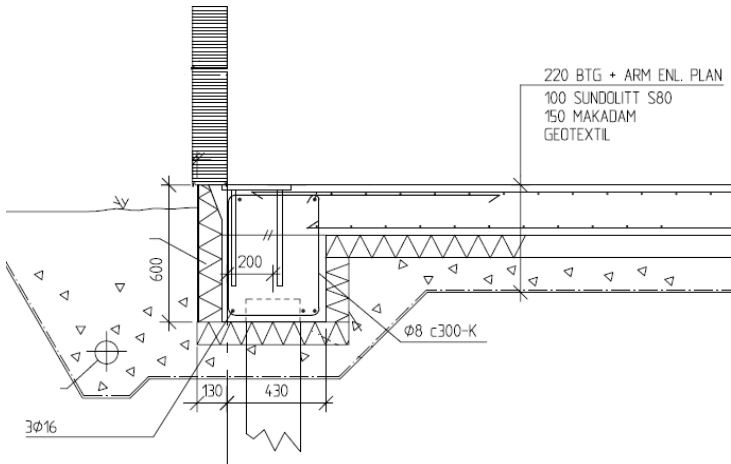
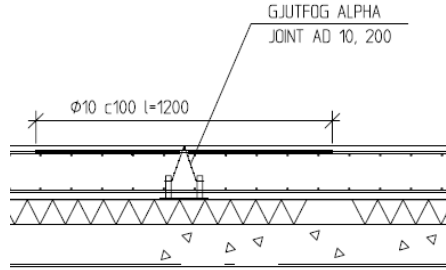
Figure 5.4 Floor plan view of object 1 illustrating measured cracks. Crack nr 1 is further illustrated in Figure 5.9. The deviating area is further illustrated in Figure 5.10.



Figure 5.5 Photo of object 1 during the construction phase.

General information regarding reinforcement and geometry for object 1 can be found in Table 5.1. Further relevant and object specific data is collected in Table 5.3.

Table 5.3 Object specific data for object 1

Age from casting	4 years
Notes on extra reinforcement	Added $\varnothing 10s_{100-1200}$ mm over all dilatation joints Also see pile detail below
Insulation	100 mm Sundolitt S80 under the whole area
Detailing	<div style="text-align: center;">  <p>Figure 5.6 Connection between pile and slab-on-ground</p> </div> <div style="text-align: center;">  <p>Figure 5.7 Perimeter strip with connection to wall</p> </div> <div style="text-align: center;">  <p>Figure 5.8 Detail of dilatation joint</p> </div>

Pile type	SP1
Distance between piles	# s 3.3 m in general
Casting sequence , see Figure 5.4 for slab section denotation.	A – B – C – D

5.3.2 Observations

Object 1 gave an overall good impression. Few cracks were found in the slab and despite that casting section D was regarded worse than the others, the overall performance of this slab was considered to be very good so far. The concrete that was used has a relatively low strength class, C20/25, resulting in a relatively high shrinkage strain due to the fact that there is a lot of water in the concrete mix that can be dried out, see Figure 4.2.

The dilatation joints (alpha type joints) allows for horizontal movement of 20 mm, see also Figure 2.8. This enhances the risk of shrinkage cracks parallel to the joints as the slab is freer to move in this direction than without the joints. The detailing work regarding these joints was found to be overall well executed.

Three measured cracks over the slab area are presented in Table 5.4. The crack locations are according to Figure 5.4, and the measured cracks do not form a well defined pattern. It should however be mentioned that only the most distinct cracks were measured. All of the mean crack width values are within the acceptable range according to EC2, see Table 4.1.

Table 5.4 Measurement data from object 1.

Crack number	Concrete cover - mean value [mm]	Crack width - max value [mm]	Crack width - mean value [mm]
1	48.8	0.25	0.14
2	24.6	0.20	0.14
3	38.3	0.15	0.11



Figure 5.9 Crack nr 1 of object 1.

The measured cover thickness was found to be larger than the nominal value of 25 mm. The deviation is on the safe side regarding degradation of the slab and reinforcement. It should however be mentioned that this deviation causes a stiffness variation in different slab sections. As the reinforcement is located lower in the slab section there will be less flexural capacity in ULS. It also leads to a decrease of reinforcement ratio due to the increased concrete amount.

In casting step D an area deviating from the average floor area of object 1 was found. The surface is crazed according to Figure 5.10. The surface showed significant similarity with the surface described in Section 3.2.4, affected by plastic shrinkage. Other deviations found in casting step D is that at some locations aggregates are exposed at the surface, see Figure 5.11.



Figure 5.10 Deviating area showing crazing for object 1.



Figure 5.11 Aggregate exposed in surface of object 1.

5.3.3 Evaluation

According to the model for determining shrinkage strain in EC2 object 1 has developed approximately 82% of the final shrinkage strain. The predicted shrinkage development for object 1 is illustrated in Figure 5.12. The calculation of developed shrinkage strain follows Equation (5.1).

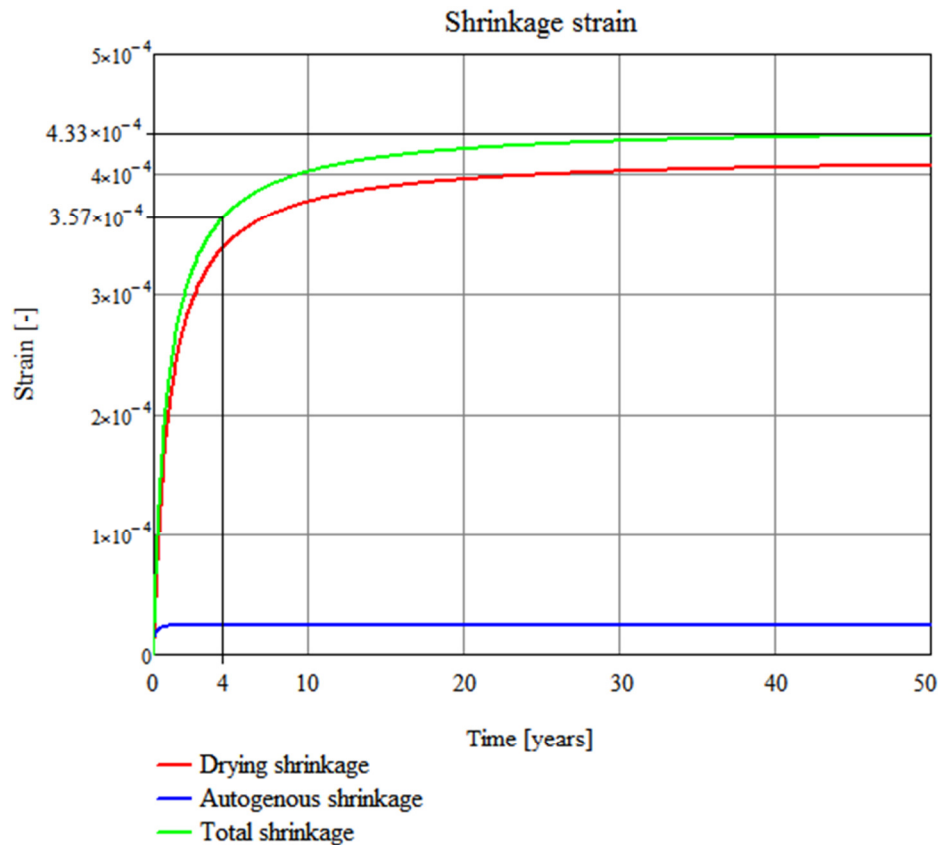


Figure 5.12 Predicted shrinkage development for object 1. The calculation was performed according to EC2 as described in Section 4.2. It was assumed that cement class N was used and that the slab was exposed to an ambient RH of 40 % after 7 days curing.

$$\frac{\varepsilon_{cs,4 \text{ years}}}{\varepsilon_{cs,50 \text{ years}}} = \frac{3.57 \cdot 10^{-4}}{4.33 \cdot 10^{-4}} = 0.824 \rightarrow 82.4 \% \quad (5.1)$$

As this slab only is 4 years old, there would still be approximately 20% left of the total shrinkage strain that the slab will be exposed to. It could be useful to carry out new measurements after a few more years to get indications on how the slab is performing over time.

Regarding the location of cracks 1-3 they are not forming a distinct pattern. The direction of the cracks is perpendicular to the long side of casting steps B and C, this indicates that it can be a matter of shrinkage cracks since the slab wants to contract more in its longer direction. The cracks could have been expected to occur in the middle of the length, but this is not the case. Local phenomena and differences in

friction against the sub-base are possible factors affecting the actual location of where the cracks are formed, in general and in this case. The restraint along the dilatation joint has most effect where the concrete connects to the joint by dowels and surface bond.

The choice of having a low concrete class in this slab reduces the need for reinforcement according to the regulations; this is of course an economical benefit as both the reinforcement and cement amount will be lowered. The chosen concrete and reinforcement in the slab-on-ground were found to respond well to the actions and impacts so far.

A windy and/or sunny day will result in faster drying of the concrete surface, with the risk of formation of plastic shrinkage cracking. The more crazed surface in casting step D could be a result of not covering the cast portion in time. As observed the surface shows similarities with plastic shrinkage cracking. The phenomena found in this casting section are suggested to be a result of mistakes during the construction process, rather than a design mistake, based on the fact that the other casting steps seemed to be performing well. It could also be a result of the material delivered on site for this casting step deviating from the material used in other casting steps.

5.4 Object 2

Object 2 is a combined store and storage building mainly housing electronics and the floor area is approximately 3600 m². Due to the large size of the floor area, measurements were focused in a region where the cracking was found to be most severe.

5.4.1 Object specific data

The area for carrying out measurements was narrowed down to approximately 1/4 of the total slab area and is illustrated in Figure 5.13. The slab over the illustrated area was cast in four steps, A-D. No measurements were however carried out in casting steps B and D.

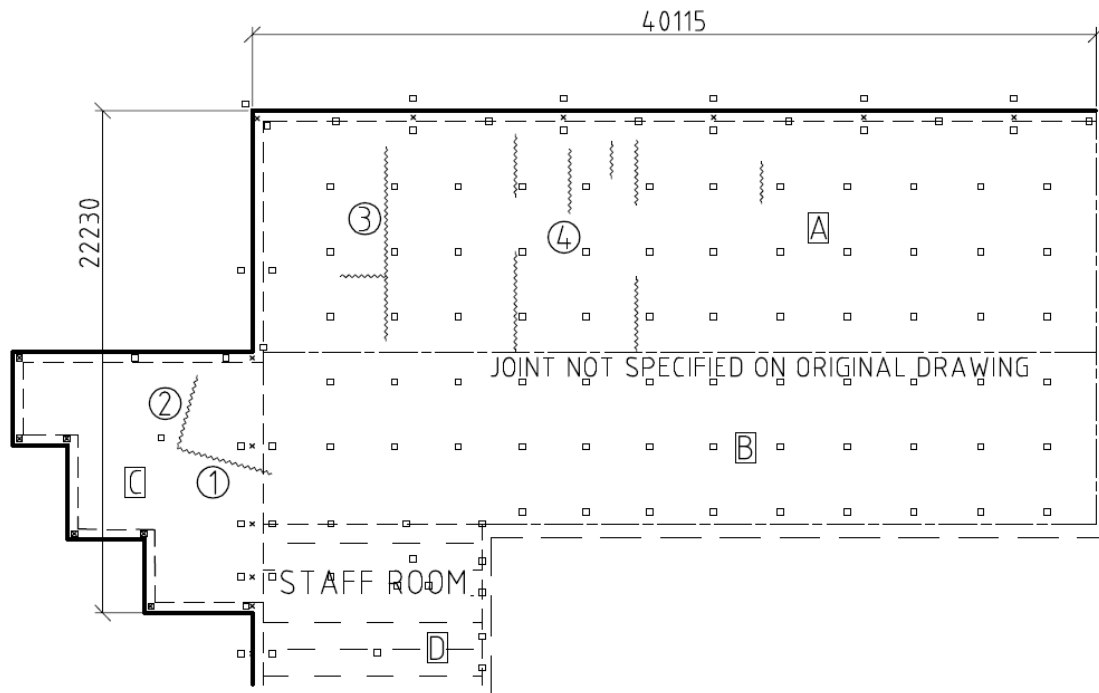


Figure 5.13 Floor plan view of object 2 illustrating measured cracks. Crack nr 4 is further illustrated in Figure 5.17.

General information regarding reinforcement and geometry for object 2 can be found in Table 5.1. Table 5.5 below lists further relevant object specific data for object 2.

Table 5.5 Object specific data for object 2

Age from casting	6 years
Notes on extra reinforcement	10Ø8s150-1600 mm added over piles
Insulation	70 mm Styrofoam G100 along perimeters
Detailing	<p>Figure 5.14 Section of pile to slab connection detailing.</p>

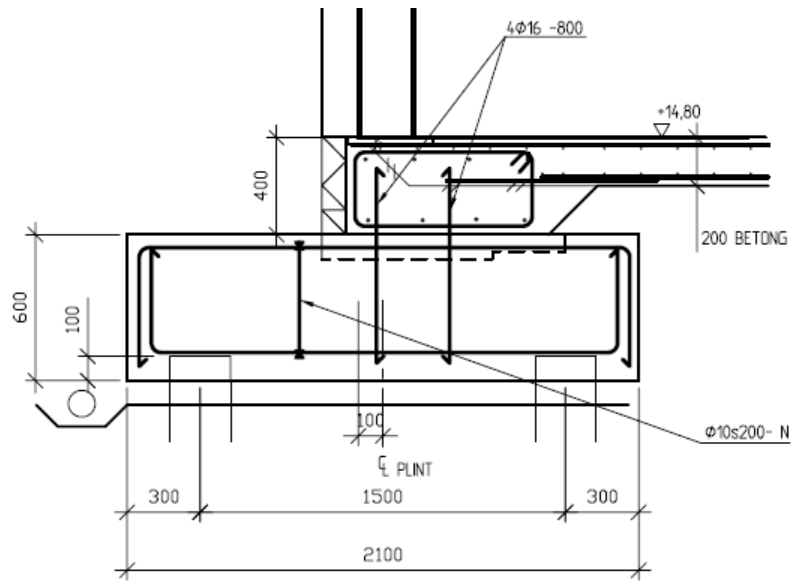


Figure 5.15 Section of perimeter strip detailing. The column is here supported on a foundation which distributes the vertical load to a pair of piles.

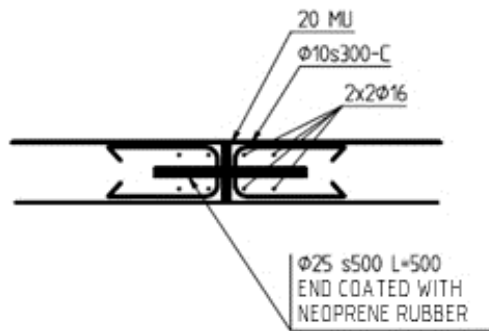


Figure 5.16 Section of joint detailing. The joint is dowelled, preventing movement in vertical direction and parallel to the joint.

Pile type	SP1
Distance between piles	# s 3.2 m
Casting sequence	Not found

5.4.2 Observations

The overall visual appearance of the concrete surface of this slab-on-ground was not found to be very satisfying. The surface was generally crazed with thin cracks in a random crack-pattern.

The most severely cracked region was found in casting step A of the building. Measurement data from this slab section can be found in Table 5.6 below. The general visual appearance of the measured cracks, Nos. 1-4, was found to be similar and Figure 5.17 illustrates a photograph of crack No. 4.

Table 5.6 Measurement data from object 2.

Crack number	Concrete cover - mean value [mm]	Crack width - max value [mm]	Crack width - mean value [mm]
1	36.4	1.20	0.96
2	36.4	1.10	0.88
3	23.0	1.10	0.74
4	30.5	1.00	0.64

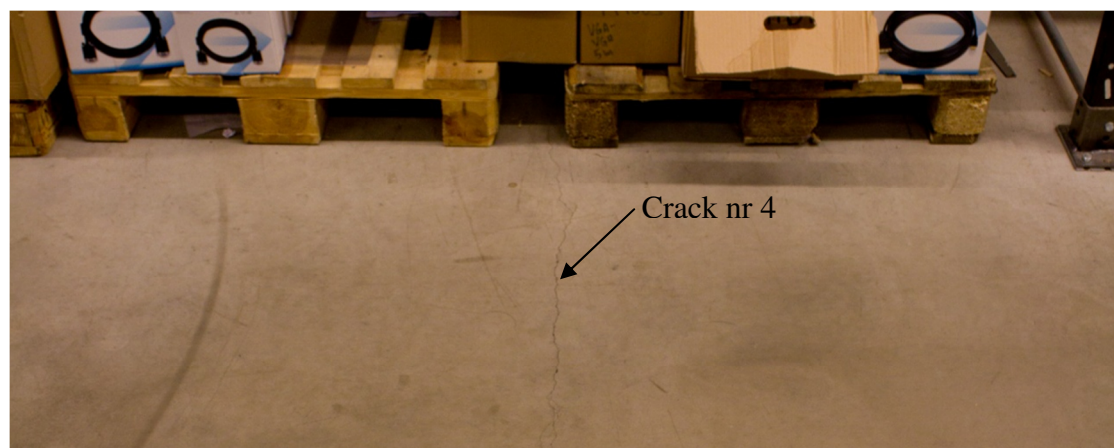


Figure 5.17 Crack nr 4 for object 2.

A major deviation from the construction drawing was also found in casting step A. During the construction, the planned casting step was divided in two by an additional joint, see Figure 5.13. The geometry of the resulting new casting steps is long in comparison to their widths.

Furthermore, the detailing regarding joints was in general found to be not carefully executed. The joints are of a simple type and are not always present where they should be according to the drawings, see Figure 5.18 and Figure 5.19.



Figure 5.18 Example of problems with joint detailing for object 2.



Figure 5.19 Example of problems with joint detailing for object 2.

5.4.3 Evaluation

The measured mean crack widths were found to exceed the recommended value in EC2 according to Table 7.1N, see Table 5.2. If the client would have specified demands on the visual appearance, these would most likely not have been fulfilled. In this case however, there are indications that the client wanted a rough warehouse feeling to give the store a “cheap” impression. Given this, the crack widths could be regarded as within the acceptable range.

The cracks are currently not causing any problems except for the fact the aesthetical appearance is lowered. However, caution should be taken since forklift traffic is passing over the cracked region, which over time might cause problems as the cracks degrade at the surface.

Two large cracks, Nos. 1 and 2, were identified in casting step C. These were both deemed to be cracks as a result of traffic load. All forklift traffic for loading and unloading of goods passes through this area of the building as the loading bay is connected to it.

As previously mentioned, the most severe cracking was found in casting step A. In addition to this, changes have been made from the design drawings in this region through the adding of an additional joint. Consequently, it is possible that the cracking is caused by the change of geometry.

The added joint creates a casting step that is 45 m long and 11.5 m wide. The section will therefore be subjected to a larger shrinkage strain in the longer direction. At the same time the shrinkage will be restrained by the larger stiffness of the perimeter strip and by the new joint that prevents this movement, see Figure 5.16. Due to the reduced width of the casting section, the restraint along the joint will have an increased effect.

Furthermore, casting section A is restrained by a perimeter strip on one short side and by a joint on the other short side. The joint allows movement perpendicular to the joint and therefore does not constitute any restraint for the shrinkage in the longer direction of the slab. Due to this unsymmetrical restraint situation the cracks have not appeared in the middle of the slab section but have been shifted closer to the perimeter strip.

The cracking behaviour could also be affected by the casting sequence of the casting steps. However, since no information has been found regarding the sequence, no conclusions can be made regarding this.

Since object 2 is approximately 6 years old at the time of observations, it is of interest to study the development of shrinkage strain for the specific slab. Following the procedure according to EC2 as described in Section 4.2 the result can be illustrated according to Figure 5.20. Together with Equation (5.2) it can be concluded that approximately 90 percent of the expected shrinkage strain during the service life has already occurred. Nevertheless, it would still be interesting to follow up the cracking behaviour after a few years.

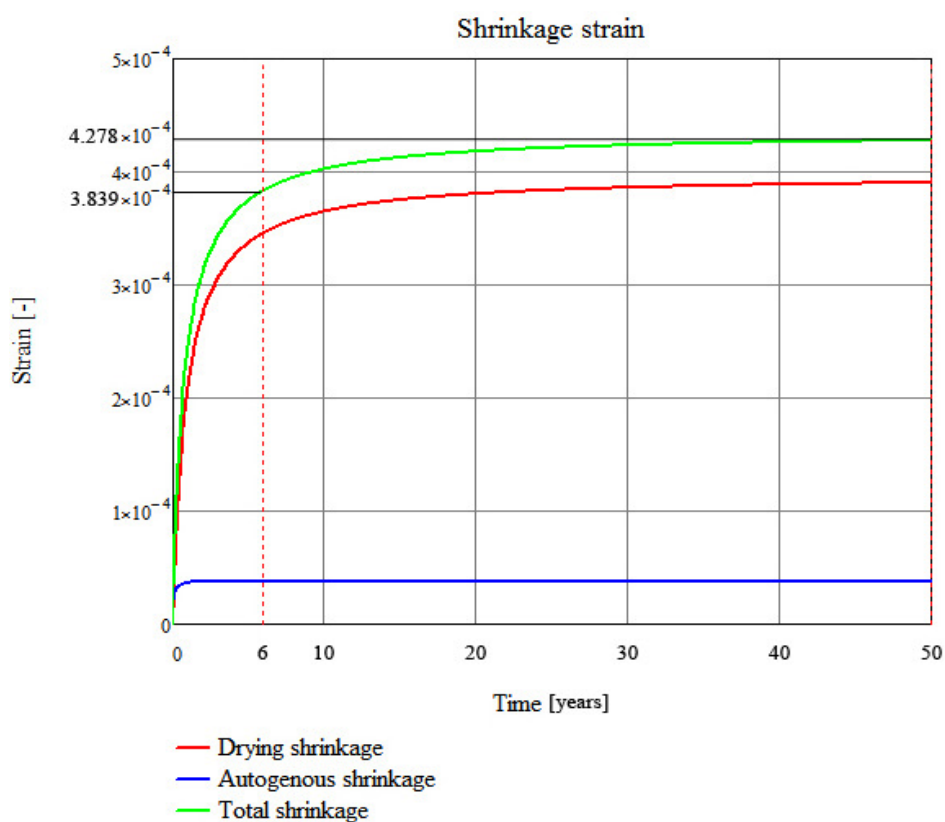


Figure 5.20 Predicted shrinkage development for object 2. The calculation was performed according to EC2 as described in Section 4.2. It was assumed that cement class N was used and that the slab was exposed to an ambient RH of 40 % after 7 days curing.

$$\frac{\varepsilon_{cs,6 \text{ years}}}{\varepsilon_{cs,50 \text{ years}}} = \frac{3.839 \cdot 10^{-4}}{4.278 \cdot 10^{-4}} = 0.897 \rightarrow 89.7 \% \quad (5.2)$$

The problems observed with joints could probably have been avoided, if more concern was given the execution. Using alpha joints, see Figure 2.8, would also have improved the result. However, considering the low demands from the client and that the fork lift traffic is limited, alpha joints would probably have been a too costly solution.

5.5 Object 3

Object 3 is a building for combined storage and store. The building is mainly housing material for heating and sanitation, but is also a detail shop for the construction industry.

5.5.1 Object specific data

It was chosen to carry out measurements on casting steps D, E, G and H as these casting sections showed worse cracking behaviour than the other sections. The office areas for this building are located one level above the slab-on-ground and the columns supporting this floor level can be seen along the two leftmost lines of columns in Figure 5.21. The total floor area is approximately 3040 m². The joints specified for this object are construction joints, see Section 2.2.3, but no details illustrating the joints were found in the original drawings.

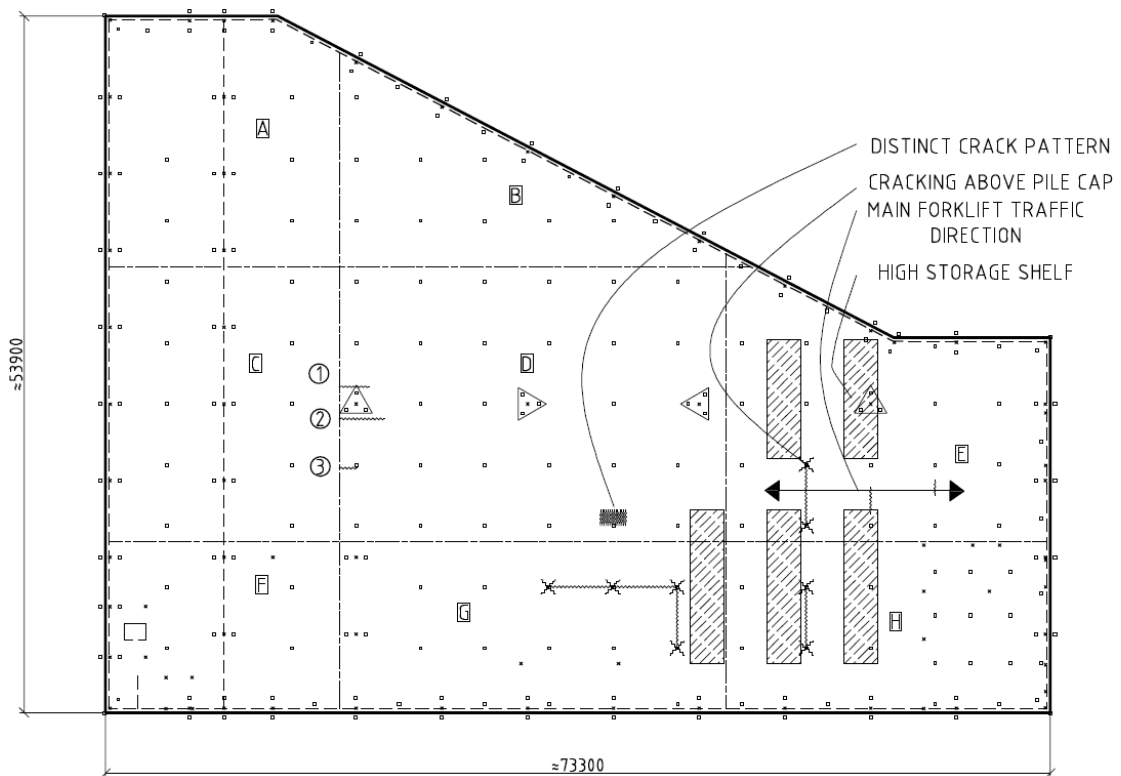


Figure 5.21 Floor plan view of object 3 illustrating measured cracks. A typical crack pattern over piles is further illustrated in Figure 5.25. The area showing a distinct crack pattern is further illustrated in Figure 5.26.

General information regarding reinforcement and geometry for object 3 can be found in Table 5.1. Further relevant and object specific data is collected in Table 5.7.

Table 5.7 Object specific data for object 3

Age from casting	5 years
Notes on extra reinforcement	16Ø16 s200-2400mm added over piles 16Ø16 s200-3500mm added over pile groups Ø10 s150-3500mm added over internal slab thickenings
Insulation	100 mm Raindisol b=1000mm following the outer perimeter No insulation under the main part of the floor area

Detailing

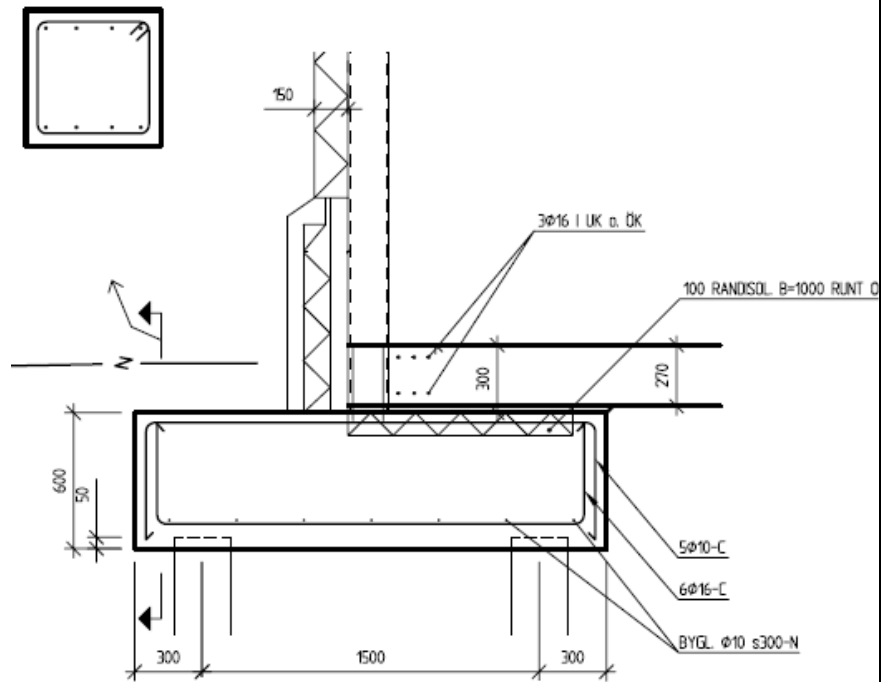


Figure 5.22 Connection between wall and floor. The column in the wall is supported on a foundation which distributes the vertical load to a pair of piles.

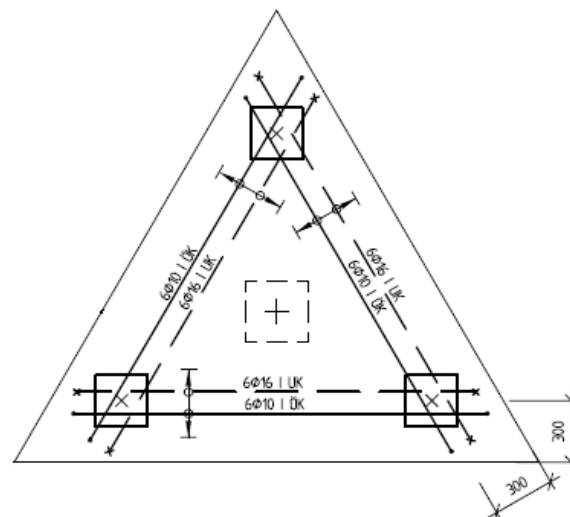
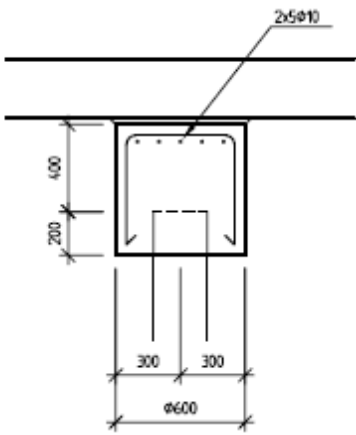


Figure 5.23 Pile group. The column in the middle is supported on a triangular foundation which distributes the vertical load to three piles.

	 <p data-bbox="491 689 1125 728"><i>Figure 5.24 Pile connection to slab-on-ground</i></p>
Pile type	SP1
Distance between piles	# s 5 m in general
Casting sequence	Not found

5.5.2 Observations

This object was the one giving the worst visual appearance. A relative large number of small cracks were found in most parts of the slab-on-ground and some larger cracks were found at specific locations, which are illustrated in Figure 5.21.

The more severe crack formations were found in casting steps E, G and H, where the forklift traffic is the most intense. It is also over these casting steps that the high storage shelves are located. Distinct crack roses above pile caps were found at several locations, see Figure 5.25. At some locations the cracks propagated from pile cap to pile cap as can be seen in Figure 5.21.



Figure 5.25 Typical crack pattern over pile for object 3.

There was also a well defined area of the slab where cracks according to Figure 5.26 were found. The documented crack pattern has similarities with the schematic sketch of plastic settlement cracks in Figure 3.10. The mean cover thickness over this area was measured to 19 mm, differing 1 mm from the nominal value of 20 mm.

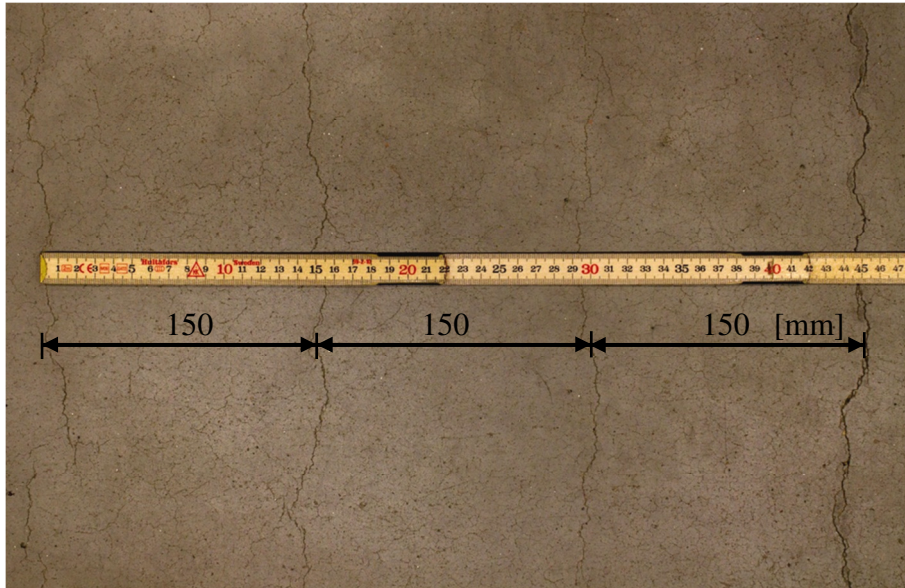


Figure 5.26 Plastic settlement cracks for object 3.

The measurement results for cracks 1-3 are presented in Table 5.8. Crack 1 and 2 are located right above and at the edge of a pile group. The pile group detail is shown in Figure 5.23. All measured cracks are located with the main crack direction perpendicular to the construction joint between casting steps C and D.

Table 5.8 Measurement data from object 3.

Crack number	Concrete cover - mean value [mm]	Crack width - max value [mm]	Crack width - mean value [mm]
1	45	0.80	0.59
2	45	2.00	1.20
3	45	0.40	0.29

Comparing the mean crack width for crack 1 and 2 with the recommended values in Table 4.2, it can be observed that the measurements are outside the recommended range.

5.5.3 Evaluation

Object 3 has developed approximately 82% of its final shrinkage strain according to the model for determining shrinkage strain according to EC2. The shrinkage development is illustrated in Figure 5.27. The formula for calculating the amount of shrinkage strain developed after 5 years is shown in Equation (5.3).

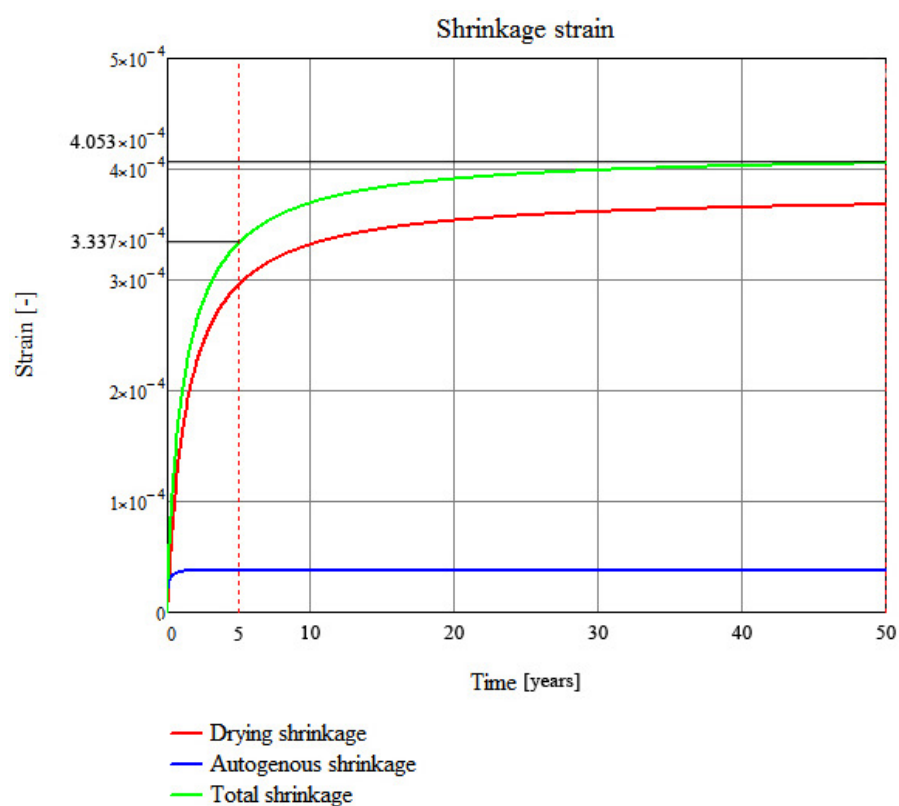


Figure 5.27 Predicted shrinkage development for object 3. The calculation was performed according to EC2 as described in Section 4.2. It was assumed that cement class N was used and that the slab was exposed to an ambient RH of 40 % after 7 days curing.

$$\frac{\varepsilon_{cs,5 \text{ years}}}{\varepsilon_{cs,50 \text{ years}}} = \frac{3.337 \cdot 10^{-4}}{4.053 \cdot 10^{-4}} = 0.823 \rightarrow 82.3 \% \quad (5.3)$$

The crack pattern found in casting steps E, G and H are probably caused by loads from the storage shelves and the forklift activity, i.e. not as a direct result of restrained shrinkage. If the ground underneath the slab-on-ground develops settlements between the piles this creates a moment above the pile caps, which can crack the concrete if the resulting stresses reach the concrete tensile strength. Studying the pile-supported slab as a column supported slab, the cracks from pile cap to pile cap can be explained as it would be along these lines the moment would create the largest tensile stresses in the top of the slab.

The well defined cracked area according to Figure 5.26 is likely to be a cause of plastic settlement cracks, compare with Section 3.2.4. The resemblance is clear comparing with this section and the sketch in Figure 3.10. Furthermore, this theory is also supported by the fact that the crack pattern matches the reinforcement spacing of 150 mm very well. The mean cover thickness for this area is not significantly deviating from the nominal value, but larger local differences could be a factor inducing cracks to these locations. The found cracks could also be cracks as a result from moment over the pile located near the studied area. However, no significant crack rose was found above this pile cap.

Cracks 1-3 could be a result of restrained shrinkage in casting step D. If casting step C was constructed before D, this would create a restraint situation where section D would have a larger need for movement than section C, leading to stresses that reach the capacity and create cracks. If casting section B or G were also constructed before section D, the cracks, if shrinkage cracks, could have been expected parallel to the shorter direction of section D. However, this is not the case. As the casting sequence is not known, further information is needed to further evaluate this.

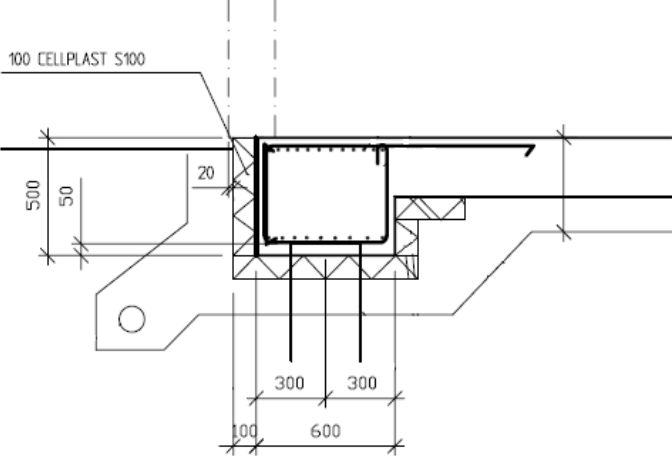
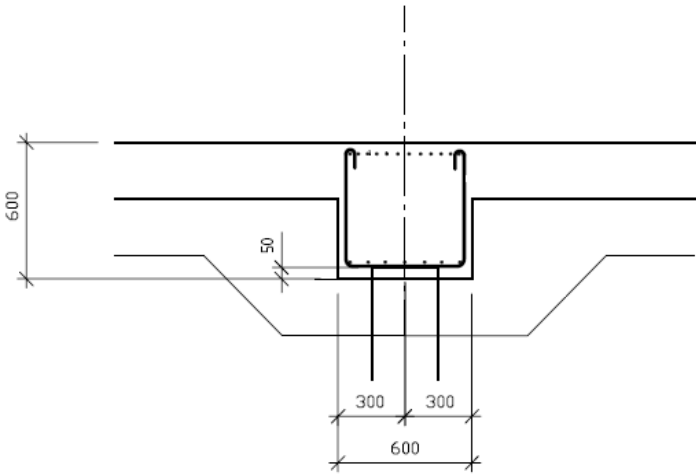
Cracks 1-2 are as mentioned located right above the ends of a pile group. If there is a moment acting above the pile group due to loads in-between the piles, this moment could have caused the cracks. Furthermore, this moment could also be increased if there are settlements in the ground between the piles. As the ground settles, the piles can be regarded as the only vertical support for the slab, forcing the slab to carry itself between the supports, creating a moment at the support.

5.6 Object 4

Object 4 is a storage combined with an office area of two storeys. The total building floor area is approximately 682 m² and slightly smaller than the other objects in this study.

5.6.1 Object specific data

The whole floor area was studied, except for the office area which was covered with clinker tiles. There were no visible joints dividing the slab into casting steps and there are no joints specified on the original drawings. A plan view with the measured cracks is found in Figure 5.28

Insulation	100 mm cellular plastic underneath the office area of the building
Detailing	 <p data-bbox="496 909 1361 981"><i>Figure 5.30 Perimeter strip following the outside perimeter of object 4. Note the connecting pile.</i></p>  <p data-bbox="496 1541 1262 1574"><i>Figure 5.31 Internal slab thickening with connecting pile.</i></p>
Pile type	SP1
Distance between piles	# s 5.5 m in general
Casting sequence	Only one casting step

5.6.2 Observations

The slab of object 4 had a good visual appearance, if not regarding the larger cracks found. No extensive crazing or other defects in the surface were found.

The found cracks form a regular pattern with cracks parallel to the shorter direction and following three main lines, see Figure 5.28. The slab has a distinct sectional variation through the two internal slab thickenings, situated parallel to the longer direction of the slab. All piles are connected to the perimeter strips and slab thickenings and the cracks are located in-between these regions. The data for the measured cracks is found in Table 5.10, and a typical crack found for this object is shown in Figure 5.32.

Table 5.10 Measurement data from object 4.

Crack number	Concrete cover - mean value [mm]	Crack width -max value [mm]	Crack width -mean value [mm]
1	69.4	1.10	0.60
2	62.4	0.50	0.30
3	54.2	0.50	0.28
4	86.3	0.50	0.31
5	72.6	0.50	0.31
6	-	1.00	0.64
7	-	1.00	0.59
8	-	1.00	0.69
9	62.6	0.50	0.38
10	-	1.00	0.66
11	-	0.60	0.45
12	-	1.00	0.67



Figure 5.32 Typical crack for object 4. The crack has been filled with an epoxy-based material.

The maximum average crack width was measured to 0.69 mm, which is outside the recommended range according to Table 4.1.

The crack widths could be accepted, if there was no demand on visual appearance on the floor. However, as the cracks have been filled with an epoxy-based material and sealed, the user is obviously not satisfied with the performance of the floor.

Additional reinforcement has been added in the perimeter strips over the piles and in the bottom of the perimeter strip between the piles. This is to be able to carry the load from the slab, if the ground would settle in between the piles and the perimeter strips. To transfer the load from the slab field extra reinforcement parallel to the shorter direction of the slab has been added in the top of the slab above the perimeter strips and slab thickenings and in the bottom of the slab portions in-between perimeter strips and slab thickenings. To locate more precisely what additional reinforcement has been provided see Figure 5.29. By incorporating additional reinforcement, the stiffness behaviour of the slab in the cracked state is changed.

5.6.3 Evaluation

The age of object 4 is 4.5 years and the predicted shrinkage development over time is shown below in Figure 5.33. From the graph it can be seen that this slab has approximately 20% left to reach the final shrinkage strain. The calculation is shown in Equation (5.4).

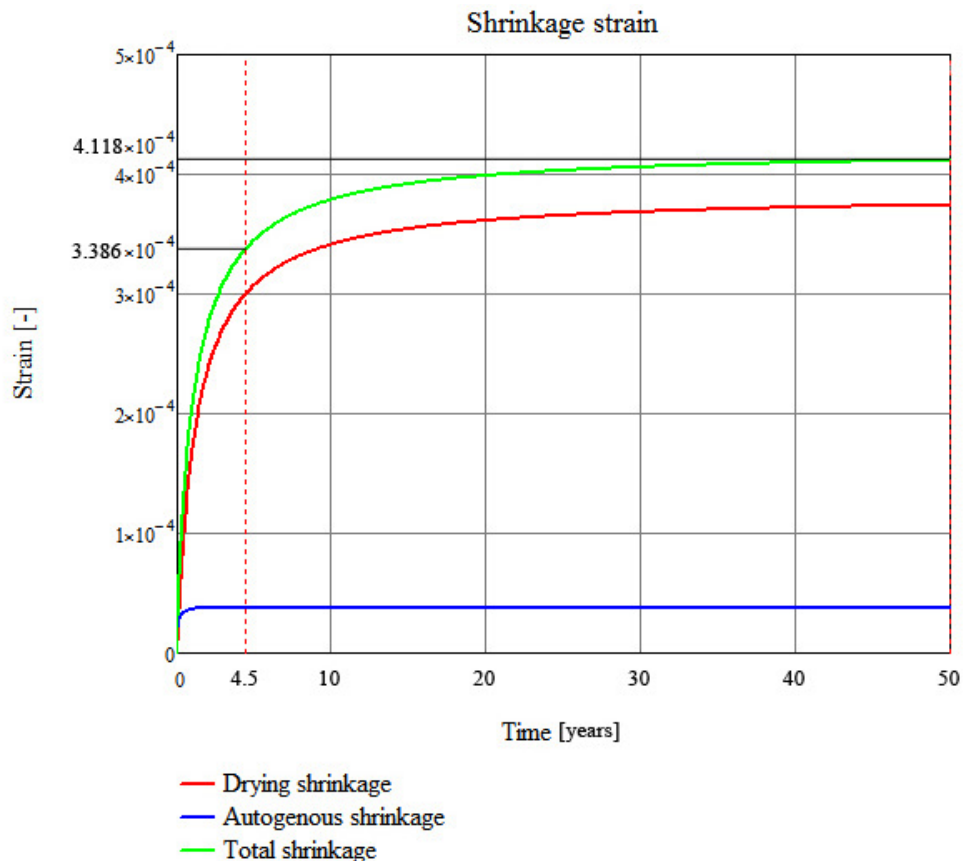


Figure 5.33 Predicted shrinkage development for object 4. The calculation was performed according to EC2 as described in Section 4.2. It was assumed that cement class N was used and that the slab was exposed to an ambient RH of 40 % after 7 days curing.

$$\frac{\varepsilon_{CS,4.5 \text{ years}}}{\varepsilon_{CS,50 \text{ years}}} = \frac{3.386 \cdot 10^{-4}}{4.053 \cdot 10^{-4}} = 0.822 \rightarrow 82.2 \% \quad (5.4)$$

Judging by the additional reinforcement layout the slab has been designed as a one way slab spanning the shorter direction of the building. In order to resist the support and field moments, additional top respectively bottom reinforcement have been added in this direction.

The perimeter strips and slab thickenings will have limited freedom of movement as they are connected to the piles and have a distinct differing geometry compared to the rest of the slab. Also the load from the roof and walls is transferred along the perimeter strips, increasing the friction and thereby the restraint. The slab portion will

be restrained both along and perpendicular to the perimeter strips. In addition to this, the sectional capacity of this slab portion will be lower than for the larger sections over the perimeter strips.

The cracks found are deemed to be caused by restrained shrinkage. The larger need for movement will be along the longer direction of the building and is restrained by perimeter strips, slab thickenings and piles both perpendicular and parallel to the main direction of the found crack pattern, as explained above. The restraints have caused stresses that have reached the tensile strength at the location of the cracks.

5.7 Evaluation

The reinforcement ratios for the different objects were compared to calculated minimum reinforcement ratios according to EC2 and BBK 04. The calculation procedure is presented in Section 4.3.2 and Section 4.3.3 respectively. The result is presented in Figure 5.34 as a bar chart diagram. The calculations were based on the following assumptions:

- The maximum allowable steel stress σ_s was assumed as 420 MPa.
- The material parameters were adopted from each project's concrete strength class and differ in definition between EC2 and BBK 04.
- The definition of concrete area used in the formulations differs between EC2 and BBK 04.
- The reduction factor of 0.7 according to BBK 04 was neglected as it does not apply for pile supported slabs-on-ground.

The percentages shown in Figure 5.34 were calculated according to Equation (5.5) below.

$$\text{percentage} = \frac{\text{actual provided reinforcement ratio} \cdot 100}{\text{min. reinforcement ratio according to regulations}} \quad (5.5)$$

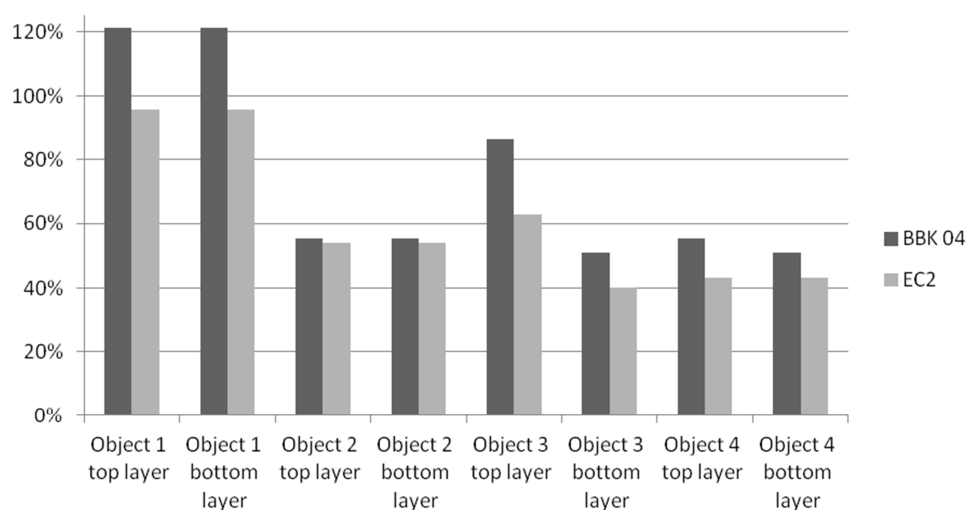


Figure 5.34 Reinforcement ratio comparison for the different objects. The percentages are compared with BBK 04 and EC2 respectively.

As can be seen it is only object 1 that has a reinforcement ratio close to the calculated minimum reinforcement ratio. All other objects have a lower reinforcement ratio than the calculations determine. It should also be noted that object 2, 3 and 4 show worse cracking than object 1.

However, if the calculations above would have taken into account the EC2 recommendation for allowable steel stress for limiting the crack widths, the calculated minimum reinforcement ratios would have been larger. Lowering the allowable crack width, decreases the maximum steel stress and consequently increases the minimum reinforcement ratios.

As was discussed in the evaluation for each object, all measured cracks were not identified as shrinkage cracks. Table 5.11 below illustrates all cracks that were argued to be caused from restrained shrinkage. In total 22 cracks were measured, but the table has been reduced to 14 cracks. The measurements were carried out according to the description in Section 5.1 and Figure 5.2.

Table 5.11 Measurement data for shrinkage cracks.

Crack nr	w_{max}	w_m	w_{max}/w_m
Object 1			
1	0.25	0.14	1.79
2	0.20	0.14	1.43
3	0.15	0.11	1.36
Object 2			
3	1.10	0.74	1.49
4	1.00	0.64	1.56
Object 4			
1	1.1	0.6	1.83
3	0.50	0.28	1.79
4	0.50	0.31	1.61
6	1.00	0.64	1.56
7	1.00	0.59	1.69
8	1.00	0.69	1.45
10	1.00	0.66	1.52
11	0.60	0.45	1.33
12	1.00	0.67	1.49

The table also illustrates the ratio between maximum crack width according to the observations and mean crack width according to the observations. Several different values for this ratio have been proposed in literature and it is therefore of interest to compare measurement results with the theoretical values.

The proposed value according to the previous Swedish design code, BBK, is 1.7. CEB (1985) on the other hand proposes two different values for the ratio, 1.7 for external loading and 1.3 for restraint loading (Engström, 2011). In addition to this, a

background document to EC2 presents a value of 1.7 for all types of loading (Corres Peiretti, et al., 2003) .

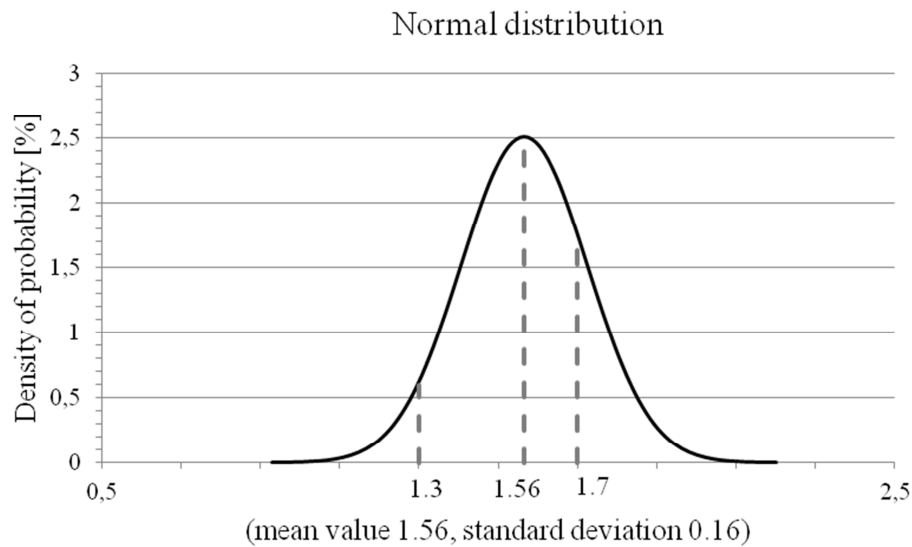


Figure 5.35 Normal distribution for ratio w_{max}/w_m of the measured cracks.

Figure 5.35 illustrates a normal distribution curve for the measured cracks. The curve was plotted using the calculated standard deviation of 0.16 and the mean value of 1.56. As can be seen from the graph, the mean value is between the two values proposed in literature. Consequently it can be argued that the measurements are likely to be accurate. Furthermore, it also indicates that it is more accurate to use 1.7 instead of 1.3 as the ratio for restrained loading.

6 Analysis using the direct stiffness method

There is no method in EC2 that directly considers shrinkage cracking as a result of external restraints. The method described in Section 4.3.6, according to Engström (2011), describes a crack risk evaluation taking into account the effect of external edge restraints. However, as discussed in Section 2.3.3, a slab-on-ground is affected by several external restraints, e.g. piles, perimeter strips and friction against the ground.

For the project a model to perform a crack risk evaluation from a more global perspective was developed. In order to efficiently consider the effect from multiple external restraints, the model was based on the direct stiffness method.

The described calculations were implemented in a Matlab program that, given inputs for a specific layout, calculates the stress distribution in a slab-on-ground as a result of restrained concrete shrinkage. The complete code of the program further explains each step in the calculation procedure and can be found in Appendix G. A brief description of the program structure is also given in Section 6.3.

6.1 Model concept

Figure 6.1 below illustrates how a slab section was idealised into a spring system. For further illustration regarding the positioning of piles in the slab see Figure 2.3.

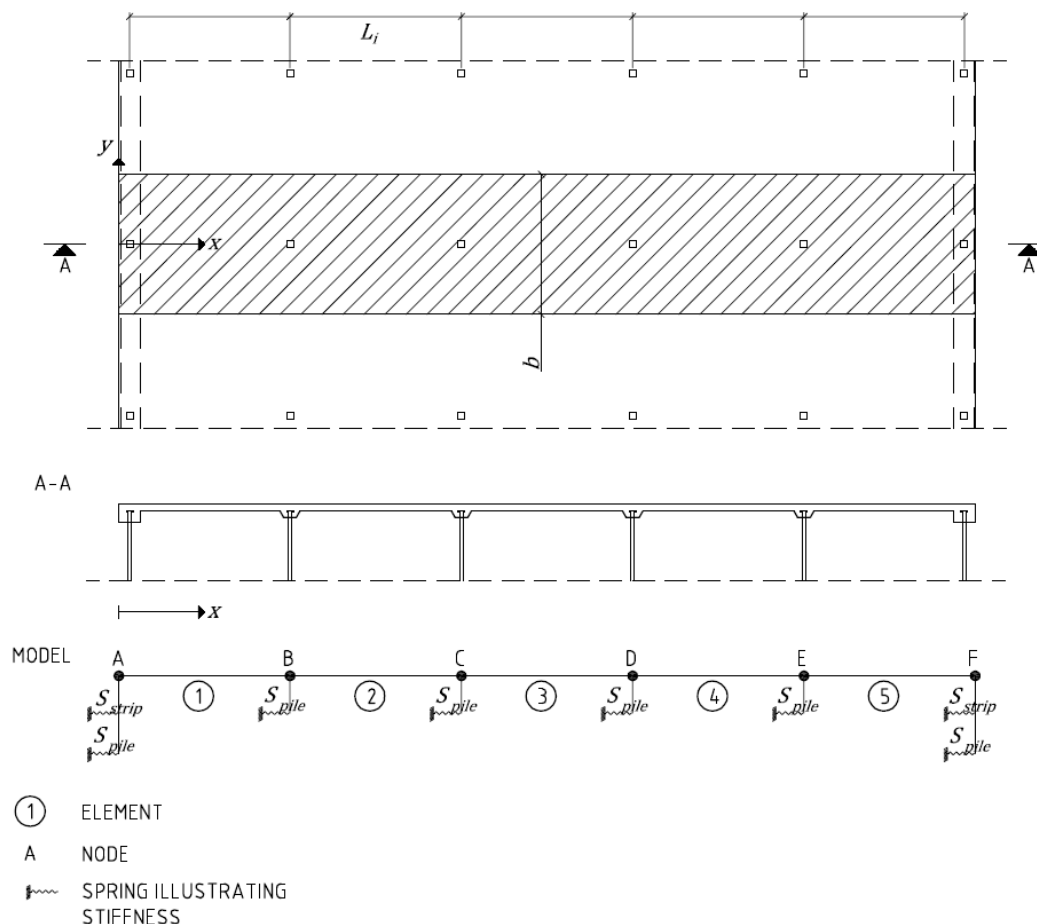


Figure 6.1 Idealisation of a pile-supported slab section into a spring system.

As previously mentioned, both piled and non-piled slabs-on-ground were covered in this project. However, for this method only piled slabs-on-ground were considered.

For a pile-supported slab the ground will settle over time and the slab will not be in contact with the ground (Hedebratt, 2005). Pile-supported slabs are therefore in most cases designed for one way or two way action, carrying imposed loads and self weight between the pile strips. Due to the settlement of the ground, for this model it was assumed that there is no contact between slab and sub-base, resulting in no friction.

6.2 General calculation procedure

This section will initially describe how the stiffness of the external restraints was determined. Followed by this it will be explained how the direct stiffness method was applied to determine the normal force distribution for a slab-on-ground. From the determined normal force the corresponding stress distribution in the slab was then calculated.

As illustrated in Figure 6.1, the influence width, b , needs to be determined. Considering the geometry of the slab, it could be assumed that the influence width should be chosen equal to the spacing of the piles. However, when b is reduced, the stiffness influence from the piles is increased and the final calculated normal force thereby increased. Since the maximum influence is equal to the spacing between the piles and since the actual influence is unknown, for this project it was generally assumed that the influence width is equal to the spacing of piles along the perimeter strip.

The stiffness of pile and perimeter strip restraints can be determined using a relationship between force, F_x , stiffness, S_i , and displacement, u_x , see Equation (6.1) below.

$$F_x = S_i * u_x \text{ [N/m]} \quad (6.1)$$

6.2.1 Stiffness of slab elements

The stiffnesses of the slab elements were modelled in accordance with the definition of axial stiffness of truss members. The model considered slabs with two layers of reinforcement, see Figure 6.2.

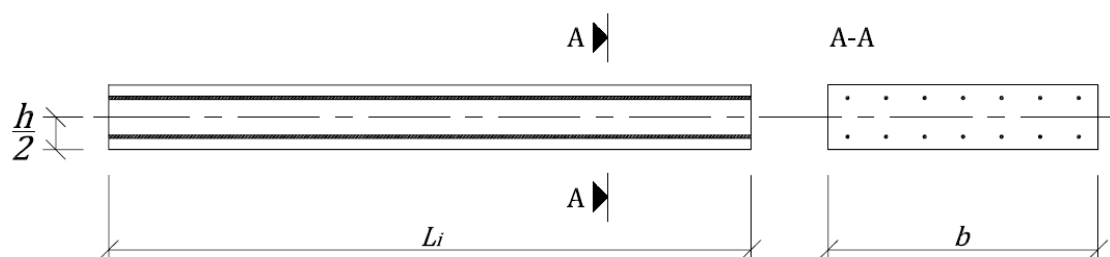


Figure 6.2 Slab section with two layers of reinforcement.

The area of the slab sections was considered as the transformed concrete area in the uncracked state, taking into account the effect of reinforcement. The following expression was used for the area of the transformed section.

$$A_{l,ef} = A_c + (\alpha_{ef} - 1) \cdot A_s \text{ [N/m]} \quad (6.2)$$

Since two layers of reinforcement were considered in the model, for simplicity reasons the calculations were performed on half the cross-sections. The transformed area can then be re-written according to Equation (6.3).

$$A_{l,ef} = \frac{h}{2} \cdot b + (\alpha_{ef} - 1) \cdot \frac{A_s}{2} \text{ [N/m]} \quad (6.3)$$

Since it is of interest to study the shrinkage effect over time, the effective elastic modulus of concrete was used. This was calculated using the creep coefficient for 50 years, following the procedure according to EC2, see Equation (6.4) below.

$$E_{c,ef} = \frac{E_{cm}}{1 + \varphi(50 \text{ years}, t_0)} \text{ [Pa]} \quad (6.4)$$

Using the above definitions, the axial stiffness of the slab elements can be expressed according to Equation (6.5).

$$S_{el,i} = \frac{E_{c,ef} A_{l,ef}}{L_i} \text{ [N/m]} \quad (6.5)$$

6.2.2 Stiffness of perimeter strips and slab thickenings

The stiffness from the perimeter strips and slab thickenings, S_{strip} , is dependent of the deformation of the subsoil, u , caused by the horizontal force, F_x . A common simplified approach when studying settlement of soil is to assume that the pressure under vertical load is distributed horizontally with an inclination of 1:2 (Sällfors, 2001). This approach was also adopted for this case, however in horizontal direction. Furthermore, it was assumed that the stress can only spread out in one direction, due to the location of the slab, see Figure 6.3.

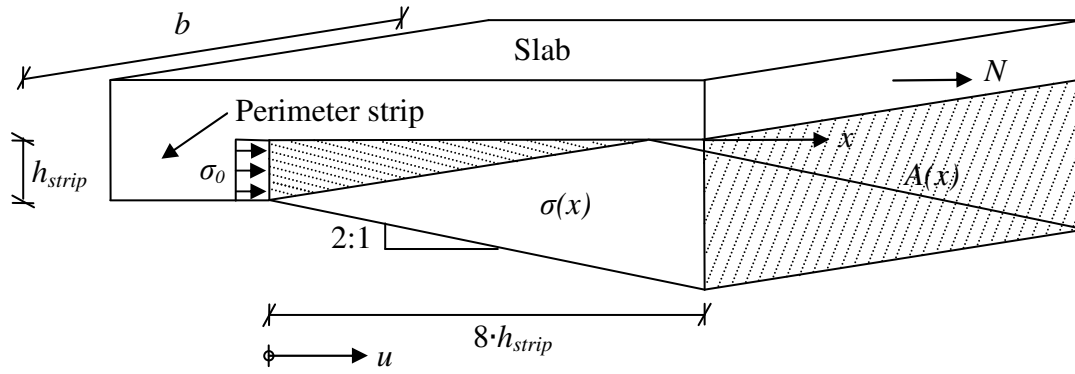


Figure 6.3 Schematic illustration of load distribution in soil from a perimeter strip.

As can be seen from the figure, the stress distribution can be described according to Equation (6.6) below.

$$\sigma(x) = \frac{N}{A(x)} = \frac{N}{b \cdot (h_{strip} + \frac{x}{2})} \text{ [Pa]} \quad (6.6)$$

Since the end displacement can be expressed as the integral of the strain, the following equation can be formulated.

$$\begin{aligned} u &= \int_0^x \varepsilon(x) dx = \{\text{Hooke's law}\} = \int_0^x \frac{\sigma(x)}{E} dx = \\ &= \frac{1}{E} \int_0^x \sigma(x) dx \text{ [m]} \end{aligned} \quad (6.7)$$

Combining Equation (6.6) and (6.7), the following equation can be derived.

$$u = \frac{N}{E \cdot b} \int_0^x \frac{1}{(h_{strip} + \frac{x}{2})} dx \text{ [m]} \quad (6.8)$$

Integration gives:

$$\begin{aligned} u &= \frac{2 \cdot N}{E \cdot b} [\ln(2 \cdot h_{strip} + x)]_0^x = \\ &= \frac{2 \cdot N}{E \cdot b} \{ \ln(2 \cdot h_{strip} + x) - \ln(2 \cdot h_{strip}) \} = \\ &= \frac{2 \cdot N}{E \cdot b} \left\{ \ln \left(\frac{2 \cdot h_{strip} + x}{2 \cdot h_{strip}} \right) \right\} \text{ [m]} \end{aligned} \quad (6.9)$$

In the above equation, the influence length of the deformation was left as a variable, x . Simplified settlement calculations of soil often consider the deformation to occur within a width equal to four times the width of the foundation (Das, 2011).

The same approach was adopted for the perimeter strip in horizontal direction. However, since the load is prevented to spread upwards due to the slab, the load was therefore considered to have an effect over a distance of eight times the width, hence $x = 8 \cdot h_{strip}$, this results in the following expression.

$$u = \frac{2 \cdot N}{E \cdot b} \left\{ \ln \left(\frac{2 \cdot h_{strip} + 8 \cdot h_{strip}}{2 \cdot h_{strip}} \right) \right\} = \frac{2 \cdot N}{E \cdot b} \ln(5) \text{ [m]} \quad (6.10)$$

By rearranging this equation, the stiffness of perimeter strips and slab thickenings can now be found.

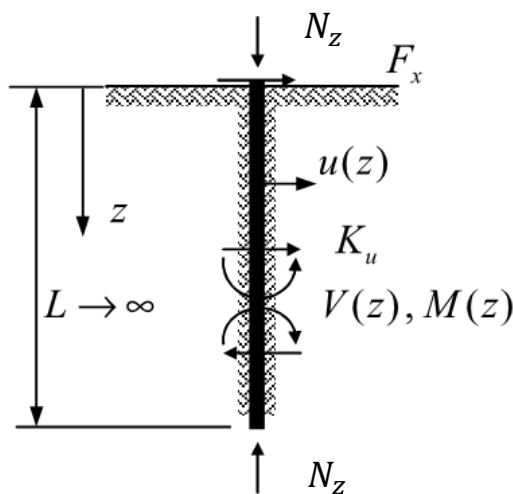
$$N = \frac{E \cdot b}{2 \cdot \ln(5)} \cdot u \text{ [N]} \quad (6.11)$$

where
$$S_{strip} = \frac{E \cdot b}{2 \cdot \ln(5)} \text{ [N/m]} \quad (6.12)$$

In order to calculate Equation (6.12), the influence width and the elastic modulus of the ground material need to be known. Since the perimeter strip only affects the top layer of the ground, the sub-base and sub-grade, which most often consists of various type of gravel, for the cases considered in this project, the elastic modulus was assumed as 100 MPa. According to Bolteus (1984), the elastic modulus of dense sand and gravel range from 80 MPa – 200 MPa.

6.2.3 Stiffness of piles

Since pile-supported slabs-on-ground are considered, the horizontal restraint from piles needs to be determined. This requires that both the deflection of the piles and the deformation of the soil are regarded. For the project this was performed by analysing the piles as beams resting on Winkler foundations. An elementary case according to Figure 6.4 below was adopted.



where:

- N_z = vertical normal force
- F_x = horizontal force
- u = horizontal displacement
- z = depth
- K_u = bed modulus
- V = shear force
- M = moment
- L = pile length

Figure 6.4 Elementary case for pile on Winkler foundation (Svahn & Alén, 2006).

For the project it was assumed that the connection of the piles to the slab is hinged and, as a result, that no moment is transferred at this point. In reality the connection is not entirely pinned, but due to the relative small thickness of the slab in relation to the length of the piles, the short embedment length of the pile motivates this assumption.

In order to determine the stiffness, as previously described, the relation between the transverse load and the deflection for $z = 0$ needs to be determined. This can be expressed as follows for pile number i .

$$N_x = S_{pile,i} \cdot u(z = 0) \text{ [N]} \quad (6.13)$$

In reality the horizontal stiffness of the pile is affected by the axial vertical load it is subjected to. When the load is increased the stiffness of the pile is reduced. However, since a large horizontal stiffness constitutes a greater restraint, the effect of vertical loads acting on the piles was neglected for this project.

Since pile-supported slabs are used when the bearing capacity of the soil is low, this mainly occurs when the soils consist of clay. As a result of this, the bed modulus, k_u , for clay was assumed to be representative for the entire ground, neglecting the top layers of sub-grade and sub-base. An approximate method according to Equation (6.14) below to determine the bed modulus, taking into account the effect of creep, proposed by Svahn & Alén (2006), was adopted.

$$k_u = 50 \cdot \frac{c_u}{b} \text{ [N/m}^3\text{]} \quad (6.14)$$

where $c_u =$ undrained shear strength [Pa]
 $b =$ pile width [m]

In accordance with the elementary case presented in Figure 6.4 for a pile without any vertical axial force, the horizontal pile stiffness can be calculated according to Equation (6.15) below.

$$S_{pile} = \frac{2 \cdot EI}{L_g^3} \text{ [N/m]} \quad (6.15)$$

where $L_g = \sqrt[4]{\frac{4 \cdot EI}{k_u}} \text{ [m}^{\frac{5}{4}}\text{]}$

Since the expression involves the second moment of inertia, the dimensions of the pile and the reinforcement amount must be known in order to determine the stiffness. For this project pile type SP1 was assumed; this is also the pile type used for all studied objects according to Section 5. Pile type SP1 has properties according to Table 6.1.

Table 6.1 Pile properties of assumed pile type.

Pile type	Dimension	Reinforcement bars	
	Pile width [mm]	Amount	Φ [mm]
SP1	235	4	16

Adopting the above pile properties, the resulting horizontal pile stiffness was determined for different soil types according to Table 6.2 below.

Table 6.2 Calculated pile stiffness in relation to soil characteristics, material data adopted from Sällfors (2001) and Svahn & Alén (2006).

Soil characteristics	c_u [kPa] (Undrained shear strength)	S_{pile} [N/m] (Pile stiffness)
Very firm	200	$12.38 \cdot 10^6$
Firm	100	$7.362 \cdot 10^6$
Semi-firm	50	$4.377 \cdot 10^6$

For this project the undrained shear strength was assumed as 50 kPa and the corresponding pile stiffness was adopted in the calculations. However, in a design situation it has to be determined for the present ground conditions. It should be noted that varying soil characteristics and pile types over a studied section will cause a stiffness variation between piles; this variation is neglected in the model.

Global stiffness matrix

Once each stiffness was determined they were assembled into a global stiffness matrix. Since the system only has one degree of freedom per node and since the elements are placed on a straight line along the x-axis, the stiffness matrix from the slab elements will have the form according to Equation (6.17) below.

$$\mathbf{K}_{el} = \begin{bmatrix} (S_{el,1}) & (-S_{el,1}) & 0 & 0 & 0 \\ (-S_{el,1}) & (S_{el,1} + S_{el,2}) & (-S_{el,2}) & 0 & 0 \\ 0 & (-S_{el,2}) & (S_{el,2} + S_{el,3}) & \dots & 0 \\ 0 & 0 & \vdots & \ddots & (-S_{el,n}) \\ 0 & 0 & 0 & (-S_{el,n}) & (S_{el,n}) \end{bmatrix} \quad (6.16)$$

Since the external stiffness are acting on the nodes, for a general case with both perimeter strips and piles, the stiffness matrix for the restraints will be according to Equation (6.17) below.

$$\mathbf{K}_{restr} = \begin{bmatrix} (S_{strip} + S_{pile}) & 0 & 0 & 0 & 0 \\ 0 & (S_{pile}) & 0 & 0 & 0 \\ 0 & 0 & (S_{pile}) & \dots & 0 \\ 0 & 0 & \vdots & \ddots & 0 \\ 0 & 0 & 0 & 0 & (S_{strip} + S_{pile}) \end{bmatrix} \quad (6.17)$$

In order to calculate the global stiffness matrix the two matrices were combined according to Equation (6.18).

$$\mathbf{K} = \mathbf{K}_{el} + \mathbf{K}_{restr} \text{ [N/m]} \quad (6.18)$$

6.2.4 Centre of movement

In order to further highlight the slab behaviour the centre of movement was determined. As the system shrinks towards the location where the stiffness is balanced, i.e. the section with no movement in x-direction, this will be a section in the region of the highest normal force and stress.

The centre of movement was determined according to Equation (6.19), which was modified from Engström (2011) in order to take the stiffness of the slab into account. The equation finds the centre of movement through weighting each stiffness with its location and then dividing with the stiffness of the entire system.

$$x_o = \frac{\sum_n (S_i \cdot x_i) + \frac{EA}{L_{tot}} \cdot \frac{L_{tot}}{2}}{\sum_n S_i + \frac{EA}{L_{tot}}} \text{ [m]} \quad (6.19)$$

The location for centre of movement is illustrated as an asterisk in the plots in Section 6.4.

6.2.5 Load definition

The force acting on each element is a result of concrete shrinkage. Studying Figure 6.5 there are two forces defined based on each element strain. The free shrinkage strain of plain concrete will be ε_{cs} and the force applied to elongate the plain concrete element to its original length will be $\varepsilon_{cs} \cdot E_{c,ef} \cdot A_c$. However, studying the reinforced concrete element the free shrinkage is restrained by the reinforcement, causing the resulting shortening to be less than the free shrinkage. The free shortening of the reinforced concrete member will be $|\varepsilon_{cs}| - \varepsilon_c$ and the corresponding force applied to elongate the element to its original length will be according to Equation (6.20). This is the force which was implemented on each element in the program.

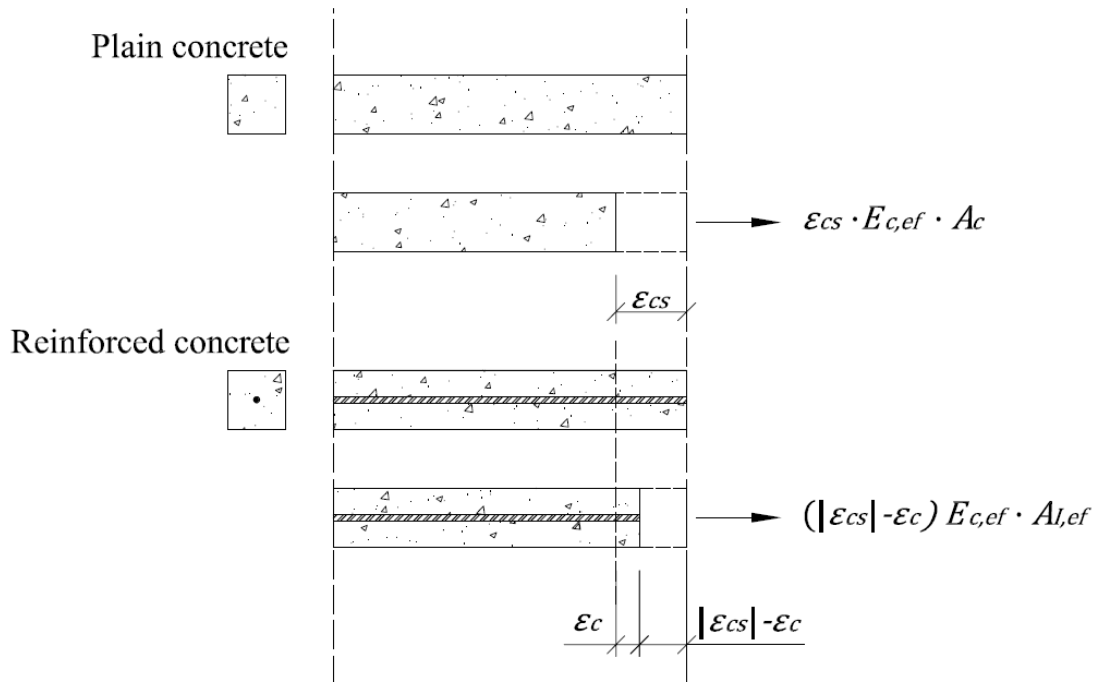


Figure 6.5 Force definition.

$$F = (|\epsilon_{cs}| - \epsilon_c) \cdot E_{c,ef} \cdot A_{l,ef} \text{ [N]} \quad (6.20)$$

Introducing the shrinkage force F_{cs} as described in Section 4.3.6 according to Engström (2011), the concrete strain can be written according to Equation (6.21).

$$\epsilon_c = \frac{F_{cs}}{E_{c,ef} \cdot A_{l,ef}} \text{ [-]} \quad (6.21)$$

where $F_{cs} = \epsilon_{cs} \cdot E_s \cdot A_s \text{ [N]}$
 = the force acting on the concrete section
 caused by the internal restraint

Inserting Equation (6.21) into Equation (6.20) the following equation for the applied force can be written.

$$F = \left(|\epsilon_{cs}| - \frac{F_{cs}}{E_{c,ef} \cdot A_{l,ef}} \right) \cdot E_{c,ef} \cdot A_{l,ef} \text{ [N]} \quad (6.22)$$

Each element force is assembled forming the global force vector \mathbf{F} , which is used to solve the system displacements.

6.2.6 Solution

Once the global stiffness matrix and the global force vector are determined the equation system can be expressed according to Equation (6.23), where \mathbf{u} is the nodal displacement vector.

$$\mathbf{F} = \mathbf{K} \cdot \mathbf{u} \text{ [N]} \quad (6.23)$$

The displacements can then be found using the inverse of the stiffness matrix according to the following matrix operation.

$$\mathbf{u} = \mathbf{K}^{-1} \cdot \mathbf{F} \text{ [m]} \quad (6.24)$$

Once the displacements are known the normal force vector caused by the external restraints, \mathbf{N} , can be calculated. The normal force vector contains normal forces for each element in the system. In order to find the concrete stress for each element Equation (6.25) is used, this equation sums up the effect from the external and internal restraints.

$$\sigma_{c,i} = \frac{N_i + F_{cs}}{A_{I,ef}} \text{ [Pa]} \quad (6.25)$$

6.3 Program structure

The described calculations were performed in a program developed in Matlab. The program structure is illustrated in Figure 6.6. The shaded areas mark the calculations and inputs, which are specified in the main file. The main file is object specific and must be adapted to each studied case. The white areas in Figure 6.6 illustrate operations performed by a function file, which is called out by the main file. The function file is of universal application and based on the input parameters in the main file it calculates and sends back the results to the main file. All program code is shown and commented in Appendix G, where three main files and one function file are presented.

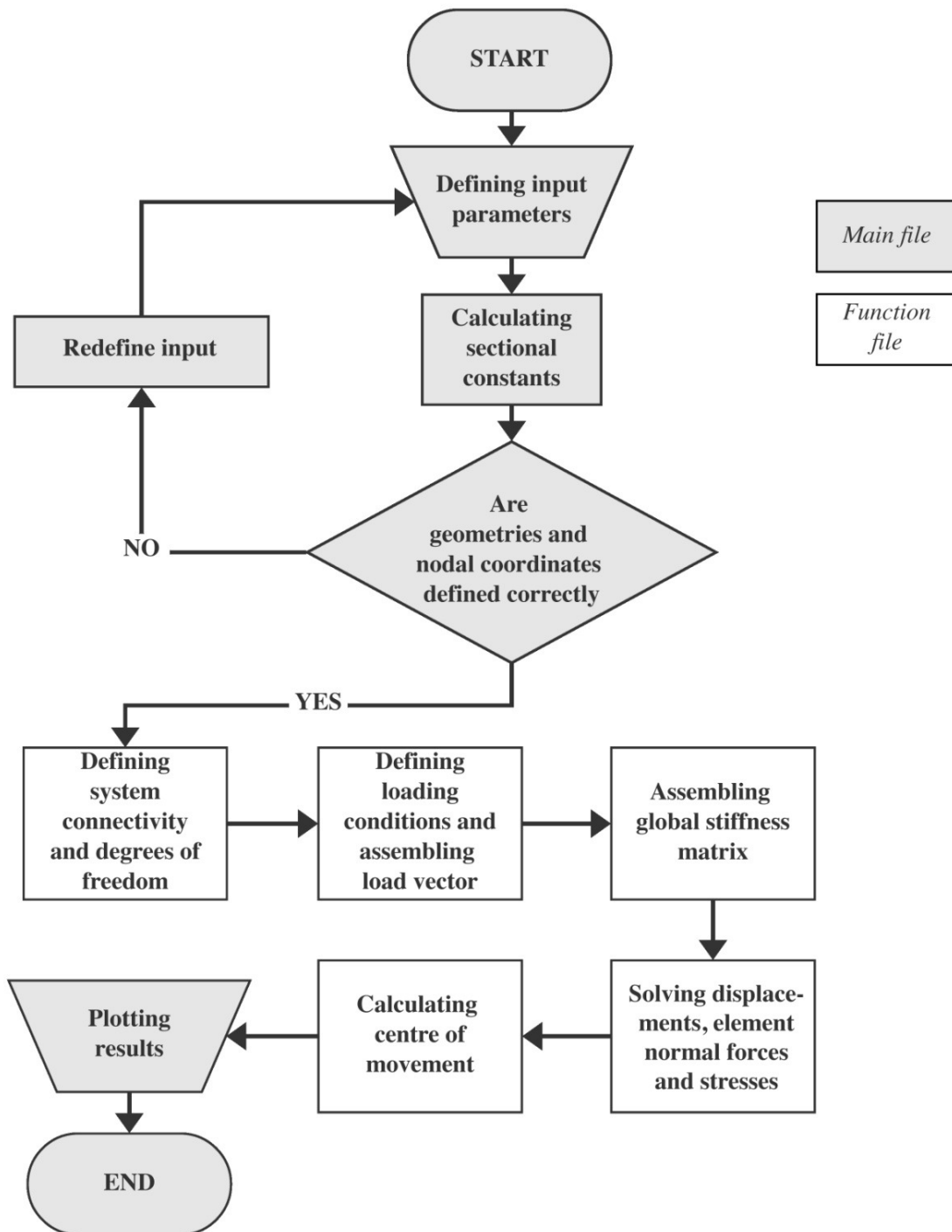


Figure 6.6 Flowchart of program structure.

6.4 Application of method

The described calculation procedure was applied to the generic model presented in Figure 6.1 and also to object 1 and 2 that were described in Section 5.

For both object 1 and 2 cracking that was suspected to be a result of restrained shrinkage was found. Due to this it was found relevant to research whether the calculation model would produce results similar to the observations.

Table 6.3 below contains input values for the Matlab program for each studied case. For the generic model the concrete class was chosen based on the recommendation from the Swedish Concrete Association (2008), see Section 4.1.

Table 6.3 Input values to the model for each studied case.

Object	Concrete class	Geometry [m]			Main reinforcement		Nominal concrete cover [mm]
		Thickness	Pile spacing along axis		Top	Bottom	
			x	y			
Generic	C30/37	0.25	8	8	Ø12s150 mm#	Ø12s150 mm#	30
1	C20/25	0.22	3.3*	3.3	Ø10s125 mm#	Ø10s125 mm#	25
2	C25/30	0.20	3.2**	3.2	Ø8s150 mm#	Ø8s150 mm#	20

* The second last pile has a perimeter strip and the last pile spacing is 5 m.
 ** The last spacing is 2.4 m and is without a pile.

Table 6.4 below shows input values for concrete properties for each case. The values were calculated considering a service life of 50 years. The effective modulus of elasticity of concrete was calculated according to Equation (7.1).

Table 6.4 Input values to the model regarding concrete properties for the different cases.

Object	Concrete class	Concrete properties (for 50 years)		
		f_{ctm} [MPa]	$E_{c,ef}$ [GPa]	ϵ_{cs} [-]
Generic	C30/37	2.9	9.272	$-4.025 \cdot 10^{-4}$
1	C20/25	2.2	6.591	$-4.326 \cdot 10^{-4}$
2	C25/30	2.6	7.173	$-4.278 \cdot 10^{-4}$

6.4.1 Calculation for generic model

The general geometry for this model is illustrated in Figure 6.1 and input data are presented in Table 6.3.

Figure 6.7 below presents the results from the calculations. The green line indicates the concrete stress in each element and the red dashed lines illustrate the tensile strength for concrete, which was calculated using the reduction due to sustained loading, see Equation (3.3). The calculated end displacement of the slab is 4.8 mm, same on each side due to symmetry.

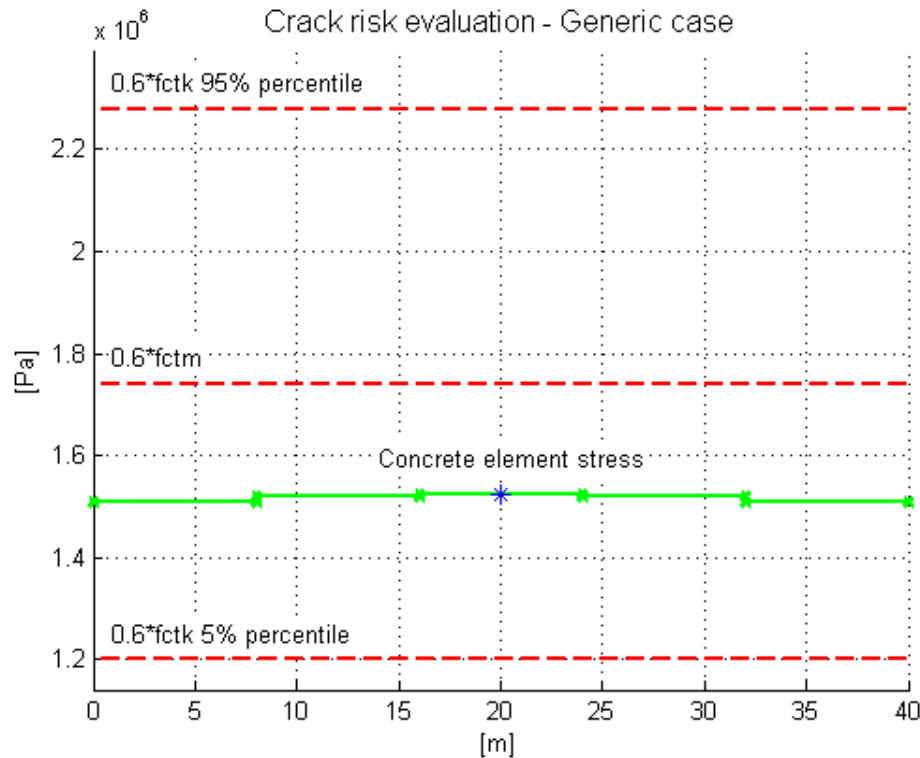


Figure 6.7 Results from calculations for the generic model. The green line indicates the concrete stress in elements and the red dashed lines indicate strength. The asterisk illustrates the region of maximum stress according to Equation (6.19).

As can be seen from the results, the calculated stress is above the reduced value of the lower percentile for strength and as a result a risk of cracking exists. The fact that the stress distribution is nearly uniform along the slab length illustrates that the influence from the piles is very small compared with the influence from the perimeter strips.

6.4.2 Object 1

For object 1 the most appropriate slab section to study was deemed to be in casting step B where crack No. 1 is located. Figure 6.8 below illustrates a plan view of the studied slab.

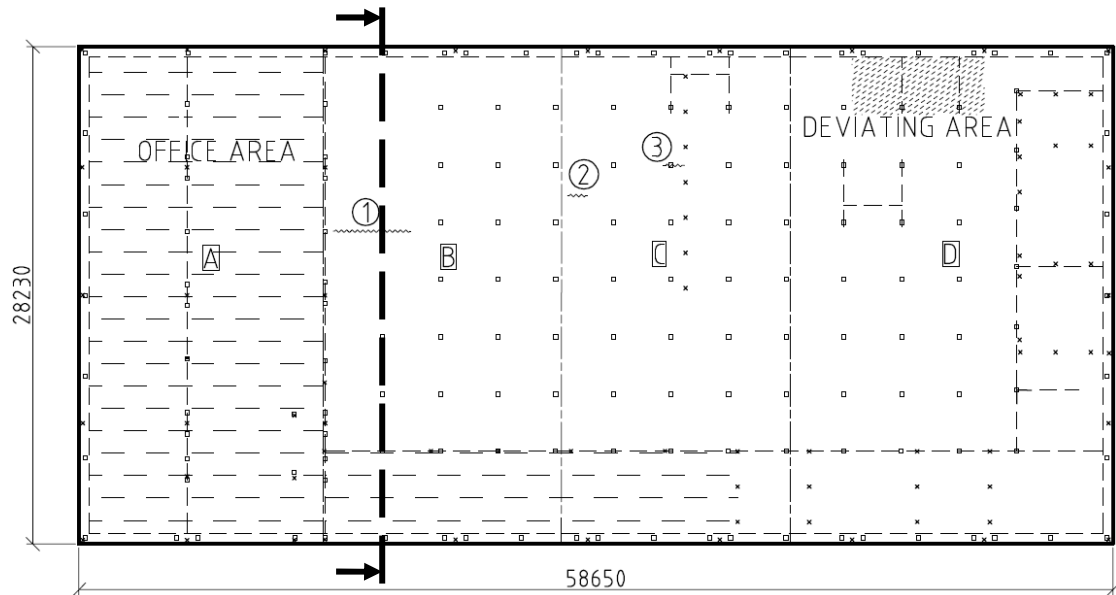


Figure 6.8 Floor plan view of object 1 illustrating the studied section of the slab.

As can be seen in Figure 6.9 below which illustrates the studied slab section, there is an additional slab thickening at node H and slab element 8 is longer than the other elements.

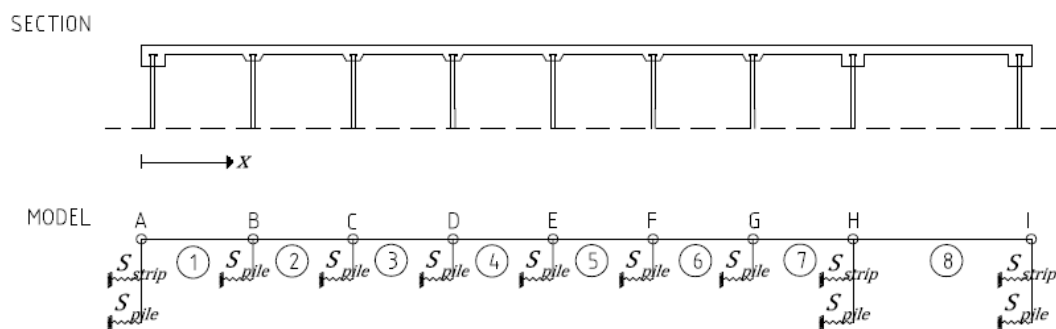


Figure 6.9 Illustration of studied slab section and corresponding stiffness model for object 1.

The results from the calculations are illustrated in Figure 6.10. As can be seen, the calculations indicate that the reduced mean strength will be reached in the slab and that the maximum stress is expected in element 5. Since the measured crack is found in element 4, the results differ slightly from the observed response of the floor. Since the last two nodes, node H and I, contain a slab thickening and a perimeter strip respectively and since the maximum concrete stress is shifted to the right, it is likely

that the additional stiffness at these nodes, S_{strip} , are too large in the calculations compared with reality.

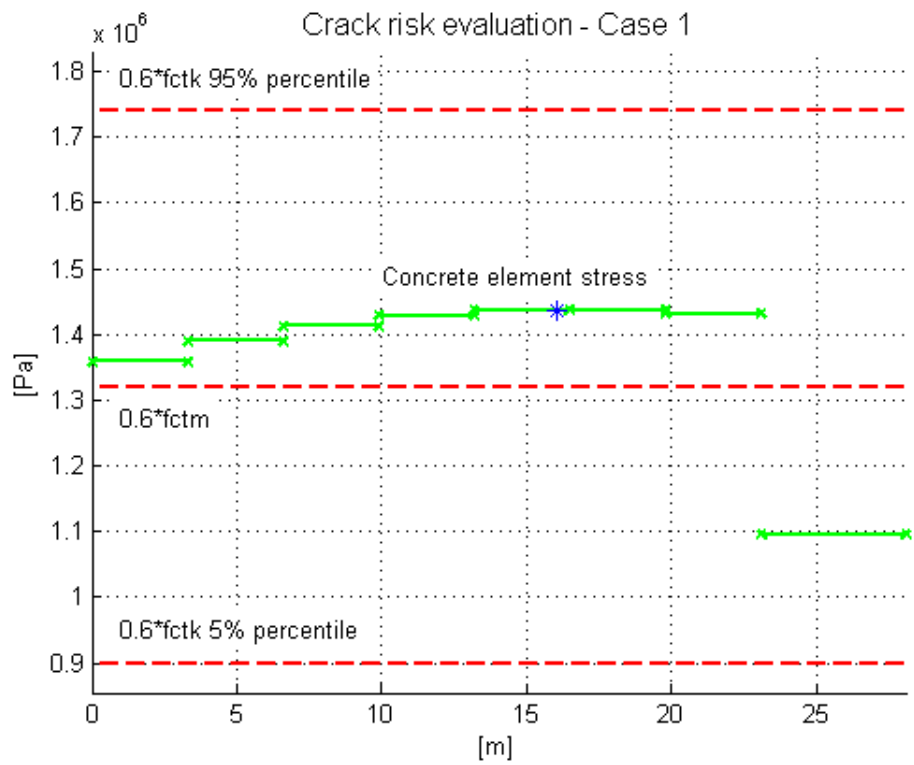


Figure 6.10 Results from calculations for object 1. The green line indicates the concrete stress in elements and the red dashed lines indicate strength. The asterisk illustrates the region of maximum stress according to Equation (6.19).

The calculated end displacement of the slab is 3.7 mm on the left side in node A and 2.7 mm on the right side in node I. The reason for the lower displacement on the right side is due to the increased stiffness of the additional perimeter strip. As a result, the centre of movement is not located in the middle of the slab.

6.4.3 Object 2

For object 2 the most appropriate area to study was deemed to be casting step A, see Figure 6.11 which illustrates which part of the slab that was studied.

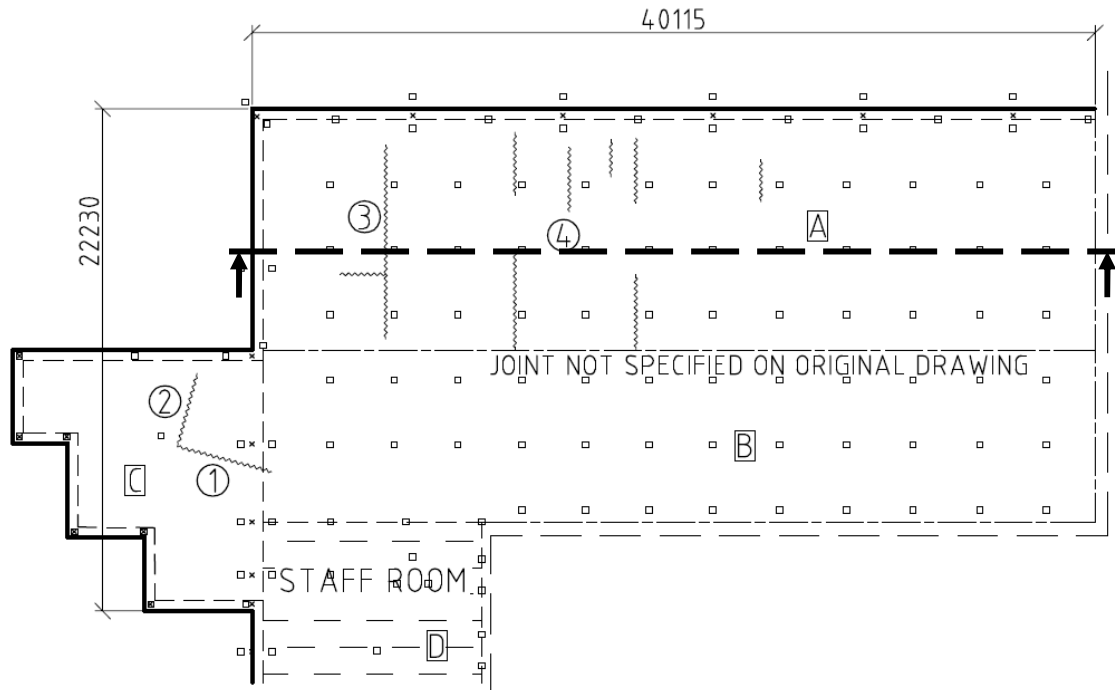


Figure 6.11 Floor plan view of object 2 illustrating studied slab section.

As can be seen from Figure 6.12 below, which illustrates the studied casting step, there is no perimeter strip on the right hand side in node N. In addition to this, element 13 is slightly shorter than the others.

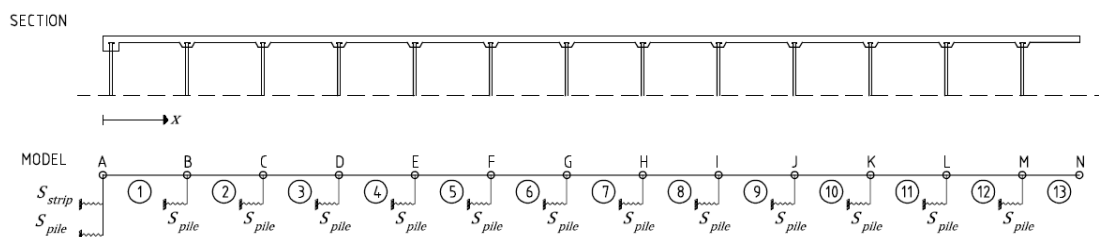


Figure 6.12 Illustration of studied slab section and corresponding stiffness model for object 2.

The results from the calculations are illustrated in Figure 6.13 below. The calculated concrete stress is lower than the reduced lower percentile of the strength. This does not coincide with the observed response of the floor, since cracking had occurred. However, the calculated stress distribution matches the area showing the most severe cracking. Due to the lack of a perimeter strip in node N, the stress distribution is shifted to the left where a perimeter strip exists. It can also be seen that the further away from the perimeter strip, the greater is the influence from the piles.

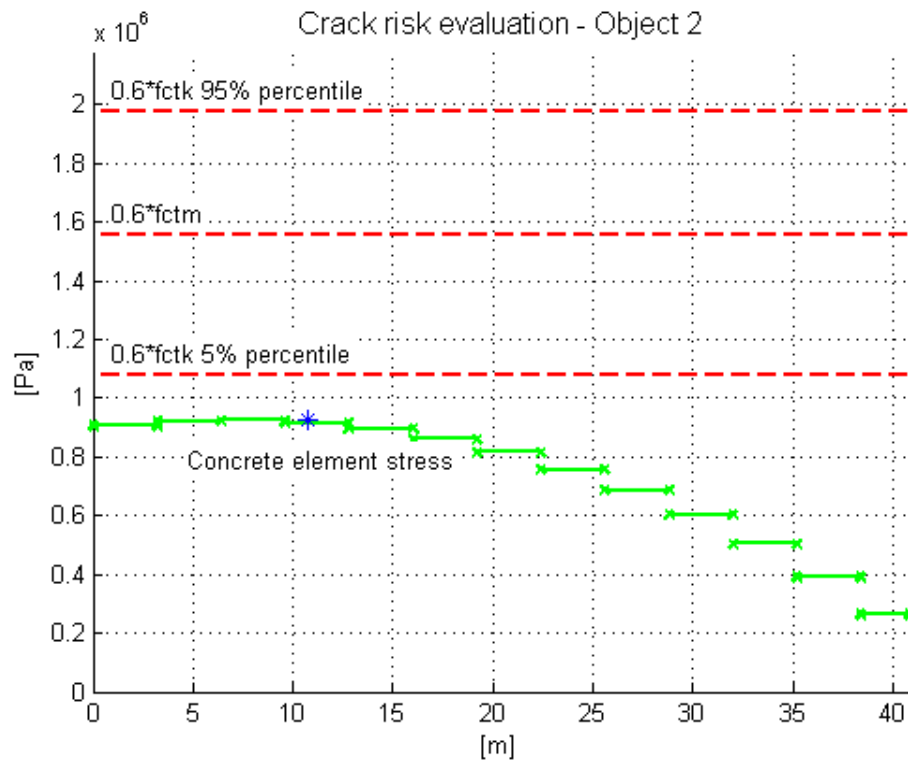


Figure 6.13 Results from calculations for object 2. The green line indicates the concrete stress in elements and the red dashed lines indicate strength. The asterisk illustrates the region of maximum stress according to Equation (6.19).

The calculated end displacement of the slab is 2.2 mm on the left side in node A and 11.1 mm on the right side in node N. The reason for the increased displacement on the right side is due to the lack of a perimeter strip. Assuming that the adjacent casting section also experiences the same end displacement, the resulting joint opening will exceed 20 mm, which is often the maximum joint opening for dilatation joints as described in Section 2.2.3. When the maximum joint opening of the dilatation joint is exceeded, the joint will transfer stresses, changing the behavior of the studied section. It is possible that this has occurred for object 2 and this could explain why stresses leading to cracking have been developed.

6.5 Evaluation

The developed method is based on several assumptions and in order to evaluate their effect, a parametric study was performed based on data for the generic case.

In addition to this, a second parametric study was performed in order to evaluate the effect from possible choices during the design process.

6.5.1 Evaluation of assumptions

The parametric study made it possible to assess which impact changing certain parameters have on the results. Figure 6.14 below illustrates the result from the parametric study. The following changes to the model were studied independently:

- Reducing the elastic modulus of the ground from 100 MPa to 75 MPa, which affects stiffness from perimeter strips and slab thickenings.
- Reducing the influence width, b , by 50%, from 8 m to 4 m.
- Increasing the undrained shear strength of clay from 50 kN/m² to 200 kN/m², which affects the stiffness from piles. This equals changing the soil characteristics from semi-firm to very firm, see Table 6.2.

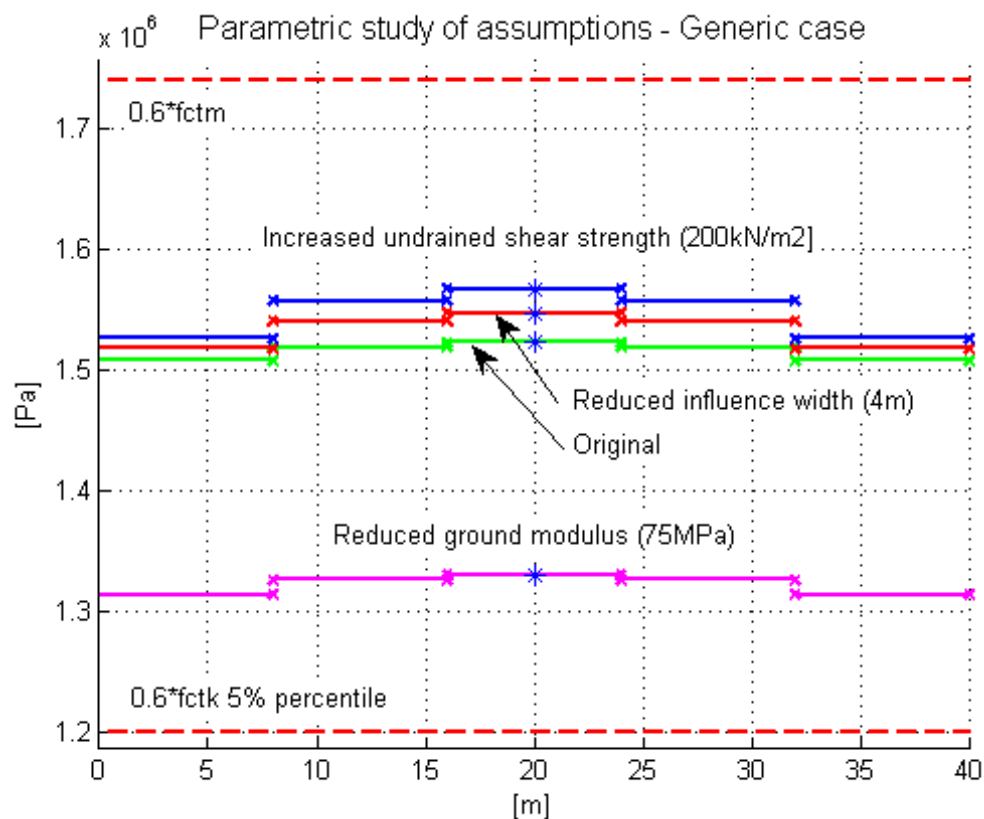


Figure 6.14 Parametric study of assumptions for the model, illustrated for the generic case.

In order to further evaluate the influence from each parameter, the change of concrete stress in percentage per change of each parameter in percentage was calculated. The results are illustrated in Table 6.5 below. As can be seen from the table, the elastic modulus of the ground has a greater influence on the concrete stress than the other parameters. If the elastic modulus is changed 1% the stress increases 0.51%.

Table 6.5 Summary of parametric study and influence on concrete stress from each parameter.

Parameter	Change of parameter			Change of stress ($\sigma_{c,max,0} = 1.53\text{MPa}$)		Influence of parameter $\left(\frac{\Delta\sigma}{\Delta par}\right)$ [%/%]
	Before	After	$\Delta_{par}[\%]$	$\sigma_{c,max}$ [MPa]	$\Delta\sigma$ [%]	
E_{ground} [MPa]	100	75	- 25	1.33	- 12.64	0.51
b [m]	8	4	- 50	1.55	+ 1.62	0.032
c_u [kPa]	50	200	+ 300	1.57	+ 2.03	0.0059

However, the influence of the parameters is in reality more complex than what the table illustrates. The normal force is also influenced by the relation between the different restraints. If the restraint from perimeter strips and slab thickenings is reduced, the influence from piles will be greater. In the present model the large restraint from the perimeter strips and slab thickenings causes the piles to have a small influence.

Since both the elastic modulus of the ground and the undrained shear strength have been assumed in the calculations, the magnitude of the calculated forces can be questioned. In a design situation these parameters would be required from a geotechnical investigation to improve the accuracy of the results.

In addition to uncertainties with the described parameters, the methods by which the stiffnesses from the external restraint have been determined also need further evaluation. This could be performed through a more detailed FEM-analysis or through full-scale testing of the restraints.

6.5.2 Evaluation of design measures

In order to reduce the tensile force in a section of a slab-on-ground studied with the developed model, several measures are possible. With the aim of evaluating their influence, a second parametric study was performed, this time varying different design measures. The different measures are listed below and the results are illustrated in Figure 6.15.

- In accordance with the recommendation by the Swedish Concrete Association (2008), as stated in Section 4.1, the original model is calculated for concrete class C30/37. The effect of lowering the recommended concrete class is evaluated by calculating the concrete stresses for a concrete class of C20/25.
- The influence of changing the reinforcement amount is illustrated by lowering the amount to a single centric layer of $\emptyset 12s150$ mm compared to the original amount of two layers of $\emptyset 12s150$ mm. The thickness of the slab was kept constant.
- As was explained in Section 3.2.6, a reduction of concrete shrinkage by up to 25-50% can be achieved by incorporating shrinkage reducing additives in the concrete mix (Fjällberg, 2002). Due to this, it was evaluated which influence a reduction of shrinkage strain by 25% would have.
- The design measure of varying the slab thickness was also evaluated by increasing the thickness from 250 mm to 350 mm.

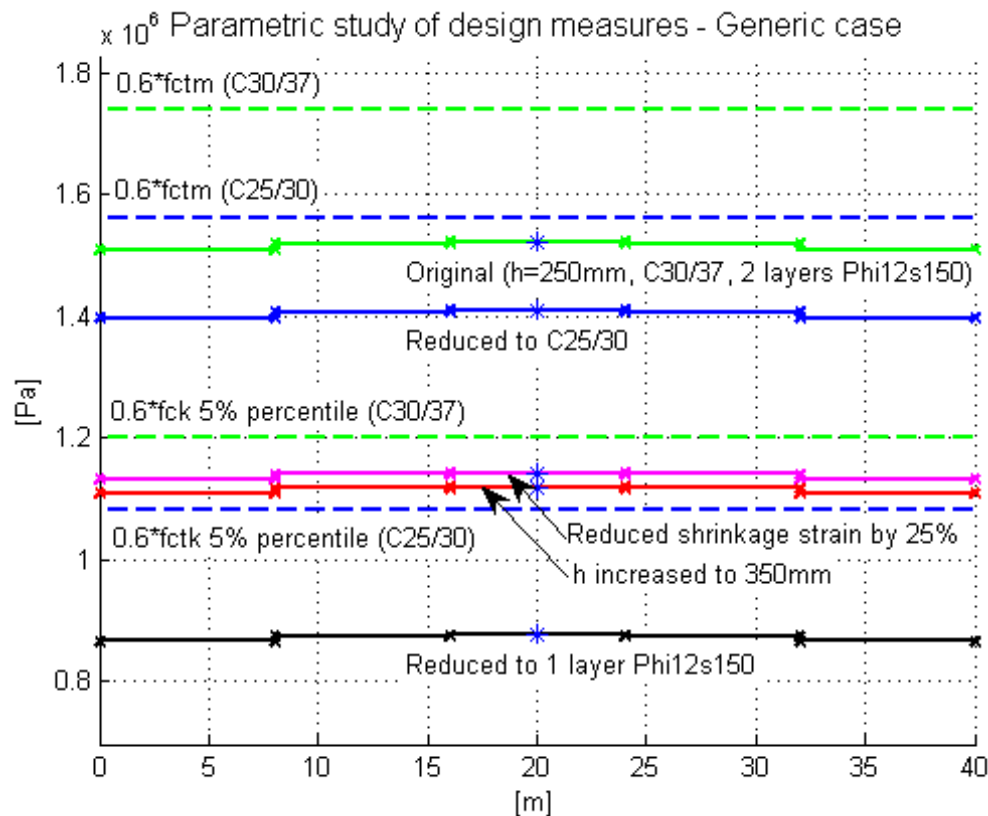


Figure 6.15 Parametric study of input parameters for the generic case.

Changing concrete strength class affects shrinkage strain, tensile strength and effective modulus of elasticity. As can be seen from Figure 6.15, both concrete stress and stress are therefore changed. Even though the concrete stress is decreased, the capacity is decreased to a greater extent, resulting in an increased risk of cracking. Reducing the concrete strength class allows for a decrease of minimum reinforcement, see Equation (4.8). This has however been neglected here.

To study the response before cracking with a lowered reinforcement amount, a section with one layer of reinforcement $\text{Ø}12\text{s}150\text{ mm}$ was studied. This is illustrated following the black line in Figure 6.15. As the reinforcement amount is lowered the internal restraint is lowered, which results in a lowered concrete stress. However, when a crack is formed, the crack width will be larger as the steel stress will increase over the crack. This lowered amount of reinforcement might not be capable of distributing the cracks sufficiently, resulting in non-controlled cracking.

The shrinkage strain was lowered by 25%, as illustrated following the purple line in Figure 6.15. As the shrinkage strain is decreased the resulting stress is also decreased. Consequently by incorporating shrinkage reducing additives in the concrete mix, the risk of cracking can be lowered.

By increasing the thickness of a slab-on-ground the sectional tensile capacity increases before cracking. Consequently the time dependent modulus of elasticity and shrinkage strain are also affected, as the shape coefficient for the section is changed. Both of these properties are lowered when increasing the slab thickness. However, it should be noted that the minimum reinforcement amount needed for an increased slab thickness will be larger, see formula (4.8).

7 Non-linear analytical friction model

As mentioned in Section 2.4, the friction between a slab-on-ground and the sub-base is commonly considered assuming a coefficient of friction. This is however a simplified method that does not accurately describe the frictional behaviour.

In the following chapter a model to analytically calculate the effect of friction against the sub-base for a slab-on-ground is described. This is performed using non-linear friction stress to slip relations, adapted from data of full-scale testing performed by Pettersson (1998).

The study was performed in analogy with the methodology used studying bond-slip of reinforcement bars in reinforced concrete. This was done in order to evaluate the resulting concrete stress due to friction stress. For detailed calculations see Appendix H.

7.1 Friction tests performed by Pettersson (1998)

The friction is not uniform along the length of a slab as it is experiencing shrinkage, but rather a function of the local slip at each point. In reality when a slab-on-ground slides along a sub-base, it needs to experience a certain slip before the maximum friction is reached. This is however neglected when a constant coefficient of friction is used. Full friction is then considered to be achieved instantaneously.

The graphs in Figure 7.1 to Figure 7.3 illustrate test results performed by Pettersson (1998). The graphs also contain approximations to the test results using different equations. Three different cases with regard to different sub-bases were considered for the model, numbered case 1-3.

The test results were all performed subjected to a vertical load of $3 * SW$. Since no friction will be present if there is no vertical load, the adapted load is assumed to have been used in order to achieve full contact between slab and sub-base.

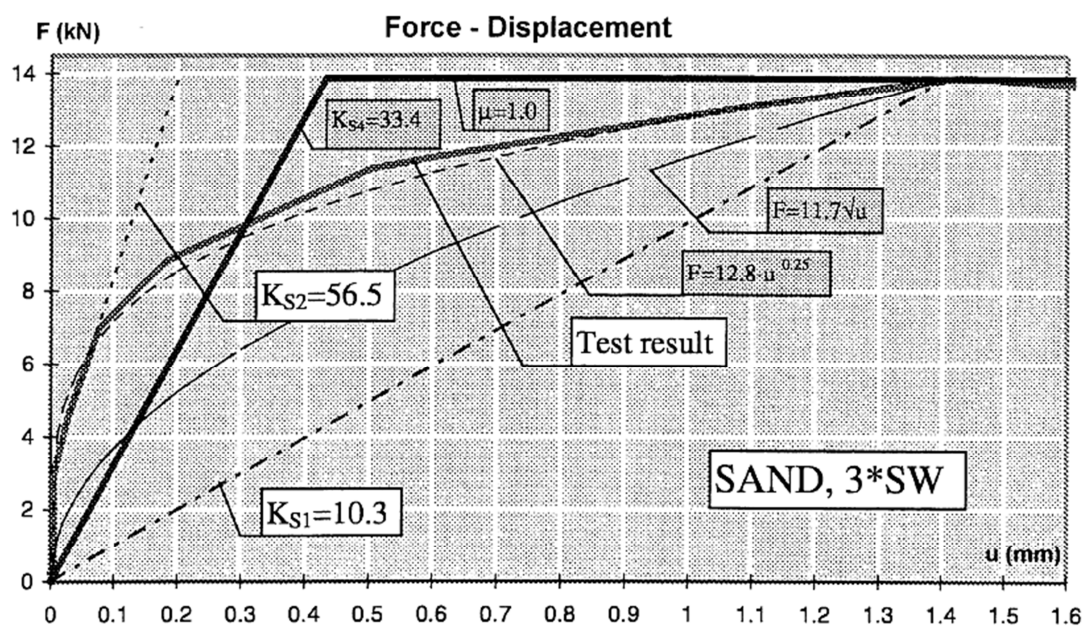


Figure 7.1 Test results for sand as sub-base (case 1) (Pettersson, 1998).

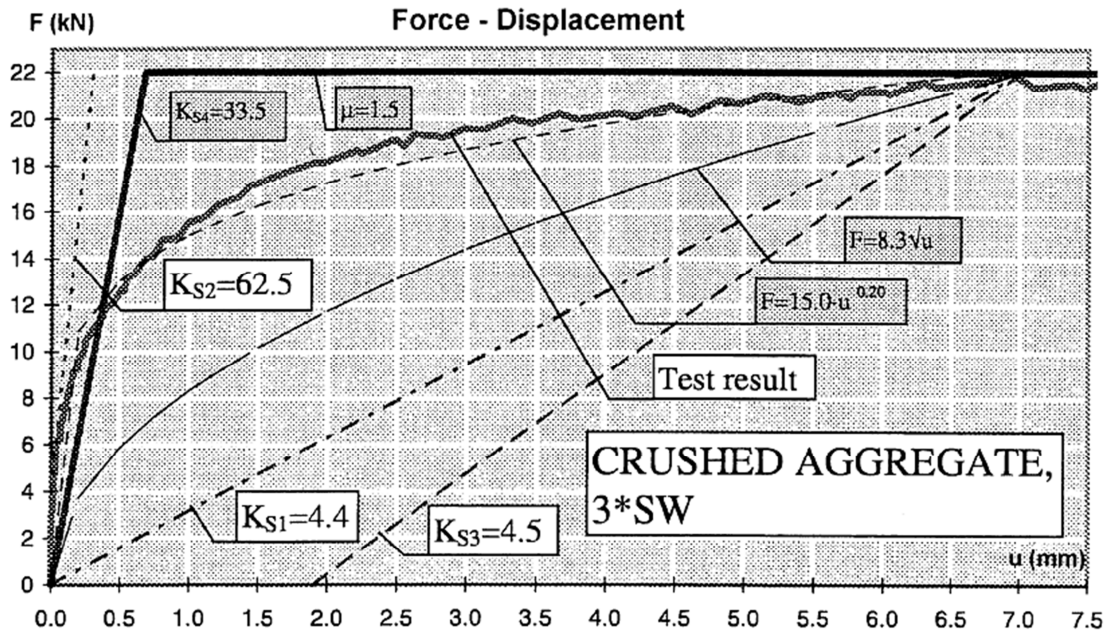


Figure 7.2 Test results for crushed aggregate as sub-base (case 2) (Pettersson, 1998).

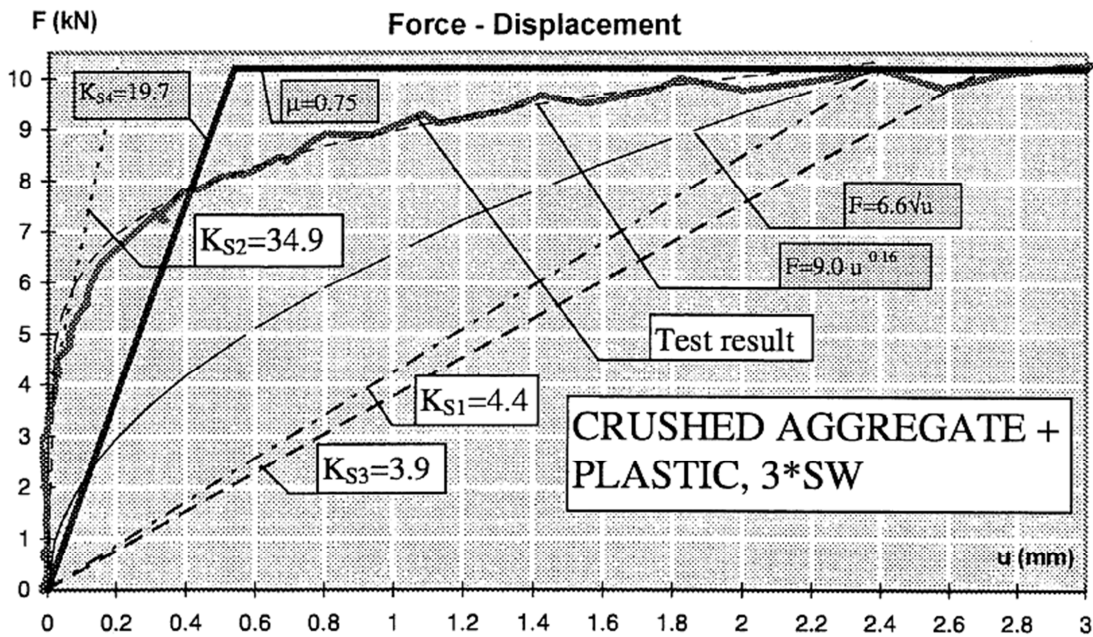


Figure 7.3 Test results for crushed aggregate and plastic film as sub-base (case 3) (Pettersson, 1998).

As can be seen in the figures, the most accurate approximations are given on the equation form $F = B \cdot u^n$. The slip is denoted u by Pettersson (1998). However, in this project the slip is denoted s . These approximations were adopted in the model and are summarised in Table 7.1. In order to convert the equations into stress functions the frictional force was divided by the area of the slab used in the test, these functions can also be found in Table 7.1.

Table 7.1 Summary of equations adapted from test results for the different cases.

Case nr	Case	Force equation on the form $F = B \cdot u^n$	Stress equation on the form $\tau = C \cdot s^n$	Slip at fully developed friction s_{max} [mm]
1	Sand	$F = 12.8 \cdot u^{0.25}$	$\tau = 13.33 \cdot s^{0.25}$	1.4
2	Crushed aggregate	$F = 15.0 \cdot u^{0.20}$	$\tau = 15.63 \cdot s^{0.20}$	6.7
3	Crushed aggregate + plastic	$F = 9.0 \cdot u^{0.16}$	$\tau = 9.34 \cdot s^{0.16}$	2.4

The stress equations are further illustrated in Figure 7.4 below. The functions are valid until the value for each s_{max} is reached, note the black dots at each curve in the figure. The validity of the adopted stress functions is evaluated in calculations by comparing the maximum slip with the value s_{max} . As can be seen in Figure 7.4, case 2 where the sub-base consists of crushed aggregate needs the largest local slip before full friction is achieved.

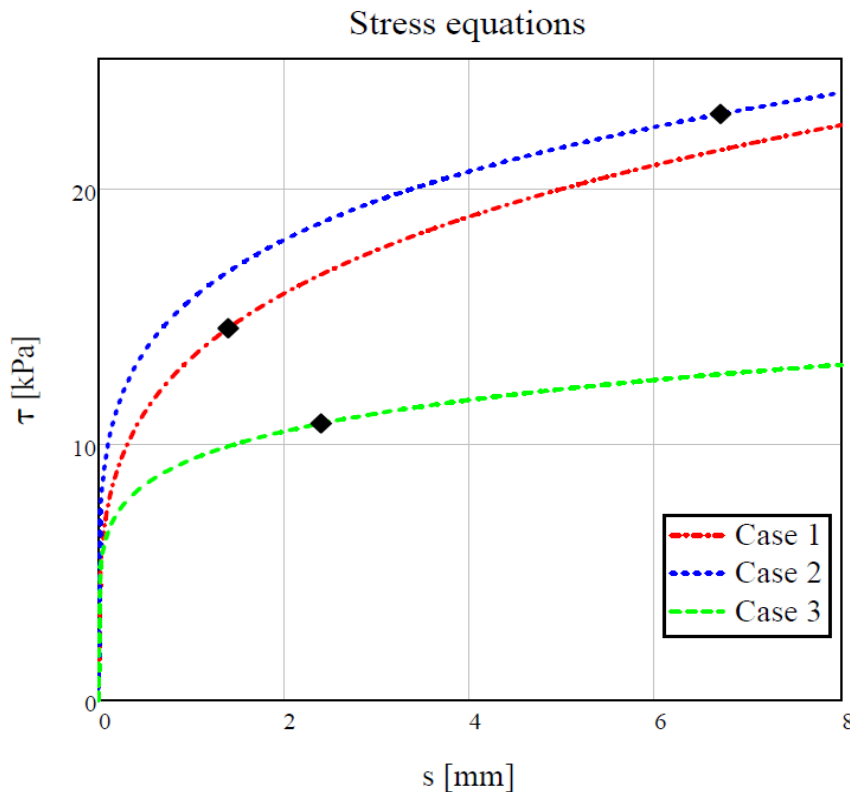


Figure 7.4 Assumed stress equations for the different cases.

7.2 Calculation procedure

The stress equations describe the stress as a function of the local slip $s(x)$. The local slip of a slab-on-ground which is subjected to shrinkage will vary along its length. Through adopting the methodology described by Tue & König (1991) to study bond-slip of reinforcement bars in reinforced concrete, the mean bond stress was found for each stress equation. This value was then used to find the normal force and the respective concrete stress acting in the middle of a slab-on-ground according to Figure 7.5.

The calculations were performed for a slab strip with a width of 1 m and a thickness of 250 mm. Concrete class C30/37 was assumed together with an ambient RH of 40% and a curing time of seven days. The shrinkage strain was considered for 50 years.

The concrete strain was calculated based on an effective modulus of elasticity, using a creep coefficient for 50 years. The calculation follows the procedure according to EC2, see Equation (7.1) below.

$$E_{c,ef} = \frac{E_{cm}}{1+\varphi(50 \text{ years}, t_o)} \text{ [Pa]} \quad (7.1)$$

where $\varphi(50 \text{ years}, t_o) = 2.68$ (for this specific case) [-]

Furthermore, since the slab was considered to be subjected to sustained loading, the concrete tensile strength was reduced by 40% as described according to Equation (3.3) in Section 3.5.

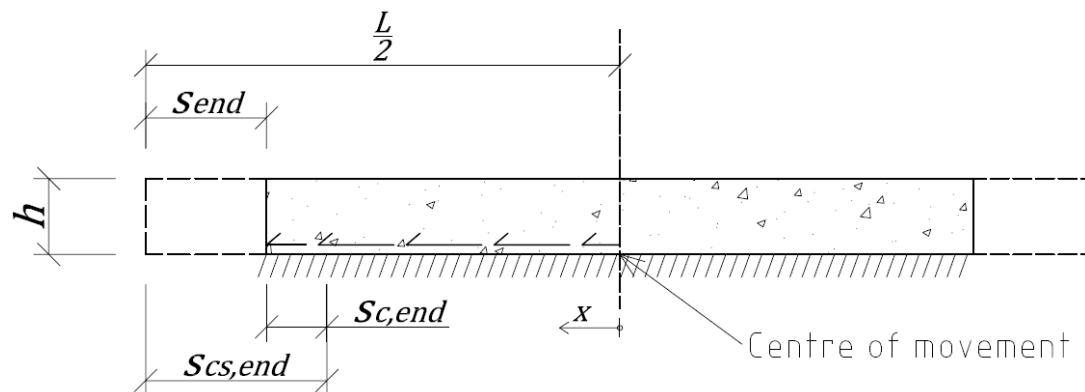


Figure 7.5 Conceptual sketch of the analytical friction model.

Figure 7.5 illustrates a conceptual sketch of the model. The calculations were performed for half the slab due to symmetry. In order to determine the stress distribution the end displacement was first needed to be determined. The end displacement can be calculated as the integral of the strain difference over the transmission length from the end to the centre of movement. This is the same as the difference between free end displacement due to shrinkage, s_{cs} , and elongation of concrete due to friction, s_c . Equation (7.2) and (7.3) summarises the relationships.

$$s_{end} = \int_0^{L/2} (-\varepsilon_{cs} + \varepsilon_c(x)) dx \text{ [m]} \quad (7.2)$$

$$s_{end} = s_{cs,end} - s_{c,end} \text{ [m]} \quad (7.3)$$

In order to calculate the elongation of the concrete, the concrete strain was calculated according to the methodology described by Tue & König (1991) for bond-slip of reinforcement bars in reinforced concrete. As the study considers the concrete member before cracking, the calculation procedure for stabilised cracking was followed. This procedure for stabilised cracking considers the behaviour between two cracks, which for this case is considered as the behaviour between the member ends.

The end slip due to the stress dependent strain of concrete in tension can be calculated according to Equation (7.4) using an integration coefficient that depends on the stress function for each considered case.

$$s_{c,end} = \frac{L}{2} \cdot \alpha_b \cdot \varepsilon_{c,max} \text{ [m]} \quad (7.4)$$

where $\alpha_b = \frac{1+b_s n_s}{2+b_s n_s} [-]$

$$b_s = \frac{2}{1-n_s} \text{ which is the positive root of}$$

$$b_s^2(1 - n_s) + b_s(-1 - 3n_s) - 2 = 0 [-]$$

$$n_s = \text{exponent in the respective stress function} [-]$$

Since this end-slip is equal to the integral of total strain over member length, Equation (7.3) can be re-written as below.

$$s_{end} = \int_0^{L/2} (-\varepsilon_{cs} + \varepsilon_{c,max}) dx = -\varepsilon_{cs} \cdot \frac{L}{2} + \alpha_b \cdot \varepsilon_{c,max} \cdot \frac{L}{2} \text{ [m]} \quad (7.5)$$

As described above, the concrete stress dependent strain was considered using an effective value for the elastic modulus and a reduced tensile strength. As a result, the concrete maximum strain can be expressed according to Equation (7.6).

$$\varepsilon_{c,max} = \frac{0.6 \cdot f_{ctm}}{E_{c,ef}} [-] \quad (7.6)$$

In accordance with the methodology described by Tue & König (1991), the mean friction stress can be expressed as below.

$$\tau_m = C \cdot \frac{s^{n_s}}{1+b_s \cdot n_s} \text{ [Pa]} \quad (7.7)$$

where $C = \text{coefficient in respective stress function}$

$$s = \text{end slip [mm]}$$

From the average friction stress the normal force can then be calculated according to Equation (7.8).

$$N = \tau_m \cdot (L/2) \cdot b \text{ [N]} \quad (7.8)$$

where $b = 1 \text{ m}$ (considered width)

The tensile stress can then be calculated from the normal force according to Equation (7.9).

$$\sigma_c = \frac{N}{b \cdot h} \text{ [Pa]} \quad (7.9)$$

where $h = \text{thickness of slab}$
(in this case assumed as 250 mm)

7.3 Results

Figure 7.6 illustrates the results from the calculations. The tensile stress is here plotted as a function of slab length for the three cases of sub-base. For evaluation purposes the tensile strength of concrete is also illustrated.

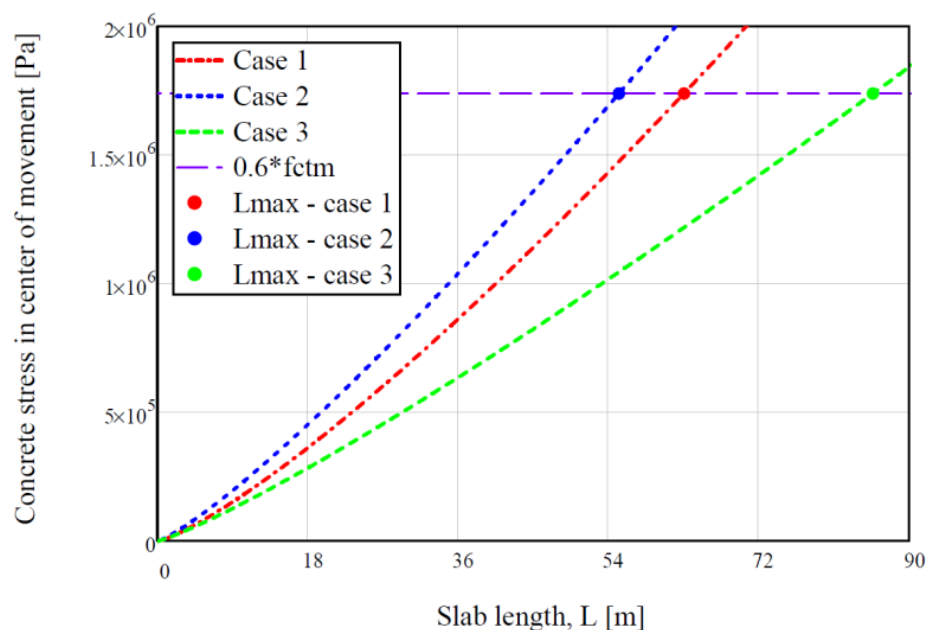


Figure 7.6 Results showing tensile stress due to restrained shrinkage in relation to slab length.

The calculated allowed maximum slab lengths together with the actual end slip, s_{end} , for each case is presented in Table 7.2. The end slip for each case will be the maximum slip any point in the slab experiences.

Table 7.2 Calculated allowed maximum slab length and calculated end slip.

Case nr	Case	Allowed maximum slab length according to calculations [m]	s_{end} [mm]
1	Sand	63.0	8.9
2	Crushed aggregate	55.2	7.9
3	Crushed aggregate + plastic	85.6	12.4

7.4 Evaluation

The described method aims at studying the friction behaviour between slabs-on-ground and sub-base more accurately than what is done in today's design procedures. In order to compare the results with other design procedures, the force equations adapted from tests by Pettersson (1998) were transformed into equations for coefficient of friction.

The tests were performed with the vertical load of $3 \cdot SW$. Using 24 kN/m^3 as unit weight for concrete, given the thickness of the test slab of 200 mm, this results in $SW = 24 \cdot 0.2 = 4.8 \text{ kPa}$. The force equations were converted into equations for coefficient of friction according to Equation (7.10) below. Figure 7.7 illustrates the converted equations.

$$\mu(u) = \frac{F(u)}{3 \cdot SW \cdot A_{test\ slab}} [-] \quad (7.10)$$

where $A_{test\ slab} = 0.96 \text{ [m}^2\text{]}$

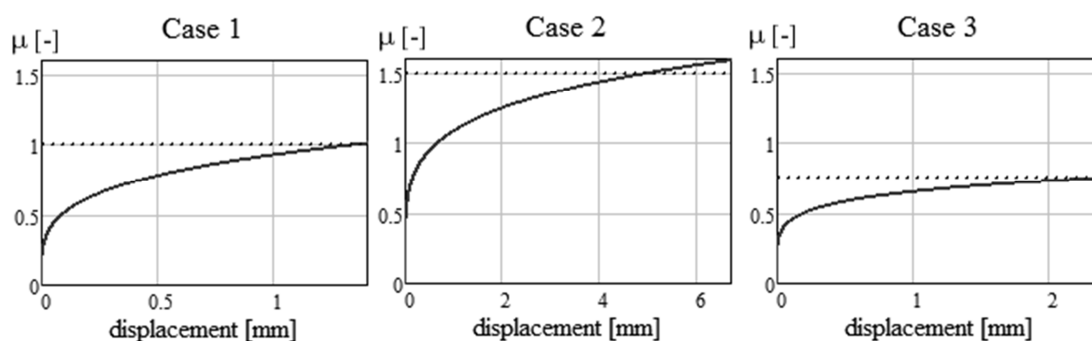


Figure 7.7 Coefficient of friction - displacement curves for the different cases.

The horizontal dotted lines indicate maximum friction values from the tests according to Pettersson (1998). As can be seen the calculated friction curves expressed using the coefficient of friction matches these maximum values well. For case 2 there is

however a small difference which is a deviation originating directly from the adopted force equations by Pettersson (1998).

Table 7.3 illustrates a comparison between the maximum values for coefficient of friction from Pettersson (1998) with the values used according to Petersons (1992). The values of coefficient of friction according to Petersons (1992) can be found in Table 2.3. According to Pettersson (1998) the crushed aggregate used in the test was compacted and is therefore comparable to the sub-base called “Crushed aggregate – compacted and smooth” according to Table 2.3. Furthermore, since no value for sub-base consisting of crushed aggregate together with plastic film is presented in Table 2.3 the value for plastic film alone was adopted.

Table 7.3 Comparison of coefficient of friction from test result with values according to Petersons (1992).

Case nr	Case	μ - coefficient of friction	
		μ_{max} described by Pettersson (1998)	Values according to Petersons (1992), see Table 2.3.
1	Sand	1	0.75
2	Crushed aggregate	1.5	1.5
3	Crushed aggregate + plastic	0.75	0.75

Except the value for sand, the table shows a strong correlation between the values, indicating that the tests, constituting the base for the developed analytical model in this report, are reliable.

To further evaluate the results from Figure 7.6, a calculation based on the procedure described in Section 4.3.1 according to Petersons (1992) was performed for a 250mm thick slab of concrete class C30/37. The considered load was $3 * SW$ and the mean tensile strength, f_{ctm} , was used. The coefficients of friction were adopted from the maximum values according the tests. Figure 7.8 illustrates how the allowable slab length varies depending on the coefficient of friction.

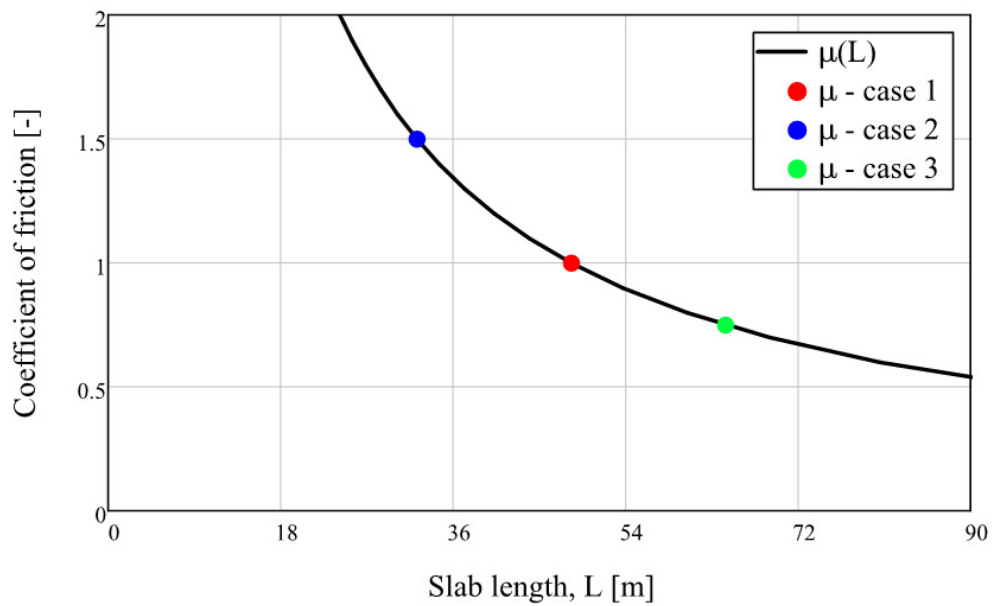


Figure 7.8 Allowable slab length depending on coefficient of friction, according to method by Petersons (1992). Coefficients of friction are adopted from maximum values according to the tests.

In Table 7.4 below the results are summarised and compared with the results from the developed analytical model. Table 7.5 illustrates the slip at which full friction is achieved, s_{max} , and the calculated end slip, s_{end} , before the first crack is formed for each case.

Table 7.4 Comparison of results with regard to slab length.

Case nr	Slab length [m]		Length difference	
	Analytical model	Using coefficient of friction according to Petersons (1992)	[m]	[%]
1	63.0	48.3	14.7	30.4
2	55.2	32.2	23.0	71.4
3	85.6	64.4	21.2	32.9

Table 7.5 Maximum end slip before full friction and calculated end slip for each case when the first crack is formed.

Case nr	End slip, s_{max} , before full friction [mm]	Calculated end slip, s_{end} [mm]
1	1.4	8.9
2	6.7	7.9
3	2.4	12.4

As can be seen from the last column in Table 7.4, the analytical model results in larger allowable slab lengths compared with using the general method assuming coefficients of friction. The largest length difference occurs for case 2 where the sub-base consists of crushed aggregates. The analytical model here allows a slab length increase of 71.4%.

Table 7.5 illustrates that, at the point of cracking, the calculated end slips are above the required end slips to achieve full friction. Consequently, the stress functions describing the friction have been used in the calculation outside their actual range. As previously explained, each function is only valid until its maximum required end slip. Since the functions are used outside their range, the friction has been allowed to continue to grow, resulting in conservative results where too much friction has been allowed for.

As a result, the calculated values of allowable increase of slab length are on the safe side. However, looking closer at case 2, which allows for the largest slab length increase, the calculated end slip matches the required end slip well and consequently only a small amount of additional friction has been included in the calculations. Due to this, the results for case 2 are the most accurate and allowable slab length increases of approximately 70 % are likely to be allowable if the friction is not overestimated.

In conclusion, it was believed that the coefficient of friction was a conservative approach to consider the effect of friction against sub-grade, overestimating the friction. This theory is confirmed from the calculations. According to the results, the analytical model results in larger allowable slab lengths. However, it should be kept in mind that this is a simplified case considering plain concrete and the only restraint is the friction. Additional external and internal restrains are not included.

8 Final remarks

8.1 Conclusions

The following section outlines conclusions drawn from the evaluation of observed responses of floors and of the two developed design models. The evaluations have been carried out under the respective section in the report.

8.1.1 Observed response of floors

In order to investigate the cracking of slabs-on-ground, four different reference objects were studied and evaluated. The following conclusion can be drawn:

- When performing crack measurement on a slab-on-ground, determining the reason for cracking is a challenging task. In order to fully understand the cracking behaviour, the location of the cracks needs to be determined in relation to other geometry, reinforcement layout and location of piles.
- 14 cracks were identified as shrinkage cracks when studying the reference objects. For these cracks the ratio between maximum crack width and mean crack width was calculated, resulting in an average ratio of 1.56 with a standard deviation of 0.16. Comparing this value with the two values proposed in literature, 1.3 and 1.7, the results indicate that 1.7 is more likely to be accurate for the studied objects.
- Comparing the reinforcement amount of the objects with the minimum reinforcement according to EC2, all objects have less reinforcement than what the regulation yields. The largest amount is found in object 1, which is the slab showing the best cracking response and the most narrow crack widths. This indicates the expected result that increasing reinforcement amount results in better control of cracks and limiting of crack widths.
- An important observation during the evaluation of the studied floors is the aspect of concrete strength class and age with regard to shrinkage cracking. Figure 4.2 illustrates the shrinkage development over time for different concrete strength classes according to EC2. It can be concluded that the calculated shrinkage strain decreases but that the proportion of autogenous shrinkage increases with higher concrete strength classes due to the increased amount of cement and lowered w/c ratio.
- As was illustrated for the example in Figure 4.3, according to EC2, a large proportion of the shrinkage development occurs during the first years after casting. After 5 years 83 percent of the shrinkage strain has already developed. However, it takes a long time to reach the final shrinkage strain, after 50 years 98 percent of the strain has developed. As a result, since the observed objects are all approximately 5 years old, the observed cracks are likely to continue developing over time and continued measurements would be of interest to further understand the cracking behaviour.

8.1.2 Analysis using the direct stiffness method

An analysis of a pile-supported slab-on-ground subjected to shrinkage was performed. The developed model evaluates the risk of cracking from a global perspective. In order to efficiently consider the effect from multiple external restraints, the model is based on the direct stiffness method.

Three cases were studied, one generic case and two cases adopted from situations found when studying the response of floors from the reference objects. The analysis was carried out in state I before the concrete cracks, and aimed at finding the normal force distribution along the chosen slab section. The corresponding stress distribution determines which element would crack first by comparing with the concrete tensional strength. The following conclusions can be drawn:

- The developed model captures the normal force distribution from a global perspective before cracking. This is a new approach that gives a better understanding of the global shrinkage response of a slab-on-ground section.
- The influence width b for the effect of piles that is assumed for each studied case has a large influence on the result and is a factor potentially causing the model to be less accurate. In the project the influence width was assumed as the maximum possible, the spacing between piles. The smaller the studied influence width, the more contribution from the pile restraints is achieved. In order to ensure that local effects from pile restraints are not neglected, further study regarding this is recommended.
- Parameters regarding the ground properties have been assumed in the calculations. These are used to determine the stiffness of the perimeter strips and piles. In a design situation, these values should however be adapted from a geotechnical investigation for the certain situation as they have great influence on the resulting stress distribution.
- The external horizontal stiffness of piles and perimeter strips has a large effect on the results and are deemed uncertain in their definition. However, the analysis indicates that the restraints from perimeter strips have a significantly larger influence on shrinkage cracking compared with pile restraints. Further studies regarding this are therefore recommended in order to improve the reliability of the model.
- Since the model includes uncertainties and assumptions, the actual concrete stress or normal force value should be questioned. However, the model is capable of determining the location of where the highest stresses are likely to occur, which is useful in a design situation in order to understand the global effect of external restraints.
- When designing a reinforced concrete member, it is common praxis to place additional reinforcement in local regions in where the highest stresses are expected to occur. However, once the location of the maximum shrinkage force is located, using the developed model in Section 6, the same approach could also be applied with regard to shrinkage restraint forces. In order to limit

the width of the first crack, the amount of reinforcement can therefore be increased in this region, since the first crack could be expected here.

8.1.3 Non-linear analytical friction model

A model of a plain concrete slab-on-ground subjected to shrinkage, taking into account the effect from friction against the sub-base, was developed and studied. The model implements non-linear friction models adopted from full-scale testing. The calculation procedure is based on the methodology for calculations of bond-slip between concrete and reinforcement. The following conclusions can be drawn:

- Since the model takes into account the slip required before full friction is developed, the model is more precise than using the general procedure assuming fully developed friction and disregarding the actual distribution of local slip. If only the maximum coefficient of friction is considered, two materials with the same maximum value but with different required slips would result in the same allowable slab length. The analytical model on the other hand would result in two separate answers.
- The results allow for a larger slab length than the general method, proving the general procedure to be conservative.
- Since the analytical model allows for larger casting steps, this could be used as a favourable method in a design situation. Larger casting steps allow for fewer joints and possibilities to rationalise the construction process.
- The actual slab length increase that can be allowed adopting this model is in direct relation to the required slip before full friction is achieved, as described by the friction curves. A larger slip before full friction is developed allows for a higher percentage in slab length increase.
- The non-linear analytical friction model has proven to be a more precise calculation procedure than using the method of assuming a coefficient of friction. It must however be noted that none of these models take into account the effect from external restraints, such as piles and perimeter strips, or internal restraints from the reinforcement.

8.2 Design recommendations

In order to achieve a good design, it is in general a matter of limiting the source of shrinkage and to facilitate possible movements due to shrinkage. It is also important to predict the most probable locations for cracking and to arrange these locations so that the cracking can be controlled. The following recommendations can be given:

- Plan for joint layout in the design phase.
- Use isolation joints around columns in order to allow for movement of the slab-on-ground.
- Combine joints in the slab into one joint type where possible. A construction joint can easily be incorporated within a dilatation joint if the project is planned carefully.
- In order to minimise the stiffness of the perimeter strips and the restraint perpendicular to the direction of the perimeter strip, it is recommended to not compact the sub-base close to the perimeter strip. This procedure would lower the elasticity of the ground, thus allowing the perimeter strip and the connected slab to move more freely.
- Another way to lower the stiffness of the perimeter strip is to incorporate an angled geometry according to the picture below. This would create less restraint than having an equivalent perimeter strip connected at 90 degrees to the slab.

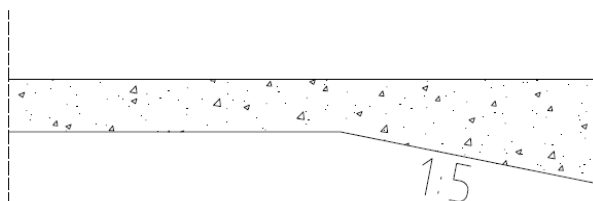


Figure 8.1 Proposed detailing of perimeter strips in order to reduce restraints.

- If there is a risk of cracking, consider using crack inducing methods to control the locations of the cracks. Contraction joints created by sawing the slab surface are recommended.
- Consider using vacuum treatment when constructing industrial floors, as this reduces the shrinkage strain.
- Choose concrete strength class with focus on functionality. A high concrete strength class will result in less final shrinkage strain, but as the concrete strength class is higher more reinforcement is needed to balance the increased tensional strength of the concrete. The recommended strength class for a slab-on-ground according to the Swedish Concrete Association (2008), as described in Section 4.1, is C30/37.

- Consider using shrinkage reducing additives in the mix design to minimise the shrinkage strain. However, this should be used with caution as not every secondary effect on the mix properties is covered.
- When a designer specifies the concrete properties for an industrial floor, it is recommended to specify both a maximum and a minimum w/c ratio, instead of only specifying a maximum value. If the contractor lowers the w/c ratio, the strength of the concrete will be higher, which was not designed for when calculating the reinforcement amounts. The balance between steel and concrete capacity is thereby changed and the reinforcement amount would need to be adjusted to assure a controlled cracking behaviour.
- The friction against the sub-base should be regarded as negative before the slab has developed the first crack. However, after the first crack is formed the friction has a positive effect. It then functions in analogy with the reinforcement, reducing the crack widths and distributing the cracks over the total length of the slab, creating a system of distributed cracks rather than a set of few large cracks.

8.3 Further investigations

When studying the cracking response of a concrete structure, for example a slab-on-ground, it is useful to be able to capture the locations of all expected cracks. However, the methods developed in this project only consider the expected location of the initial crack. An improvement would therefore be to further develop the models in order to determine the crack locations after finished cracking.

For the model using the direct stiffness method, the Matlab program could be further developed to model cracks by incorporating spring elements at points determined by a fixed stress threshold value. It would then be required to recalculate the system each time this threshold value is reached, in analogy with the method for crack evaluation described in Section 4.3.7. Through this procedure the need for reinforcement to control the cracks can also be determined.

Further research and development could be to incorporate reinforcement in the analytical non-linear friction model and thereby be able to capture the behaviour between concrete, steel and the sub-base.

A future project is also suggested to combine the two models developed in this project. A direct stiffness method solution for a slab-on-ground subjected to shrinkage that also captures the non-linear friction against the sub-grade could thereby be achieved.

To further verify and adjust the non-linear analytical solution, full-scale testing is recommended. The model could also be verified and compared to a numerical solution of the same problem.

Tests could also be carried out to evaluate and improve the direct stiffness model. The calculated horizontal stiffness of piles and perimeter strips could be investigated using full-scale testing.

9 References

- AB Jacobson & Widmark, 2000. *Slabs-on-ground (Betonggolv på mark)*, Stockholm: Teknikrådet J&W Byggprojektering.
- AB Jacobson & Widmark, 2001. *Slab-on-ground industrial floors - Design guide (Industrigolv av betong på mark - Projekteringsguide)*, Karlstad: Teknikorganisationen J&W Byggprojektering.
- American Concrete Institute, 1992. *Design of slabs on grade, Report 360R-92*, Farmington Hills, Michigan: ACI.
- Balvac inc., 2007. *Balvac inc.*. [Online]
Available at: <http://www.balvac.com>
[Accessed 4 May 2012].
- BASF, n.d. *BASF - The Chemical Company*. [Online]
Available at: <http://www.basf-cc.se>
[Accessed 13 February 2012].
- Bernander, S., Emborg, M. & Jonasson, J.-E., 1994. *Temperature, maturity development and eigenstresses in young concrete (Temperatur, mognadsutveckling och egenspanningar i ung betong)*. *Betonghandbok - Material, Chapter 16*. 2 ed. Stockholm: AB Svensk Byggtjänst och Cementa AB.
- Bolteus, L., 1984. *Soil-structure interaction - A study based on numerical methods*, Göteborg: Chalmers University of Technology .
- Boverket, 2004. *Boverket's guide book to concrete structures, BBK04 (Boverkets handbok om betongkonstruktioner, BBK04)*. 3 ed. Vällingby: Boverket.
- Brooks, J., 2003. *Advanced Concrete Technology - Concrete Properties, Chapter 7*. Oxford: Elsevier Ltd. .
- Celsa Steel Service, n.d. *Celsa Steel Service AB*. [Online]
Available at: <http://www.celsa-steelservice.com>
[Accessed 13 April 2012].
- Corres Peiretti, H., Pérez Caldentey, A. & Petschke, T., 2003. *PrEN Chapter 7 – Servicability limit*, Madrid: Universidad politécnica de Madrid.
- Das, B., 2011. *Principles of Foundation Engineering*, Stamford: Cengage Learning.
- Day, R. & Clarke, J., 2003. *Advanced Concrete Technology - Concrete Properties, Chapter 2*. Oxford : Elsevier Ltd. .
- Domone, P. & Illston, J., 2010. *Construction materials, their nature and behaviour*, Oxon: Spon Press.
- Engström, B., 2008. *Load-bearing structures: Part 2 (Bärande konstruktioner: Del 2)*. Göteborg: Chalmers tekniska högskola.
- Engström, B., 2011. *Restraint cracking of reinforced concrete structures*, Göteborg: Chalmers University of Technology.
- European committee for standardization, 2004. *Eurocode 2: Design of concrete structures*. Brussels: CEN.
- European Concrete Platform ASBL, 2008. *Eurocode 2 Commentary*, Brussels: European Concrete Platform ASBL.

- Fjällberg, L., 2002. *The effect of shrinkage-reducing admixtures on the shrinkage of cement based materials (Krympreducerares inverkan på cementbaserade materials krympning)*. CBI rapport 1:2002, Stockholm: Cement och Betong Institutet.
- Hedebratt, J., 2005. *Integrated design and construction of industrial floors - Methods to increase the quality (Integrerad projektering och produktion av industrigolv - Metoder för att öka kvaliteten)*, Stockholm: Licentiatavhandling, bulletin 78, brobyggnad, institutionen för byggvetenskap, KTH.
- International Federation for Structural Concrete, 2012. *Model Code 2010*, Lausanne: International Federation for Structural Concrete.
- Khairallah, R. S., 2009. *Analysis of Autogenous and Drying Shrinkage of Concrete. Master's thesis, paper 4546*, Hamilton, Ontario: McMaster University.
- Knapton, J., 2003. *Ground bearing concrete slabs*. London: Thomas Telford Limited.
- Ljungkrantz, C., Möller, G. & Petersons, N., 1994. *Special properties (Speciella egenskaper)*. *Betonghandbok - Material, Chapter 18.3*. 2 ed. Stockholm: AB Svensk Byggtjänst och Cementa AB.
- National Ready Mixed Concrete Association, 1998. *CIP 6 - Joints in Concrete Slabs on Grade*, Silver Spring: National Ready Mixed Concrete Association.
- New Construction Group, n.d. *New Construction Group*. [Online] Available at: <http://ncg-bg.com> [Accessed 13 February 2012].
- Permaban, n.d. *Permaban*. [Online] Available at: <http://www.permaban.com> [Accessed 01 05 2012].
- Petersons, N., 1992. *Concrete floors (Betonggolv)*. *Betonghandbok - Arbetsutförande, Chapter 19.4:3.2*. 2 ed. Örebro: AB Svensk Byggtjänst och Cementa AB.
- Petersons, N., 1994. *Cracks (Sprickor)*. *Betonghandbok - Material, Edition 2, Chapter 19*. Stockholm: AB Svensk Byggtjänst och Cementa AB.
- Pettersson, D., 1998. *Stresses in concrete Structures from ground restraints*, Lund: Lund Institute of Technology. Department of Structural Engineering.
- Pettersson, D., 2000. *Control of Cracking due to Imposed Strains in Concrete Structures, Doctoral Thesis*. Lund: Division of Structural Engineering, Lund Institute of Technology, Lund University.
- Portland Cement Association, n.d. *Portland Cement Association*. [Online] Available at: <http://www.cement.org> [Accessed 10 February 2012].
- Sällfors, G., 2001. *Geoteknik*. 3 ed. Göteborg: s.n.
- Svahn, P.-O. & Alén, C., 2006. *Laterally loaded piles (Transversalbelastade pålar)*. *Report 101*, Linköping: Commission on Pile Research (Pålkommisionen).
- Swedish Concrete Association, 2008. *Concrete report nr 13. Industrial floors - Recommendations regarding planning, choosing materials, production, management and maintenance (Betongrapport nr 13. Industrigolv - Rekommendationer för projektering, materialval, produktion, drift och underhåll)*, Stockholm: Swedish Concrete Association (Svenska Betongföreningen).

Tue, N. & König, G., 1991. *Darmstadt concrete - Annual journal on concrete and concrete structures, Vol. 6. Calculating the mean bond and steel stress in reinforced and prestressed concrete members.* , Darmstadt: Institute für Massivbau, Technische Hochschule Darmstadt.

Williamson, N., 2003. *Advanced concrete technology - Processes, Chapter 24.* Oxford: Elsevier Ltd..

Wire Reinforcement Institute, Inc., 2003. *Innovative Ways to Reinforce Slabs-On-Ground*, Hartford, Connecticut: WRI.

Appendix A Shrinkage and creep calculation

Input parameters

Geometry

Slab thickness [mm]: $t_h = 250\text{-mm}$

Concrete cover top [mm]: $c_t = 30\text{-mm}$

Concrete cover bottom, to ground [mm]: $c_{bg} = 50\text{-mm}$

Concrete cover bottom, to insulation [mm] $c_{bi} = 30\text{-mm}$

Material properties

Concrete class (recommended value: C30/37)

- C 12/15
- C 16/20
- C 20/25
- C 25/30
- C 30/37
- C 35/45
- C 40/50
- C 45/55
- C 50/60
- C 55/67
- C 60/67
- C 70/85
- C 80/95
- C 90/105

Mechanical Properties of concrete according to EC2

Class	12/15	16/20	20/25	25/30	30/37	35/45	40/50	45/55	50/60	55/67	60/75	70/85	80/95	90/105
f_{ck} [MPa]	12	16	20	25	30	35	40	45	50	55	60	70	80	90
f_{cm} [MPa]	20	24	28	33	38	43	48	53	58	63	68	78	88	98
$f_{ctk0.05}$ [MPa]	1.1	1.3	1.5	1.8	2.0	2.2	2.5	2.7	2.9	3.0	3.1	3.2	3.4	3.5
f_{ctm} [MPa]	1.6	1.9	2.2	2.6	2.9	3.2	3.5	3.8	4.1	4.2	4.4	4.6	4.8	5.0
$f_{ctk0.95}$ [MPa]	2.0	2.5	2.9	3.3	3.8	4.2	4.6	4.9	5.3	5.5	5.7	6.0	6.3	6.6
E_{cm} [GPa]	27	29	30	31	33	34	35	36	37	38	39	41	42	44

- $f_{ck} = 30\text{-MPa}$ characteristic compressive strength (5%-fractile)
- $f_{cm} = 38\text{-MPa}$ mean value compressive strength
- $f_{ctk0.05} = 2\text{-MPa}$ lower characteristic tensile strength (5%-fractile)
- $f_{ctm} = 2.9\text{-MPa}$ mean value tensile strength
- $f_{ctk0.95} = 3.8\text{-MPa}$ upper characteristic tensile strength (95%-fractile)
- $E_{cm} = 33\text{-GPa}$ young's modulus
- $f_{cmo} := 10\text{MPa}$ reference strength
- $f_{ct,eff} := f_{ctm} = 2.9\text{-MPa}$ (Assuming cracks to appear after 28 days or more)

Cement class

- Cement class S
 - Cement class N
 - Cement class R
- $$\alpha_{ds1} := \begin{cases} 3 & \text{if CemC} = 1 \\ 4 & \text{if CemC} = 2 \\ 5 & \text{if CemC} = 3 \end{cases} = 4$$
- $$\alpha_{ds2} := \begin{cases} 0.13 & \text{if CemC} = 1 \\ 0.12 & \text{if CemC} = 2 \\ 0.11 & \text{if CemC} = 3 \end{cases} = 0.12$$

Ambient relative humidity

- RH 20%
- RH 40%
- RH 60%
- RH 80%
- RH 90%
- RH 100%

$$RH_{amb} = 0.4$$

$$RH_0 := 1$$

Time values

$$t_{fin} := 50 \cdot 365 \text{ day}$$

$$t_s := 7 \text{ day}$$

Steel data

$$E_s := 200 \text{ GPa}$$

Creep

The creep coefficient can be determined according to equations below:

$$\varphi(t, t_0) = \beta_c(t, t_0) \cdot \varphi_0$$

Where: $\beta_c(t, t_0) = \left[\frac{(t - t_0)}{\beta_H + (t - t_0)} \right]^{0.3}$ = time function of the creep coefficient

$\varphi_0 = \varphi_{RH} \cdot \beta(f_{cm}) \cdot \beta(t_0)$ = notional creep coefficient

notional size of cross section

studying one unit length of the slab

$$l_u := 1 \text{ m}$$

$$u_u := 1 \text{ m}$$

$$h_0 := \frac{2 \cdot l_u \cdot t_h}{u_u} = 500 \cdot \text{mm}$$

Notional creep coefficient

φ_{RH} - Factor that considers relative humidity

$$\varphi_{RH} := \begin{cases} 1 + \left(\frac{1 - RH_{amb}}{0.1 \cdot \sqrt{h_0 \cdot 1000 \cdot \text{m}^{-1}}} \right) & \text{if } f_{cm} \leq 35 \text{ MPa} \\ 1 + \frac{1 - RH_{amb}}{0.1 \cdot \sqrt{h_0 \cdot 1000 \cdot \text{m}^{-1}}} \cdot \left(\frac{35 \text{ MPa}}{f_{cm}} \right)^{0.7} \cdot \left(\frac{35 \text{ MPa}}{f_{cm}} \right)^{0.2} & \text{if } f_{cm} > 35 \text{ MPa} \end{cases} = 1.686 \quad (\text{B.3a})$$

$$\left[\begin{aligned} & 1 + \frac{1 - RH_{amb}}{0.1 \cdot \sqrt{h_0 \cdot 1000 \cdot \text{m}^{-1}}} \cdot \left(\frac{35 \text{ MPa}}{f_{cm}} \right)^{0.7} \cdot \left(\frac{35 \text{ MPa}}{f_{cm}} \right)^{0.2} & \text{if } f_{cm} > 35 \text{ MPa} \end{aligned} \right] \quad (\text{B.3b})$$

$\beta_{f,cm}$ - Factor that considers concrete strength

$$\beta_{f,cm} := \frac{16.8}{\sqrt{f_{cm} \cdot \text{MPa}^{-1}}} = 2.725 \quad (\text{B.4})$$

β_{t_0} - Factor that considers concrete age at loading

Assuming loading to occur when controlled curing stops: $t_{0,T} := t_s = 7 \cdot \text{day}$
(not adjusted with regard to temperature)

Effect of cement class: $\alpha_t := \begin{cases} -1 & \text{if CemC} = 1 = 0 \\ 0 & \text{if CemC} = 2 \\ 1 & \text{if CemC} = 3 \end{cases}$

$$t_0 := \max \left[0.5 \text{day}, t_{0,T} \cdot \left[\frac{9}{2 + (t_{0,T} \cdot \text{day}^{-1})^{1.2}} + 1 \right]^{\alpha_t} \right] = 7 \cdot \text{day} \quad (\text{B.9})$$

$$\beta_{t_0} := \frac{1}{0.1 + (t_0 \cdot \text{day}^{-1})^{0.2}} = 0.635$$

$$\varphi_0 := \varphi_{RH} \cdot \beta_{f,cm} \cdot \beta_{t_0} = 2.915$$

Time function of the creep coefficient

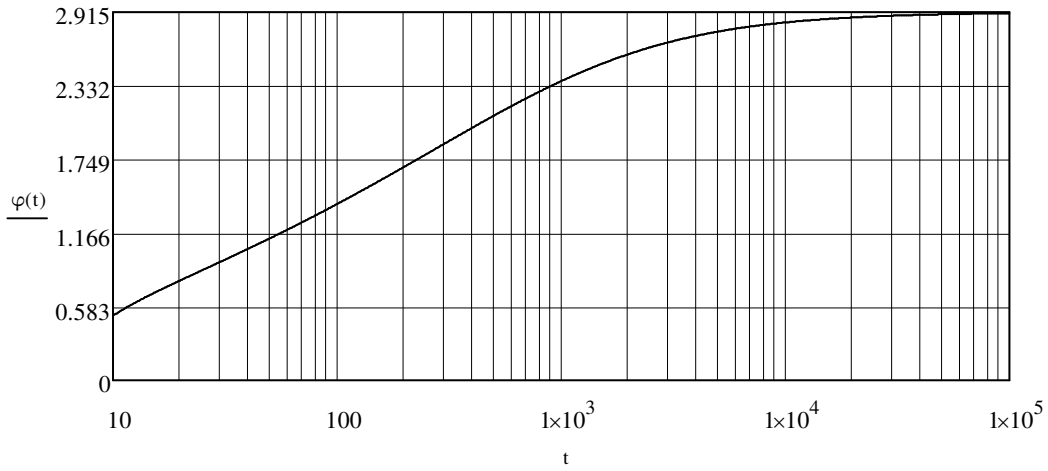
β_H - Factor that considers RH and h_0

$$\beta_H := \begin{cases} \min \left[1.5 \left[1 + (1.2 \cdot \text{RH}_{\text{amb}})^{18} \right] \cdot h_0 \cdot \frac{1000}{\text{m}} + 250, 1500 \right] & \text{if } f_{cm} \leq 35 \text{MPa} \\ \min \left[1.5 \left[1 + (1.2 \cdot \text{RH}_{\text{amb}})^{18} \right] \cdot h_0 \cdot \frac{1000}{\text{m}} + 250 \cdot \left(\frac{35 \text{MPa}}{f_{cm}} \right)^{0.5}, 1500 \cdot \left(\frac{35 \text{MPa}}{f_{cm}} \right)^{0.5} \right] & \text{if } f_{cm} > 35 \text{MPa} \end{cases}$$

$$\beta_H = 989.93$$

$$\beta_c(t) := \left[\frac{(t - t_0 \cdot \text{day}^{-1})}{\beta_H + (t - t_0 \cdot \text{day}^{-1})} \right]^{0.3} \quad (t_0 \text{ is treated as a constant})$$

$$\varphi(t) := \beta_c(t) \cdot \varphi_0$$



Shrinkage

Drying shrinkage strain

nominal shrinkage

$$\beta_{RH} := 1.55 \left[1 - \left(\frac{RH_{amb}}{RH_0} \right)^3 \right] = 1.451 \quad (B.11)$$

$$\epsilon_{cd,0} := 0.85 \left[(220 + 110 \cdot \alpha_{ds1}) \cdot e^{\left(-\alpha_{ds2} \cdot \frac{f_{cm}}{f_{cmo}} \right)} \right] \cdot 10^{-6} \cdot \beta_{RH} = 5.159 \times 10^{-4} \quad (B.12)$$

shape coefficient

linear interpolation using table 3.3

$$h_{0v} := \begin{pmatrix} 100 \\ 200 \\ 300 \\ 500 \end{pmatrix} \text{mm} \quad k_{hv} := \begin{pmatrix} 1 \\ 0.85 \\ 0.75 \\ 0.7 \end{pmatrix}$$

$$k_h := \text{linterp}(h_{0v}, k_{hv}, h_0) = 0.7$$

adapted from (table 3.3)

time function

$$\beta_{ds} := \frac{(t_{fin,day}^{-1} - t_{s,day}^{-1})}{(t_{fin,day}^{-1} - t_{s,day}^{-1}) + 0.04 \cdot \sqrt{(h_0 \cdot \text{mm}^{-1})^3}} = 0.976 \quad (3.10)$$

concrete drying shrinkage

$$\epsilon_{cd} := \beta_{ds} \cdot k_h \cdot \epsilon_{cd,0} = 3.525 \times 10^{-4} \quad (3.9)$$

Autogenous shrinkage strain

shrinkage over unlimited time

$$\epsilon_{ca,\infty} := 2.5 \cdot (f_{ck} - 10 \text{MPa}) \cdot 10^{-6} \cdot \text{MPa}^{-1} = 5 \times 10^{-5} \quad (3.11)$$

time function

$$\beta_{as} := 1 - e^{\left[-0.2 \cdot t_{fin}^{0.5} \cdot \text{day}^{-(0.5)}\right]} = 1 \quad (3.12)$$

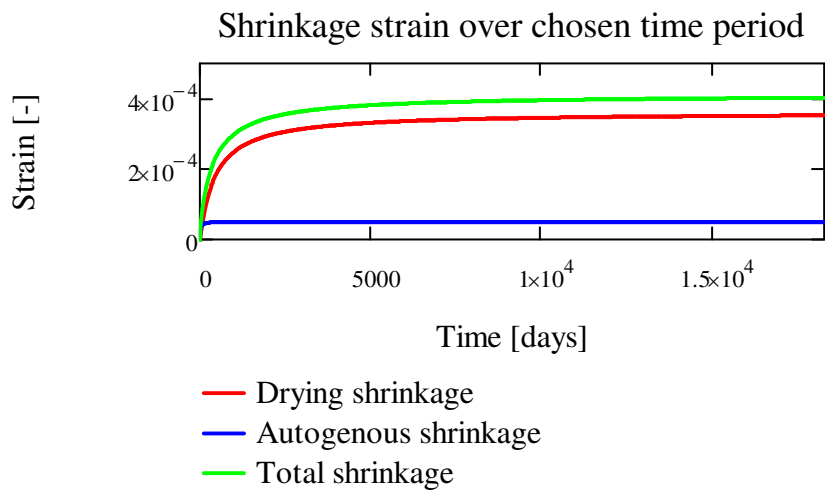
concrete autogenous shrinkage

$$\epsilon_{ca} := \beta_{as} \cdot \epsilon_{ca,\infty} = 5 \times 10^{-5} \quad (3.13)$$

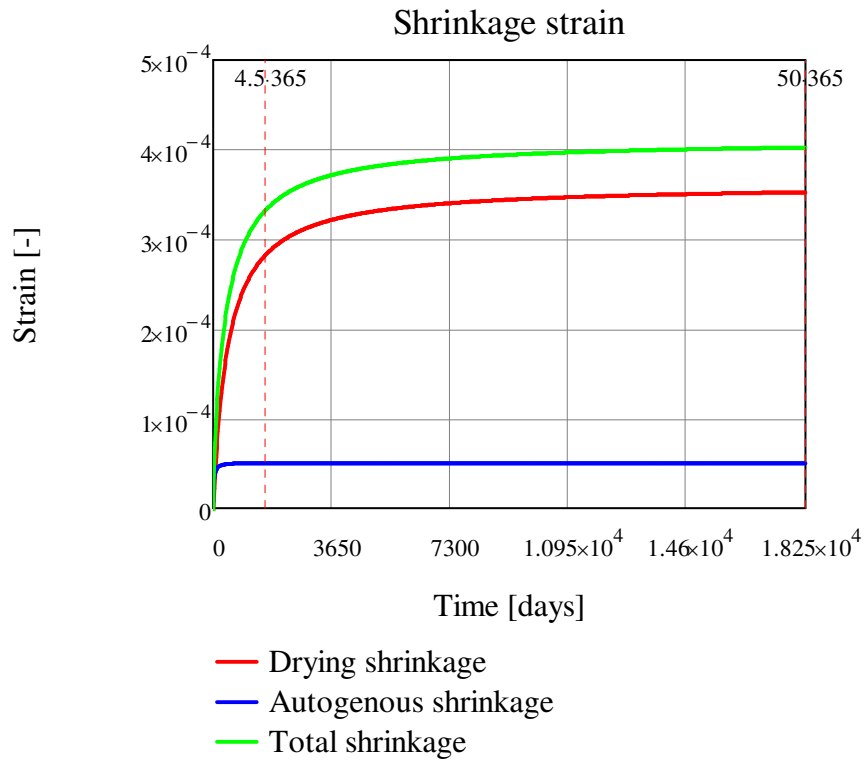
Total shrinkage strain

total shrinkage at chosen time

$$\epsilon_{cs} := \epsilon_{ca} + \epsilon_{cd} = 4.025 \times 10^{-4} \quad (3.8)$$



Plot of shrinkage variation over 50 years



$$\epsilon_{cd.func}(50 \cdot 365) + \epsilon_{ca.func}(50 \cdot 365) = 4.025 \times 10^{-4}$$

$$\epsilon_{cd.func}(4.5 \cdot 365) + \epsilon_{ca.func}(4.5 \cdot 365) = 3.335 \times 10^{-4}$$

Finding after which time convergence is found:

$$\epsilon_{cs,\infty}(t) := \epsilon_{cd.func}(t) + \epsilon_{ca.func}(t)$$

$$\epsilon_{cd,\infty} := k_h \cdot \epsilon_{cd,0} = 3.611 \times 10^{-4}$$

$$\epsilon_{ca,\infty} = 5 \times 10^{-5}$$

$$\epsilon_{cs,\infty} := \epsilon_{ca,\infty} + \epsilon_{cd,\infty} = 4.111 \times 10^{-4}$$

$$\text{Limit} := 0.98$$

$$f_{conv}(t) := \epsilon_{cd.func}(t) + \epsilon_{ca.func}(t) - \epsilon_{cs,\infty} \cdot \text{Limit}$$

$$\text{guess} := 1$$

$$t_{conv} := \text{root}(f_{conv}(\text{guess}), \text{guess}) = 1.92 \times 10^4$$

$$t_{conv.yrs} := \frac{t_{conv}}{365} = 52.605$$

Percent of shrinkage that has occurred after 50 years:

$$t_{50} := 50.365$$

$$\text{Percent}_{50.years} := \frac{(\epsilon_{cd.func}(t_{50}) + \epsilon_{ca.func}(t_{50}))}{\epsilon_{cs,\infty}} \cdot 100 = 97.898$$

Appendix B Data and drawings, object 1

Name:	Object 1	
Building type:	Industrial building, workshop/storage	
Construction time:	2008-2009, casting period spring	
Geographical position:	Industrial area, approximately 200 m from the river Göta älv.	
Ground conditions:	Not specified	
Groundwater:	Not specified	
Generic demands:	Mainly demands on functionality as a combined workshop and storage facility	
Demands on shrinkage cracking:	Not specified	
Applied code:	BBK	
Calculated crack width:	BBK	
Exposure class:	XC1	
Life time class:	L50	
Slab thickness:	220mm	
Surface tolerances:	Not specified	
Surface treatment:	Troweled surface	
Piles or no piles:	Piles, location according to drawing	
Perimeter strip:	According to drawing	
Cast-in connections:	Columns fixed on steel plates casted in the slab. Foundations to heavy equipment. Grease pit and drainage.	
Casting against ground:	Yes	
Insulation:	100mm Sundolitt S80	
Plastic film:	No	
Macadam:	150mm	
Geotextile:	Yes	
Cover thickness top:	25	[mm]
Cover thickness bottom:	30 against insulation 50 against ground	[mm]
Total floor area:	1360	[m ²]
Sawn joints:	No	[mm]
Dilatation joints:	Yes, alpha-joints	[mm]
w/c ratio:	wct=0.75 (max)	
Water ratio:	not specified	
Cement ratio:	not specified	
Cement type:	not specified	
Strength class:	C20/25	
Max aggregate size:	not specified	
Consistency class:	not specified	
Reference shrinkage:	not specified	
Shrinkage reducer:	not specified	
Water reducer:	not specified	

Other additives:	not specified
------------------	---------------

Reinforcement type:	NPS500 / B500BT
Steel properties:	$f_{yk} = 500\text{MPa}$
Double reinforcement:	Yes, $\Phi 10s125\text{mm} / \Phi 10s125\text{mm}$
Centric reinforcement:	-
Overlaps detailing:	Not specified on drawings

Construction method:	
Casting period:	May 2008 - April 2008
Casting sections:	According to drawing
Casting sequence:	-
Water curing:	Special surface sealer and sprinkler curing, 7 days
Plastic cover:	Before curing with sprinkler system
Air curing:	No
Receipts from fabricant of concrete:	-

Code name:	Object 1
------------	----------

Crack number	1
Location	According to sketch
CC measurement points	200 [mm]
Crack width - Series	0,1 0,15 0,2 0,1 0,05 0,2 0,25 0,15 0,05 0,15 [mm]
Crack width - Max	0,250 [mm]
Crack width - Mean	0,140 [mm]
Concrete cover - Series	45 51 41 52 52 52 [mm]
Concrete cover - Mean	48,8 [mm]

Crack number	2
Location	According to sketch
CC measurement points	200 [mm]
Crack width - Series	0,15 0,1 0,15 0,2 0,15 0,1 [mm]
Crack width - Max	0,20 [mm]
Crack width - Mean	0,142 [mm]
Concrete cover - Series	26 25 26 25 25 23 22 [mm]
Concrete cover - Mean	24,6 [mm]

Crack number	3
Location	According to sketch
CC measurement points	200 [mm]
Crack width - Series	0,1 0,1 0,15 0,1 0,1 0,15 0,1 [mm]
Crack width - Max	0,150 [mm]
Crack width - Mean	0,114 [mm]
Concrete cover - Series	39 38 36 36 39 42 [mm]
Concrete cover - Mean	38,3 [mm]

Appendix C Data and drawings, object 2

Name:	Object 2	
Building type:	Store / Storage	
Construction time:	Spring 2006	
Geographical position:	Industrial area, approximately 200 m from the river Göta älv.	
Ground conditions:	Not specified	
Groundwater:	Not specified	
Generic demands:	Low demands on visual appearance though functionality is expected	
Demands on shrinkage cracking:	Not specified	
Applied code:	BBK	
Calculated crack width:	Not specified	
Exposure class	XC1* (corrosivity class), XF2* (exposure class), C1 (environmental class) *Applies to outside environment.	
Life time class	Not specified	
Slab thickness	200mm	
Surface tolerances	Not specified	
Surface treatment	Trowelled	
Piles or no piles	Piles according to drawing	
Perimeter strip?	Yes, according to drawing	
Cast-in connections	Columns pinned on steel plates which are casted into the floor construction. Pile caps on certain pile groups. Installation channel.	
Casting against ground	Yes	
Insulation:	70mm G100 (only in certain regions, for example in the perimeter)	
Plastic film:	No	
Macadam:	150mm	
Geotextile:	Yes	
Cover thickness top:	20 indoors, 30 outdoors	[mm]
Cover thickness bottom:	30 against insulation 50 against ground	[mm]
Total floor area:	3600	[m ²]
Sawn joints:	No	[mm]
Dilatation joints:	Yes, but poorly constructed	[mm]
w/c ratio	not specified for indoors	
Water ratio	not specified	
Cement ratio	not specified	
Cement type	Std, btg 2	
Strength class	C25/30	
Max aggregate size	not specified	
Consistency class	not specified	
Reference shrinkage	not specified	
Shrinkage reducer	not specified	

Water reducer	not specified
Other additives	not specified

Reinforcement type	NPS500 / B500BT
Steel properties	500MPa
Double reinforcement	Yes, $\Phi 8s150mm / \Phi 8s150mm$
Centric reinforcement	-
Overlaps detailing	Not specified on drawings
Notes	Extra reinforcement added over piles $10\Phi 8s150mm$ in each direction 1600mm

Casting period	Early spring 2006
Casting sections	Changed compared to drawing!
Casting sequence	Unknown
Water curing	Unknown
Plastic cover	Unknown
Air curing	Unknown
Receptions from fabricant of concrete	Unknown

Name:	Object 2
-------	----------

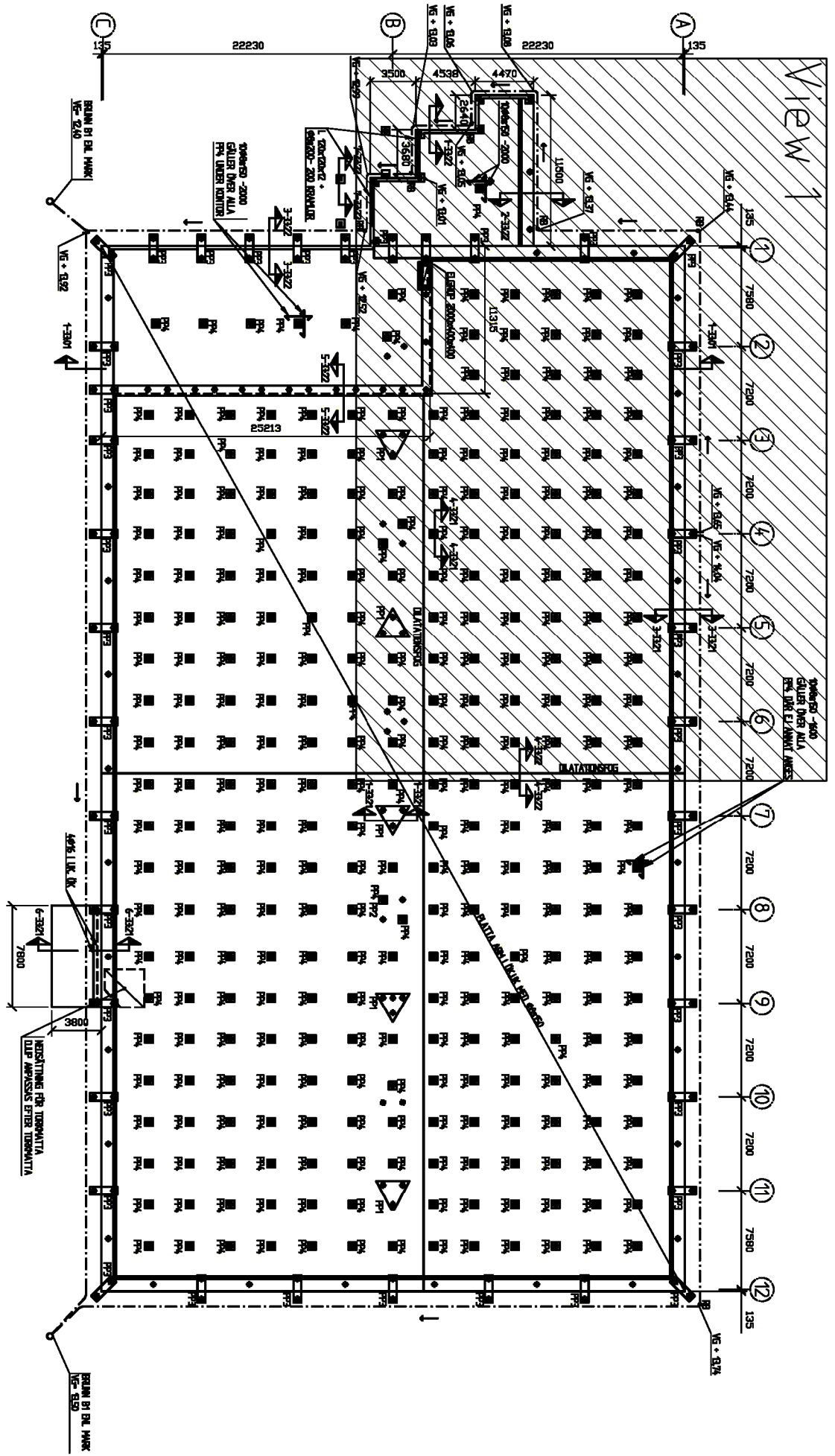
Crack number	1
Location	According to sketch , in cold storage
CC measurement points	500 [mm]
Crack width - Series	0,9 1,2 1,1 0,6 1,0 1,1 0,8 1,2 1,1 0,6 [mm]
Crack width - Max	1,200 [mm]
Crack width - Mean	0,960 [mm]
Concrete cover - Series	37 33 34 33 35 36 38 38 40 40 [mm]
Concrete cover - Mean	36,4 [mm]

Crack number	2
Location	According to sketch , in cold storage
CC measurement points	500 [mm]
Crack width - Series	1,1 1,0 0,8 0,5 1,0 [mm]
Crack width - Max	1,100 [mm]
Crack width - Mean	0,880 [mm]
Concrete cover - Series	37 33 34 33 35 36 38 38 40 40 [mm]
Concrete cover - Mean	36,4 [mm]

Crack number	3
Location	According to sketch
CC measurement points	1000 [mm]
Crack width - Series	0,5 0,4 0,4 0,8 1,0 1,1 0,8 0,9 0,7 0,8 [mm]
Crack width - Max	1,100 [mm]
Crack width - Mean	0,740 [mm]
Concrete cover - Series	22 24 24 24 23 21 [mm]
Concrete cover - Mean	23,0 [mm]

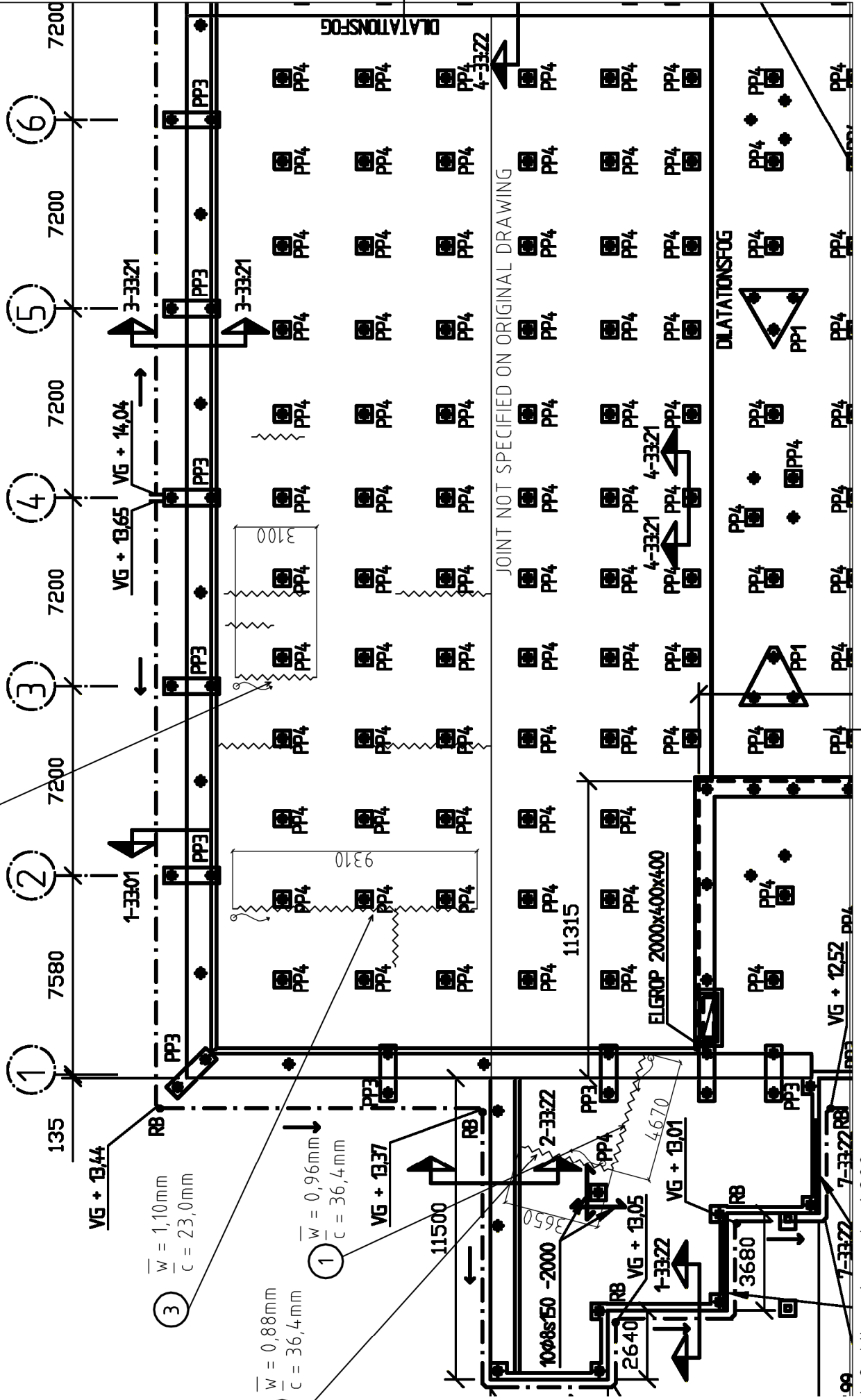
Crack number	4
Location	According to sketch
CC measurement points	500 [mm]
Crack width - Series	0,6 0,5 1,0 0,9 0,5 0,7 0,3 [mm]
Crack width - Max	1,000 [mm]
Crack width - Mean	0,643 [mm]
Concrete cover - Series	29 29 31 33 [mm]
Concrete cover - Mean	30,5 [mm]

Object 2, Orientation figure



1008s150 -1600
 GÄLLER ÖVER ALLA
 PP4 DÄR EJ ANNAT ANGES

$\bar{w} = 0,64\text{mm}$
 $\bar{c} = 30,5\text{mm}$



$\bar{w} = 1,10\text{mm}$
 $\bar{c} = 23,0\text{mm}$

$\bar{w} = 0,88\text{mm}$
 $\bar{c} = 36,4\text{mm}$

$\bar{w} = 0,96\text{mm}$
 $\bar{c} = 36,4\text{mm}$

Appendix D Data and drawings, object 3

Name:	Object 3
-------	----------

Building type:	Store / Storage
Construction time:	First half of 2007

Geographical position:	Industrial area, approximately 4km from the coast.
Ground conditions:	Not specified
Groundwater:	Not specified

Generic demands:	No special client demands found. A functioning storage/store is expected.
Demands on shrinkage cracking:	Not specified

Applied code:	BBK
Calculated crack width:	Unknown

Exposure class	XC1* (corrosivity class), XF2* (exposure class), C1 (environmental class) *Applies to outside environment.
Life time class	Not specified
Slab thickness	270mm
Surface tolerances	Not specified
Surface treatment	Not specified

Piles or no piles	Piles, according to drawing K30:103 - K30:104
Perimeter strip	Isolated from column foundations
Cast-in connections	Columns pinned on steel plates which are casted into the floor construction. Pile caps on certain pile groups. Installation channel
Casting against ground	Yes, mainly
Insulation:	At points where wall meets floor and around freeze sensible installations
Plastic film:	Not specified
Macadam:	Not specified, but control following BBK is requested
Geotextile:	Not specified

Cover thickness top:	20 indoors	[mm]
Cover thickness bottom:	30 against insulation 50 against ground	[mm]
Total floor area:	3040	[m ²]
Sawn joints:	No	[mm]
Dilatation joints:	No, but casting joints are specified on drawings.	

w/c ratio	not specified
Water ratio	not specified
Cement ratio	not specified
Cement type	Std, btg 2
Strength class	C25/30
Max aggregate size	not specified
Consistency class	not specified
Reference shrinkage	not specified
Shrinkage reducer	not specified

Water reducer	not specified
Other additives	not specified

Reinforcement type	NPS500 / B500BT
Steel properties	500MPa
Double reinforcement	Yes, # Φ 10s150mm / # Φ 8s150mm
Centric reinforcement	-
Overlaps detailing	Not specified on drawings
Notes	Extra reinforcement according to drawing K30:02

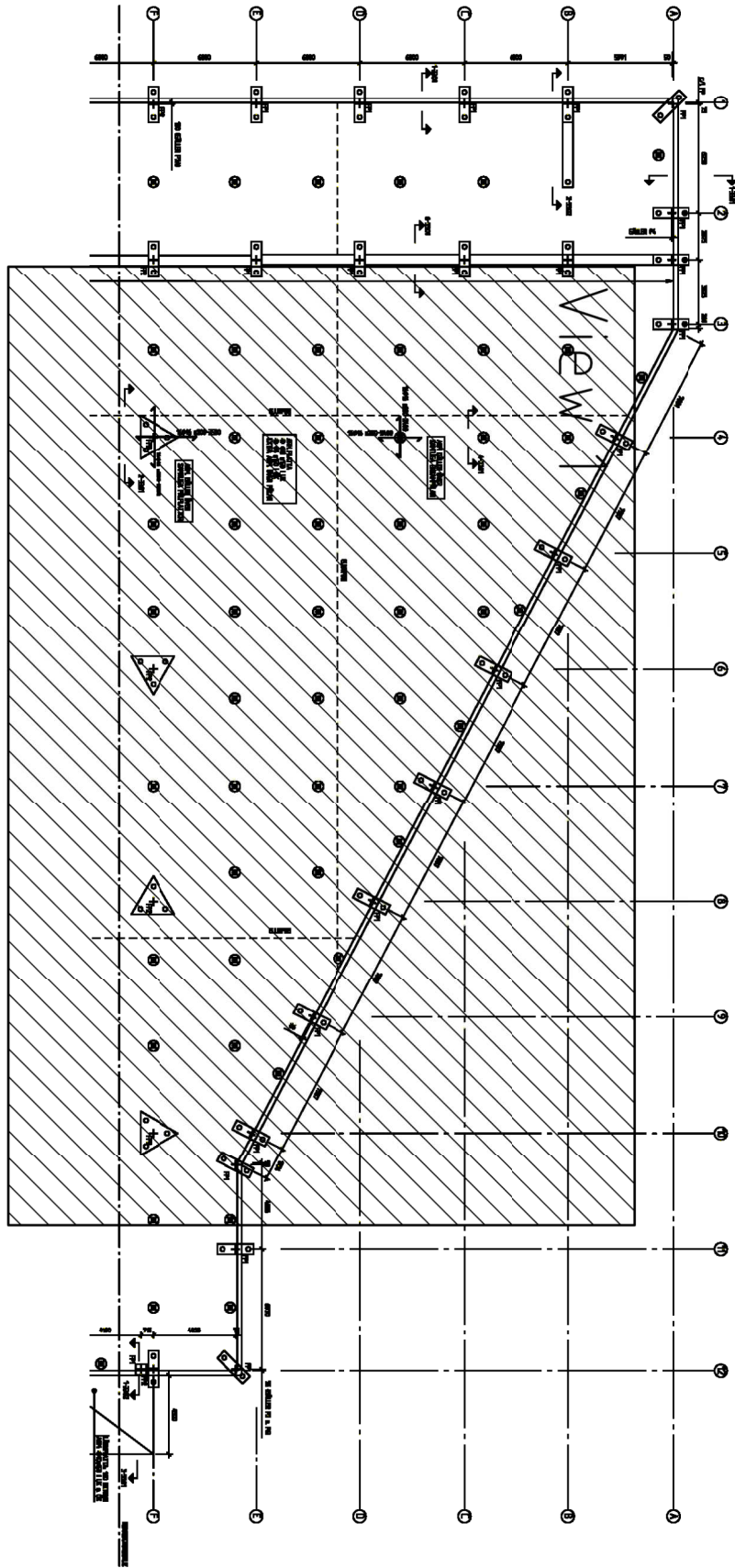
Casting period	Spring 2007
Casting sections	Specified on drawings
Casting sequence	Unknown
Water curing	Unknown
Plastic cover	Unknown
Air curing	Unknown
Receipts from fabricant of concrete	-

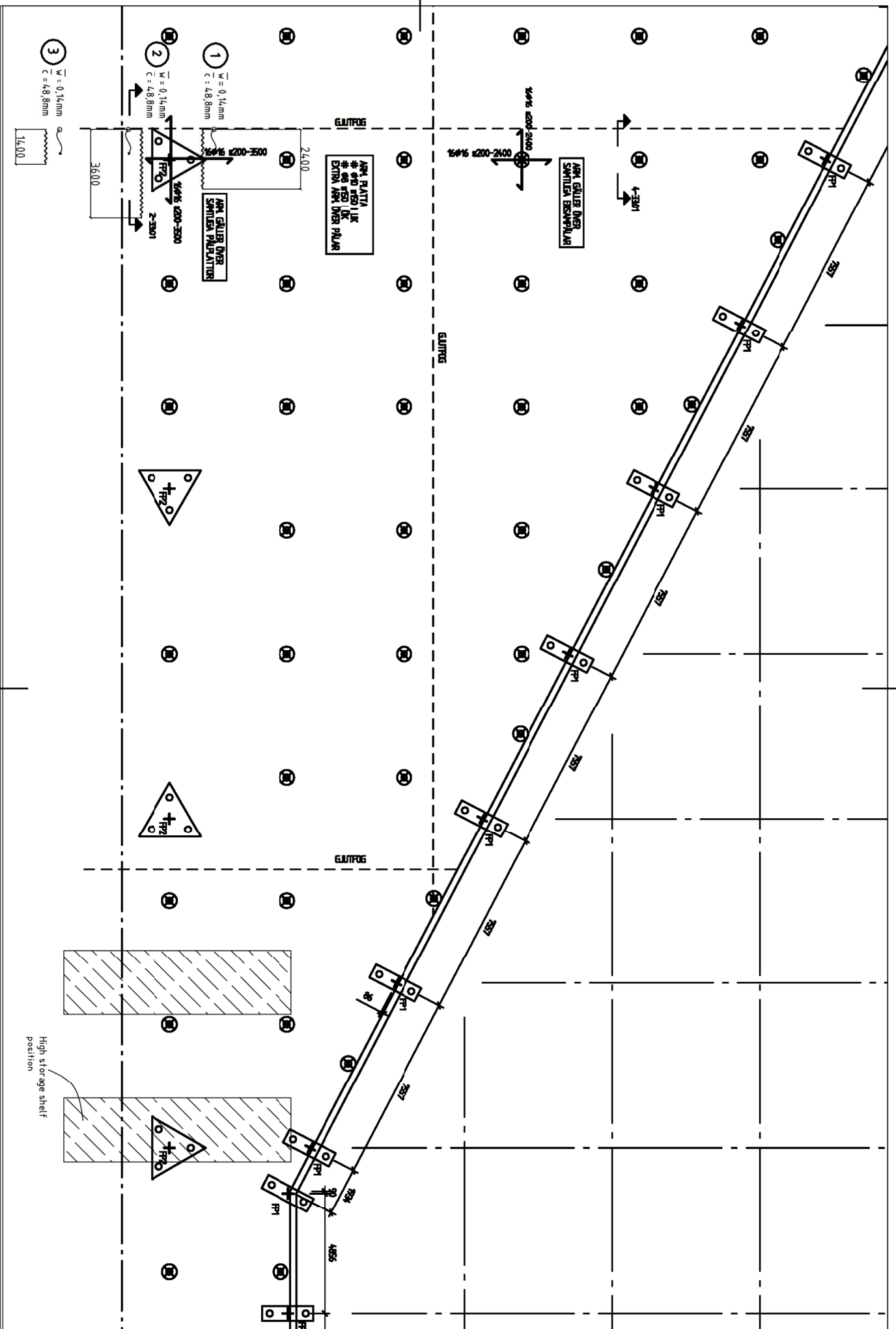
Code name:	Object 3
------------	----------

Crack number	1
Location	According to sketch
CC measurement	150 [mm]
Crack width: Series	0,6 0,4 0,4 0,4 0,5 0,6 0,8 0,5 0,8 0,8 0,4 0,7 0,6 0,8 [mm]
Crack width: Max	0,800 [mm]
Crack width: Mean	0,593 [mm]
Concrete cover: Series	45 <i>very hard to measure, the equipment did not give reliable measurements</i> [mm]
Concrete cover: Mean	45,0 [mm]

Crack number	2
Location	According to sketch
CC measurement	200 [mm]
Crack width: Series	1,0 0,9 1,0 1,0 0,8 1,1 0,6 1,6 1,2 1 2 1,4 1,5 1,4 1,5 1,3 [mm]
Crack width: Max	2,000 [mm]
Crack width: Mean	1,200 [mm]
Concrete cover: Series	45 <i>very hard to measure, the equipment did not give reliable measurements</i> [mm]
Concrete cover: Mean	45,0 [mm]

Crack number	3
Location	According to sketch
CC measurement	150 [mm]
Crack width: Series	0,1 0,2 0,3 0,3 0,4 0,3 0,3 0,4 0,3 0,3 [mm]
Crack width: Max	0,400 [mm]
Crack width: Mean	0,290 [mm]
Concrete cover: Series	45 <i>very hard to measure, the equipment did not give reliable measurements</i> [mm]
Concrete cover: Mean	45,0 [mm]





Appendix E Data and drawings, object 4

Code name:	Object 4
------------	----------

Building type:	Store / Storage
Construction time:	Autumn 2007 - Spring 2008

Geographical position:	Industrial area, approximately 4km from the coast.
Ground conditions:	Not specified
Groundwater:	Not specified

Generic demands:	<i>The client is more aware of cracks than in the other projects. As a result they have filled existing cracks.</i>
Demands on shrinkage cracking:	Not specified

Applied code:	BBK
Calculated crack width:	Not specified

Exposure class	XC1 (corrosivity class), C1 (environmental class)
Life time class	Not specified
Slab thickness	250mm
Surface tolerances	Not specified
Surface treatment	Not specified

Piles or no piles	Piles, according to drawings
Perimeter strip	All around and two along main direction in the middle.
Cast-in connections	Columns pinned on steel plates which are casted into the floor construction. Installation channel. Elevator located in connection to office area.
Casting against ground	Yes and no. Insulation under the office area.
Insulation:	In office area (100mm), not in storage.
Plastic film:	Not specified
Macadam:	150mm (16-32)
Geotextile:	Possibly according to drawing.

Cover thickness top:	20 indoors	[mm]
Cover thickness bottom:	30 against insulation 50 against ground	[mm]
Total floor area:	682	[m ²]
Sawn joints:	No	
Dilatation joints:	No	

w/c ratio	Not specified
Water ratio	Not specified
Cement ratio	Not specified
Cement type	Std, btg 2
Strength class	C25/30
Max aggregate size	Not specified
Consistency class	Not specified
Reference shrinkage	Not specified
Shrinkage reducer	Not specified

Water reducer	Not specified
Other additives	Not specified

Reinforcement type	NPS500 / B500BT
Steel properties	500MPa
Double reinforcement	Yes, $\Phi 8s150mm / \Phi 8s150mm$
Centric reinforcement	-
Overlaps detailing	Not specified on drawings
Notes	Extra reinforcement according to drawing

Casting period	Autumn 2007 - Spring 2008
Casting sections	According to drawing.
Casting sequence	Unknown
Water curing	Unknown
Plastic cover	Unknown
Air curing	Unknown
Receipts from fabricant of concrete	-

Code name:	Object 4
------------	----------

Crack number	1
Location	According to sketch
CC measurement	200 [mm]
Crack width: Series	0,2 0,3 0,4 0,8 0,4 0,2 0,8 0,7 1,1 0,8 0,8 0,4 1,0 0,8 0,3 [mm]
Crack width: Max	1,100 [mm]
Crack width: Mean	0,600 [mm]
Concrete cover: Series	66 68 67 71 75 [mm]
Concrete cover: Mean	69,4 [mm]

Crack number	2
Location	According to sketch
CC measurement	200 [mm]
Crack width: Series	0,2 0,2 0,2 0,3 0,3 0,3 0,4 0,4 0,5 0,3 0,2 0,2 0,4 0,4 0,3 0,4 0,3 [mm]
Crack width: Max	0,500 [mm]
Crack width: Mean	0,303 [mm]
Concrete cover: Series	56 59 67 67 63 [mm]
Concrete cover: Mean	62,4 [mm]

Crack number	3
Location	According to sketch
CC measurement	200 [mm]
Crack width: Series	0,1 0,2 0,1 0,4 0,4 0,5 [mm]
Crack width: Max	0,500 [mm]
Crack width: Mean	0,283 [mm]
Concrete cover: Series	56 55 53 54 53 [mm]
Concrete cover: Mean	54,2 [mm]

Crack number	4
Location	According to sketch
CC measurement	200 [mm]
Crack width: Series	0,2 0,2 0,3 0,4 0,3 0,5 0,2 0,1 0,3 0,4 0,4 0,5 0,3 0,3 [mm]
Crack width: Max	0,500 [mm]
Crack width: Mean	0,311 [mm]
Concrete cover: Series	77 77 91 100 [mm]
Concrete cover: Mean	86,3 [mm]

Crack number	5
Location	According to sketch
CC measurement	200 [mm]
Crack width: Series	0,1 0,2 0,3 0,2 0,5 0,2 0,3 0,3 0,4 0,4 0,4 0,4 0,2 0,4 0,4 0,5 0,2 [mm]
	0,2 0,3 0,3
Crack width: Max	0,500 [mm]
Crack width: Mean	0,310 [mm]
Concrete cover: Series	69 77 74 70 73 [mm]
Concrete cover: Mean	72,6 [mm]

Crack width: Max	0,500	[mm]
Crack width: Mean	0,310	[mm]
Concrete cover: Series	69 77 74 70 73	[mm]
Concrete cover: Mean	72,6	[mm]

Crack number	6	
Location	According to sketch	
CC measurement	200	[mm]
Crack width: Series	0,4 0,5 0,5 0,8 0,6 0,7 0,6 0,7 1,0 0,4 0,8 0,8 0,6 0,7 0,5 0,7	[mm]
Crack width: Max	1,000	[mm]
Crack width: Mean	0,644	[mm]

Crack number	7	
Location	According to sketch	
CC measurement	500	[mm]
Crack width: Series	0,5 0,3 0,8 1,0 0,4 0,5 0,6	[mm]
Crack width: Max	1,000	[mm]
Crack width: Mean	0,586	[mm]

Crack number	8	
Location	According to sketch	
CC measurement	500	[mm]
Crack width: Series	0,5 0,4 0,6 1,0 1,0 0,8 0,5	[mm]
Crack width: Max	1,000	[mm]
Crack width: Mean	0,686	[mm]

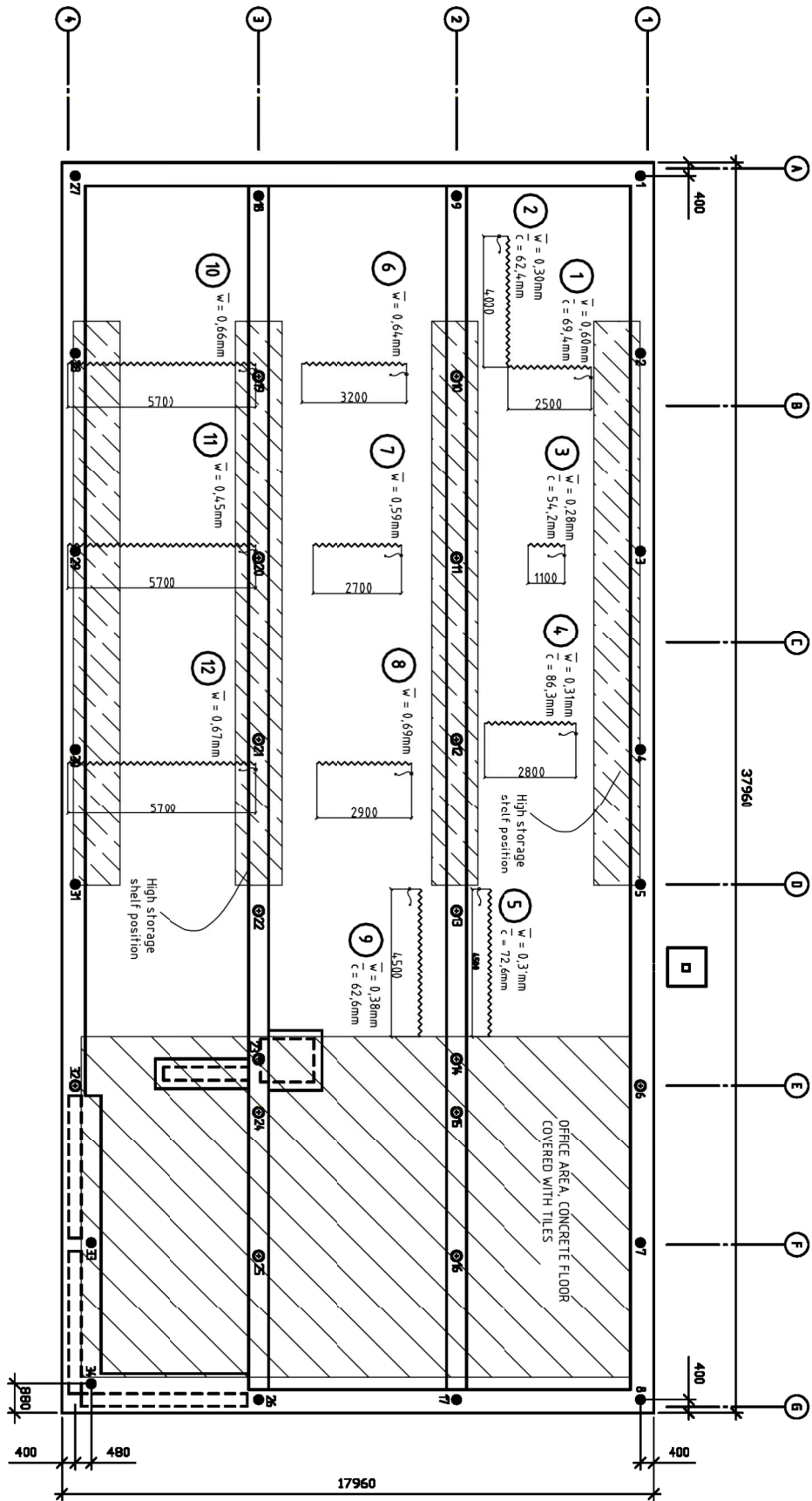
Crack number	9	
Location	According to sketch	
CC measurement	200	[mm]
Crack width: Series	0,5 0,2 0,3 0,3 0,4 0,5 0,3 0,4 0,3 0,5 0,4 0,5 0,3	[mm]
Crack width: Max	0,500	[mm]
Crack width: Mean	0,377	[mm]
Concrete cover: Series	65 61 63 57 67	[mm]
Concrete cover: Mean	62,6	[mm]

Crack number	10	
Location	According to sketch	
CC measurement	400	[mm]
Crack width: Series	0,4 0,7 0,7 0,7 0,8 0,6 0,5 0,5 1,0	[mm]
Crack width: Max	1,000	[mm]
Crack width: Mean	0,656	[mm]

Crack number	11	
Location	According to sketch	
CC measurement	300	[mm]
Crack width: Series	0,2 0,2 0,3 0,6 0,4 0,5 0,6 0,5 0,5 0,5 0,6 0,5 0,4 0,5 0,4 0,5	[mm]
Crack width: Max	0,600	[mm]
Crack width: Mean	0,450	[mm]

Crack number	12	
--------------	----	--

Location	According to sketch	
CC measurement	500	[mm]
Crack width: Series	0,4 0,8 0,8 1,0 1,0 0,3 0,4	[mm]
Crack width: Max	1,000	[mm]
Crack width: Mean	0,671	[mm]



Appendix F Stiffness calculations for piles

Input parameters

Geometry of piles

- SP1 (235mm)
- SP2 (270mm)
- SP2 (275mm)
- SP3 (270mm)
- SP3 (275mm)

$$\text{Pile}_{\text{data}} := \begin{pmatrix} 235 & 4 & 16 \\ 270 & 8 & 12 \\ 275 & 8 & 12 \\ 270 & 8 & 16 \\ 275 & 8 & 16 \end{pmatrix}$$

Pile type	Dimension	Reinforcement	
	Pile width [mm]	Number of bars	ϕ [mm]
SP1	235	4	16
SP2	270	8	12
SP2	275	8	12
SP3	270	8	16
SP3	275	8	16

$$b_p := \text{Pile}_{\text{data}}[\text{Pile}_{\text{type}}, 0] \cdot \text{mm} = 235 \cdot \text{mm} \quad (\text{Pile width})$$

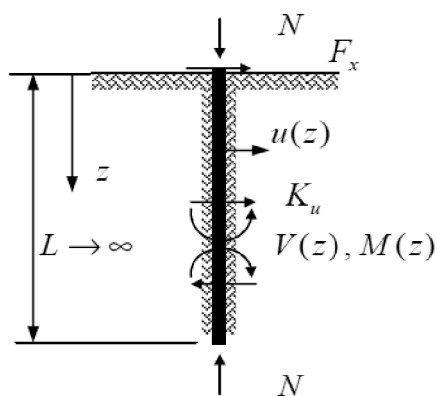
$$h_p := b_p = 235 \cdot \text{mm} \quad (\text{Pile height})$$

$$n_p := \text{Pile}_{\text{data}}[\text{Pile}_{\text{type}}, 1] = 4 \quad (\text{Number of bars})$$

$$\phi_p := \text{Pile}_{\text{data}}[\text{Pile}_{\text{type}}, 2] \cdot \text{mm} = 16 \cdot \text{mm} \quad (\text{Bar dimension})$$

Elementary Case:

Horizontally loaded pile



	$N = 0$	$N > 0$
$u(z)$	$\frac{F_x L_g^3}{2 EI} C_{\delta 0}(z)$	$\frac{F_x L_{g1}^3}{2 EI} C_{F \delta N}(z)$
$u'(z)$	$-\frac{F_x L_g^2}{2 EI} C_{\alpha 0}(z)$	$-\frac{F_x L_{g1}^2}{2 EI} C_{F \alpha N}(z)$
$M(z)$	$F_x L_g C_{\beta 0}(z)$	$F_x L_{g1} C_{F \beta N}(z)$
$V(z)$	$-F_x C_{\gamma 0}(z)$	$-F_x C_{F \gamma N}(z)$

Assuming concrete cover of 30mm

$$c_p := 30\text{mm}$$

$$A_{c,p} := h_p \cdot b_p = 5.523 \times 10^4 \cdot \text{mm}^2$$

$$A_{s,p} := n_p \cdot \frac{\pi \cdot [(12\text{mm})^2]}{4} = 452.389 \cdot \text{mm}^2$$

$$I_{c,p} := \frac{b_p \cdot h_p^3}{12} = 2.542 \times 10^8 \cdot \text{mm}^4$$

$$I_{s,p} := A_{s,p} \cdot \left[\frac{b_p}{2} - [c_p + (\phi_p)] \right]^2 = 2.313 \times 10^6 \cdot \text{mm}^4$$

Safety factors correcting the strength classes with regard to handling and storing procedures. There is more info about the choice of the below values in Svahn & Alén (2006).

$$\mu_c := 0.6$$

$$\mu_{sc} := 0.6 \quad (\text{steel in compression})$$

$$\mu_{st} := 1 \quad (\text{steel in tension})$$

$$\text{safety class 1} \quad \gamma_n := 1$$

Material data

Concrete properties

Assuming C45/55

$$f_{ck,p} := 45\text{MPa}$$

$$f_{cm,p} := 53\text{MPa}$$

$$f_{ctk0.05,p} := 2.7\text{MPa}$$

$$E_{cm,p} := 36\text{GPa}$$

reduced:

$$E_{cr,p} := \frac{E_{cm,p}}{\gamma_n \cdot 1.2} = 30 \cdot \text{GPa}$$

$$f_{cr,p} := \mu_c \cdot \frac{f_{ck,p}}{\gamma_n \cdot 1.5} = 18 \cdot \text{MPa}$$

$$f_{ctr,p} := \mu_c \cdot \frac{f_{ctk0.05,p}}{\gamma_n \cdot 1.5} = 1.08 \cdot \text{MPa}$$

Steel properties

B500B

$$E_{s,p} := 200\text{GPa}$$

$$f_{yk,p} := 500\text{MPa}$$

reduced:

$$E_{sr,p} := \frac{E_{s,p}}{\gamma_n \cdot 1.05} = 190.476 \cdot \text{GPa}$$

$$f_{src,p} := \mu_{sc} \cdot \frac{f_{yk,p}}{\gamma_n \cdot 1.15} = 260.87 \cdot \text{MPa}$$

$$f_{srt,p} := \mu_{st} \cdot \frac{f_{yk,p}}{\gamma_n \cdot 1.15} = 434.783 \cdot \text{MPa}$$

Effective creep coefficient (assumed)

$$\varphi_{c,ef,p} := 1.5$$

Bending stiffness of the pile

This is done according to old standards BBK94, but will be on safe side (stiffer) as long as the axial load of the pile does not exceed approximately 750kN

$$EI_p := \max\left(\frac{0.4 \cdot E_{cr,p} \cdot I_{c,p}}{1 + \varphi_{c,ef,p}}, \frac{0.2 \cdot E_{cr,p} \cdot I_{c,p}}{1 + \varphi_{c,ef,p}} + E_{sr,p} \cdot I_{s,p}\right) = 1.22 \cdot \text{MN} \cdot \text{m}^2$$

Piles without vertical load

Following procedure according to Svahn & Alén (2006).

$$z = 0 \quad N = 0$$

$$L_g = \sqrt[4]{\left(\frac{4 \cdot E \cdot I}{k_u}\right)}$$

$$k_u = 50 \cdot \frac{c_u}{b_p}$$

$$c_u := 200 \frac{\text{kN}}{\text{m}^2}$$

$$k_u := 50 \cdot \frac{c_u}{b_p} = 4.255 \times 10^4 \cdot \frac{\text{kN}}{\text{m}^3}$$

$$\text{cor} := \text{m} \cdot \text{m}^{-1.25}$$

$$L_{g,p} := \sqrt[4]{\left(\frac{4 \cdot EI_p}{k_u}\right)} \cdot \text{cor} = 0.582 \text{ m}$$

Horizontal stiffness of pile:

$$S_{\text{pile},0,i} := \frac{2 \cdot EI_p}{L_{g,p}^3} = 1.238 \times 10^4 \cdot \frac{\text{kN}}{\text{m}}$$

Appendix G Matlab code for direct stiffness method

```
%% =====%
% Slab_Crack_Evaluation_Generic.m
%
% Program that calculates the stress distribution for a slab-on-ground
% subjected to shrinkage. The program regards the slab as uncracked and
% divides it into elements. It then uses the Direct Stiffness Method
% to find the displacements and corresponding stresses.
%
% Authors: Fabian Narin, 860114-4010, narin@student.chalmers.se
%          Olle Wiklund, 850114-0779, wiklundo@student.chalmers.se
%
% Subject: Calculations for master's thesis work
%
% Version 1.0
%=====%%

clear all
close all
clc

%%
% --- Input: Defining the slab section, coordinates in x-direction

%Nodal coordinates
nCord =[0 8 16 24 32 40]; %Input to define the system [m]

%Defining positions of external restraints
pileloc= [1 1 1 1 1 1]; % 1 equals position for pile
perloc= [1 0 0 0 0 1]; % 1 equals position for perimeter strip

%Slab geometry
b = 8; % [m] Centre to centre between piles
      % (into the plane)
th = 0.25; % [m] Thickness of slab
c = 0.03; % [m] Concrete cover

%%
% --- Input: Defining material constants

%Concrete data (time-dependent values are taken after 50 years)
      % Concrete class: C30/37
fctm = 2.9e6; % [Pa] Tensile capacity, mean value
fctk5 = 2e6; % [Pa] Tensile capacity, 5% percentile
fctk95 = 3.8e6; % [Pa] Tensile capacity, 95% percentile
Ecef = 9.272e9; % [Pa] Effective modulus of concrete
ecs = -4.025e-4; % [-] Shrinkage strain of concrete, 50years

%Steel reinforcement (two layers, calculations are for one layer)
Es = 200e9; % [Pa] Modulus of elasticity for steel
Phi = 0.012; % [m] Bar diameter
```

```

s = 0.150; % [m] Bar spacing

%Material data for the sub-base
Eground = 100e6; % [Pa] Modulus of elasticity for ground

%%
% --- Calculations of sectional constants

%Reinforcement
Asi = pi*Phi^2/4; % [m^2] Bar cross-sectional area
n = b/s; % [-] Number of bars in cross section
As = n*Asi; % [m^2] Steel area in cross section
Ac = b*th/2; % [m^2] Concrete area in tensile zone
% Studying response of one layer of r.f.

%Transformed section using effective concrete area
alpha = Es/Ecef; % [-] Modular ratio
Atrans = (Ac+(alpha-1)*As); % [m^2] Transformed concrete section

%%
% --- External stiffnesses

Sper = Eground*b/(2*log(5)); % [N/m] Stiffness of perimiter strip
% log is the natural logarithm
Spile = 4.377e6; % [N/m] Stiffness of pile

% --- Defining positions for additional stiffness
nCordpiles = Spile*pileloc;
nCordper = Sper*perloc;

% --- Checking input coordinates
if length(nCordpiles) ~= length(nCord)
    disp('Pile coordinates do not match element coordinates, check input')
    break
end

if length(nCordper) ~= length(nCord)
    disp('Perimiter strip coordinates do not match element coordinates,')
    disp('check input')
    break
end

%%
% --- Calculating stresses, non moving point and connectivity parameters

[sigma_c, nCord, nDofs, nEl, x_0] = Slab_Stress_Calculation(nCord, Es,...
    ecs, As, Atrans, Ac, Ecef, nCordpiles, nCordper);

%%
% --- Plotting results

%Axis limits
yminS=0.6*fctk5*0.95;
ymaxS=0.6*fctk95*1.05;
xminS=0;

```

```

xmaxS=nCord(length(nCord));

%Plotting element stresses
figure (1)
hold on
grid on

for i=1:nEl
    hold on
    plot([nCord(i) nCord(i+1)],(sigma_c(i)*[1 1])...
        , 'gx-', 'LineWidth',2, 'MarkerSize',5)
end

%Plotting non moving point on specific element
plot(x_0,max(sigma_c), 'b*', 'MarkerSize',8)

%Plotting reduced capacities (sustained loading)
plot([0 nCord(nDofs)], (0.6*fctm*[1 1]), '--r'...
    , 'LineWidth',2, 'MarkerSize',5)
plot([0 nCord(nDofs)], (0.6*fctk5*[1 1]), '--r'...
    , 'LineWidth',2, 'MarkerSize',5)
plot([0 nCord(nDofs)], (0.6*fctk95*[1 1]), '--r'...
    , 'LineWidth',2, 'MarkerSize',5)

%Labels
ylabel('[Pa]')
xlabel('[m]')
axis([xminS xmaxS yminS ymaxS])
title('Crack risk evaluation - Generic case','FontSize',12)

%Texts
position_x=x_0;
position_y=0.07e6+max(sigma_c);
text(position_x-6,position_y,'Concrete element stress',...
    'BackgroundColor',[1 1 1]);
position_fctm=0.05e6+0.6*fctm;
text(1,position_fctm,'0.6*fctm','BackgroundColor',[1 1 1]);
position_fctk5=0.05e6+0.6*fctk5;
text(1,position_fctk5,'0.6*fctk 5% percentile',...
    'BackgroundColor',[1 1 1]);
position_fctk95=0.05e6+0.6*fctk95;
text(1,position_fctk95,'0.6*fctk 95% percentile',...
    'BackgroundColor',[1 1 1]);

%=====

```

```

%% =====
% Slab_Crack_Evaluation_Object1.m
%
% Program that calculates the stress distribution for a slab-on-ground
% subjected to shrinkage. The program regards the slab as uncracked and
% divides it into elements. It then uses the Direct Stiffness Method
% to find the displacements and corresponding stresses.
%
% Authors: Fabian Narin, 860114-4010, narin@student.chalmers.se
%          Olle Wiklund, 850114-0779, wiklundo@student.chalmers.se

% Subject: Calculations for master's thesis work
%
% Version 1.0
%=====

clear all
close all
clc

%%
% --- Input: Defining the slab section, coordinates in x-direction

%Nodal coordinates
nCord = [0 3.3 6.6 9.9 13.2 16.5 19.8 23.1 28.1]; %[m]

%Defining positions of external restraints
pileloc= [1 1 1 1 1 1 1 1 1];
perloc= [1 0 0 0 0 0 0 1 1];

%Slab geometry
b = 3.3; % [m] Centre to centre between piles
% (into the plane)
th = 0.22; % [m] Thickness of slab
c = 0.025; % [m] Concrete cover

%%
% --- Input: Defining material constants

%Concrete data (time-dependent values are taken after 50 years)
% Concrete class: C20/25
fctm = 2.2e6; % [Pa] Tensile capacity, mean value
fctk5 = 1.5e6; % [Pa] Tensile capacity, 5% percentile
fctk95 = 2.9e6; % [Pa] Tensile capacity, 95% percentile
Ecef = 6.591e9; % [Pa] Effective modulus of concrete
ecs = -4.326e-4; % [-] Shrinkage strain of concrete, 50years

%Steel reinforcement (two layers, calculations are for one layer)
Es = 200e9; % [Pa] Modulus of elasticity for steel
Phi = 0.010; % [m] Bar diameter
s = 0.125; % [m] Bar spacing

%Material data for the sub-base
Eground = 100e6; % [Pa] Modulus of elasticity for ground

```

```

%%
% --- Calculations of sectional constants

%Reinforcement
Asi = pi*Phi^2/4;           % [m^2] Bar cross-sectional area
n = b/s;                   % [-] Number of bars in cross section
As = n*Asi;                % [m^2] Steel area in cross section
Ac = b*th/2;               % [m^2] Concrete area in tensile zone
                             % Studying response of one layer of r.f.

%Transformed section using effective concrete area
alpha = Es/Ecef;           % [-] Modular ratio
Atrans = (Ac+(alpha-1)*As);% [m^2] Transformed concrete section

%%
% --- External stiffnesses

Sper = Eground*b/(2*log(5));% [N/m] Stiffness of perimeter strip
                             % log is the natural logarithm
Spile = 4.377e6;           % [N/m] Stiffness of pile

% --- Defining positions for additional stiffness
nCordpiles = Spile*pileloc;
nCordper = Sper*perloc;

% --- Checking input coordinates
if length(nCordpiles) ~= length(nCord)
    disp('Pile coordinates do not match element coordinates, check input')
    break
end

if length(nCordper) ~= length(nCord)
    disp('Perimeter strip coordinates do not match element coordinates,')
    disp('check input')
    break
end

%%
% --- Calculating stresses, non moving point and connectivity parameters

[sigma_c, nCord, nDofs, nEl, x_0] = Slab_Stress_Calculation(nCord, Es,...
    ecs, As, Atrans, Ac, Ecef, nCordpiles, nCordper);

%%
% --- Plotting results

%Axis limits
yminS=0.6*fctk5*0.95;
ymaxS=0.6*fctk95*1.05;
xminS=0;
xmaxS=nCord(length(nCord));

%Plotting element stresses
figure (1)
hold on

```

```

grid on

for i=1:nEl
    hold on
    plot([nCord(i) nCord(i+1)],(sigma_c(i)*[1 1])...
        , 'gx-', 'LineWidth', 2, 'MarkerSize', 5)
end

%Plotting non moving point on specific element
plot(x_0,max(sigma_c), 'b*', 'MarkerSize', 8)

%Plotting reduced capacities (sustained loading)
plot([0 nCord(nDofs)], (0.6*fctm*[1 1]), '--r'...
    , 'LineWidth', 2, 'MarkerSize', 5)
plot([0 nCord(nDofs)], (0.6*fctk5*[1 1]), '--r'...
    , 'LineWidth', 2, 'MarkerSize', 5)
plot([0 nCord(nDofs)], (0.6*fctk95*[1 1]), '--r'...
    , 'LineWidth', 2, 'MarkerSize', 5)

%Labels
ylabel(' [Pa] ')
xlabel(' [m] ')
axis([xminS xmaxS yminS ymaxS])
title('Crack risk evaluation - Case 1', 'FontSize', 12)

%Texts
position_x=x_0;
position_y=0.05e6+max(sigma_c);
text(position_x-6,position_y, 'Concrete element stress',...
    'BackgroundColor', [1 1 1]);
position_fctm=-0.05e6+0.6*fctm;
text(1,position_fctm, '0.6*fctm', 'BackgroundColor', [1 1 1]);
position_fctk5=0.05e6+0.6*fctk5;
text(1,position_fctk5, '0.6*fctk 5% percentile',...
    'BackgroundColor', [1 1 1]);
position_fctk95=0.05e6+0.6*fctk95;
text(1,position_fctk95, '0.6*fctk 95% percentile',...
    'BackgroundColor', [1 1 1]);

%=====

```

```

%% =====%
% Slab_Crack_Evaluation_Object2.m
%
% Program that calculates the stress distribution for a slab-on-ground
% subjected to shrinkage. The program regards the slab as uncracked and
% divides it into elements. It then uses the Direct Stiffness Method
% to find the displacements and corresponding stresses.
%
% Authors: Fabian Narin, 860114-4010, narin@student.chalmers.se
%          Olle Wiklund, 850114-0779, wiklundo@student.chalmers.se

% Subject: Calculations for master's thesis work
%
% Version 1.0
%=====%%

clear all
close all
clc

%%
% --- Input: Defining the slab section, coordinates in x-direction

%Nodal coordinates
nCord =[0 3.2 6.4 9.6 12.8 16 19.2 22.4 25.6 28.8 32 35.2 38.4 40.8];

%Defining positions of external restraints
pileloc=[1 1 1 1 1 1 1 1 1 1 1 1 1 0];
perloc= [1 0 0 0 0 0 0 0 0 0 0 0 0 0];

%Slab geometry
b = 3.2; % [m] Centre to centre between piles
% (into the plane)
th = 0.20; % [m] Thickness of slab
c = 0.02; % [m] Concrete cover

%%
% --- Input: Defining material constants

%Concrete data (time-dependent values are taken after 50 years)
% Concrete class: C25/30
fctm = 2.6e6; % [Pa] Tensile capacity, mean value
fctk5 = 1.8e6; % [Pa] Tensile capacity, 5% percentile
fctk95 = 3.3e6; % [Pa] Tensile capacity, 95% percentile
Ecef = 7.173e9; % [Pa] Effective modulus of concrete
ecs = -4.278e-4; % [-] Shrinkage strain of concrete, 50years

%Steel reinforcement (two layers, calculations are for one layer)
Es = 200e9; % [Pa] Modulus of elasticity for steel
Phi = 0.008; % [m] Bar diameter
s = 0.150; % [m] Bar spacing

%Material data for the sub-base
Eground = 100e6; % [Pa] Modulus of elasticity for ground

```

```

%%
% --- Calculations of sectional constants

%Reinforcement
Asi = pi*Phi^2/4;           % [m^2] Bar cross-sectional area
n = b/s;                   % [-] Number of bars in cross section
As = n*Asi;                % [m^2] Steel area in cross section
Ac = b*th/2;               % [m^2] Concrete area in tensile zone
                           % Studying response of one layer of r.f.

%Transformed section using effective concrete area
alpha = Es/Ecef;           % [-] Modular ratio
Atrans = (Ac+(alpha-1)*As);% [m^2] Transformed concrete section

%%
% --- External stiffnesses

Sper = Eground*b/(2*log(5));% [N/m] Stiffness of perimeter strip
                           % log is the natural logarithm
Spile = 4.377e6;           % [N/m] Stiffness of pile

% --- Defining positions for additional stiffness
nCordpiles = Spile*pileloc;
nCordper = Sper*perloc;

% --- Checking input coordinates
if length(nCordpiles) ~= length(nCord)
    disp('Pile coordinates do not match element coordinates, check input')
    break
end

if length(nCordper) ~= length(nCord)
    disp('Perimeter strip coordinates do not match element coordinates,')
    disp('check input')
    break
end

%%
% --- Calculating stresses, non moving point and connectivity parameters

[sigma_c, nCord, nDofs, nEl, x_0] = Slab_Stress_Calculation(nCord, Es,...
    ecs, As, Atrans, Ac, Ecef, nCordpiles, nCordper);

%%
% --- Plotting results

%Axis limits
yminS=0.6*fctk5*0.9*0;
ymaxS=0.6*fctk95*1.1;
xminS=0;
xmaxS=nCord(length(nCord));

%Plotting element stresses
figure (1)
hold on

```

```

grid on

for i=1:nEl
    hold on
    plot([nCord(i) nCord(i+1)],(sigma_c(i)*[1 1]))...
        , 'gx-', 'LineWidth', 2, 'MarkerSize', 5)
end

%Plotting non moving point on specific element
plot(x_0, max(sigma_c), 'b*', 'MarkerSize', 8)

%Plotting reduced capacities (sustained loading)
plot([0 nCord(nDofs)], (0.6*fctm*[1 1]), '--r'...
    , 'LineWidth', 2, 'MarkerSize', 5)
plot([0 nCord(nDofs)], (0.6*fctk5*[1 1]), '--r'...
    , 'LineWidth', 2, 'MarkerSize', 5)
plot([0 nCord(nDofs)], (0.6*fctk95*[1 1]), '--r'...
    , 'LineWidth', 2, 'MarkerSize', 5)

%Labels
ylabel(' [Pa] ')
xlabel(' [m] ')
axis([xminS xmaxS yminS ymaxS])
title('Crack risk evaluation - Object 2', 'FontSize', 12)

%Texts
position_x=x_0;
position_y=-0.14e6+max(sigma_c);
text(position_x-6, position_y, 'Concrete element stress',...
    'BackgroundColor', [1 1 1]);
position_fctm=0.07e6+0.6*fctm;
text(1, position_fctm, '0.6*fctm', 'BackgroundColor', [1 1 1]);
position_fctk5=0.07e6+0.6*fctk5;
text(1, position_fctk5, '0.6*fctk 5% percentile',...
    'BackgroundColor', [1 1 1]);
position_fctk95=0.07e6+0.6*fctk95;
text(1, position_fctk95, '0.6*fctk 95% percentile',...
    'BackgroundColor', [1 1 1]);
%=====

```

```

=====
% Slab_Stress_Calculation.m
%
% Calculates sigma_c, nCord, nDofs och x_0 be the defined variables.
%
% Authors: Fabian Narin, 860114-4010, narin@student.chalmers.se
%          Olle Wiklund, 850114-0779, wiklundo@student.chalmers.se
%
% Subject: Calculations for master's thesis work
%
% Version 1.0
=====
%%

function [sigma_c, nCord, nDofs, nEl, x_0] = Slab_Stress_Calculation...
    (nCord, Es, ecs, As, Atrans, Ac, Ecef, nCordpiles, nCordper)

%% DEGREES OF FREEDOM AND SYSTEM CONNECTIVITY

% --- Defining system geometries, nodes and elements
nCords = length(nCord); % Number of degrees of freedom
% (one per node)
Length = zeros((nCords-1), 1); % [m] Element length vector
for j = 1:(nCords-1)
    Length(j) = nCord(j+1) - nCord(j);
end

% --- Degrees of freedom (horizontal movement)
Dofs = 1:nCords;

% --- Defining element connectivity
nEl = length(Length); % Number of elements
Elcon = zeros(nEl, 2);
for j = 1:nEl
    Elcon(j,1) = Dofs(j);
    Elcon(j,2) = Dofs(j+1);
end

%% LOAD
% --- Pre-defining loading conditions

% Shrinkage force
Fcs = Es*ecs*As;

% Element load vector
Npre = (abs(ecs) - abs(Fcs) / (Ecef*Atrans)) * Ecef*Atrans*ones...
    (1, length(nCord) - 1);

% --- Assembly of load vector
Np = zeros(nCords, 1);
for el = 1:nEl
    Npe = Npre(el) * [1; -1];
    Eldofs = [Dofs(Elcon(el,1)), Dofs(Elcon(el,2))];
    Np(Eldofs) = Np(Eldofs) + Npe;
end

```

```

end

%% STIFFNESS
% --- Pre-defining element stiffness

Spre = Ecef*Atrans./Elength;

% --- Assembly of stiffness matrix
S = zeros(nDofs);
for el = 1:nEl
    Se = Spre(el)*[1 -1; -1 1];
    Eldofs = [Dofs(Elcon(el,1)),Dofs(Elcon(el,2))];
    S(Eldofs,Eldofs) = S(Eldofs,Eldofs) + Se;
end

% --- Adding horisontal stiffeners
Sad = zeros(nDofs);
for i = 1:nDofs
    Sad(i,i)=nCordpiles(i)+nCordper(i);
end

% --- Assembly of global stiffness matrix
Stot=S+Sad;

%% SOLVING SYSTEM

% --- Calc. displacements in system & rearrangin for node w. zero displ.

u = Stot\Np;

% --- Calculating normal forces in elements

Nke=zeros(nEl,1);

for el=1:nEl;
    Eldofs = [Dofs(Elcon(el,1)),Dofs(Elcon(el,2))];
    ue=u(Eldofs);
    Nke(el)=Spre(el)*(ue(2)-ue(1));
    Npe(el)=Npre(el);
end

Ne=Nke+Npe;

% --- Calculating stresses in elements

sigma_c = (Ne+abs(Fcs))/Atrans;

%% CALCULATING NON MOVING POINT

% --- Sum of total stiffness
L_tot = nCord(length(nCord));
S_sum = Atrans*Ecef/L_tot+sum(nCordpiles)+sum(nCordper);

% --- Sum of weighted stiffness
S_sum_pile = 0;

```

```
S_sum_per = 0;
for i =1:nDofs
    S_sum_pile = S_sum_pile+nCord(i)*nCordpiles(i);
    S_sum_per = S_sum_per+nCord(i)*nCordper(i);
end
S_sum_weighted = (Atrans*Ecef/L_tot)*(L_tot/2)+S_sum_pile+S_sum_per;

% --- Identifying centre of movement, x_0
x_0 = S_sum_weighted/S_sum;
```

Appendix H Analytical friction model

Test curves according to Pettersson (1998)

Input parameters

Concrete class C30/37 gives: $f_{ctm} := 2.9\text{MPa}$ $f_{ctk.0.05} := 2\text{MPa}$ $E_{cm} := 33\text{GPa}$ $\varphi_{50yr} := 2.684$

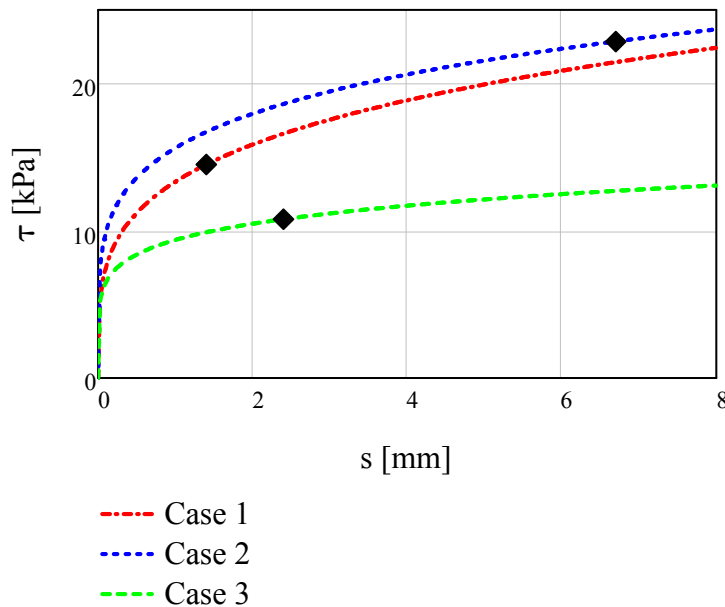
$$E_{c.ef} := \frac{E_{cm}}{1 + \varphi_{50yr}} = 8.958\text{GPa}$$

Geometry of slab used in tests: $A_{test} := 1.2 \cdot 0.8 = 0.96$

Geometry of studied slab: $b := 1\text{m}$ (one metre strip) $h := 250\text{mm}$

	<u>Force - Displacement</u>	<u>Stress - Displacement</u>
1 - Sand:	$u_{max.1} := 1.4$ $F_1(u) := 12.8 \cdot u^{0.25}$	$\tau_1(u) := \frac{F_1(u)}{A_{test}}$
2 - Crushed aggregate:	$u_{max.2} := 6.7$ $F_2(u) := 15 \cdot u^{0.2}$	$\tau_2(u) := \frac{F_2(u)}{A_{test}}$
3 - Crushed aggregate + plastic:	$u_{max.3} := 2.4$ $F_3(u) := 9 \cdot u^{0.16}$	$\tau_3(u) := \frac{F_3(u)}{A_{test}}$

Stress equations



Writing stress functions on the form $\tau_x = C \cdot s_x^n$

1 - Sand:	$C_1 := \frac{12.8}{A_{\text{test}}} = 13.333$	$n_1 := 0.25$	$\tau_{x,1}(s_{x,1}) := C_1 \cdot s_{x,1}^{n_1}$
2 - Crushed aggregate:	$C_2 := \frac{15}{A_{\text{test}}} = 15.625$	$n_2 := 0.20$	$\tau_{x,2}(s_{x,2}) := C_2 \cdot s_{x,2}^{n_2}$
3 - Crushed aggregate + plastic:	$C_3 := \frac{9}{A_{\text{test}}} = 9.375$	$n_3 := 0.16$	$\tau_{x,3}(s_{x,3}) := C_3 \cdot s_{x,3}^{n_3}$

Integration coefficients

the formulation for b_s is derived from equation (12) in the report by Tue and Köning (1991)

α_b is found in the same report according to equation (21)

1 -
Sand:

$$b_{s,1} := 0.5 \left(\frac{1 + 3 \cdot n_1}{1 - n_1^2} \right) + \sqrt{\left[0.5 \left(\frac{1 + 3 \cdot n_1}{1 - n_1^2} \right) \right]^2 + \frac{2}{(1 - n_1^2)}} = 2.667$$

$$\alpha_{b,1} := \frac{1 + b_{s,1} \cdot n_1}{2 + b_{s,1} \cdot n_1} = 0.625$$

2 -
Crushed
aggregate:

$$b_{s,2} := 0.5 \left(\frac{1 + 3 \cdot n_2}{1 - n_2^2} \right) + \sqrt{\left[0.5 \left(\frac{1 + 3 \cdot n_2}{1 - n_2^2} \right) \right]^2 + \frac{2}{(1 - n_2^2)}} = 2.5$$

$$\alpha_{b,2} := \frac{1 + b_{s,2} \cdot n_2}{2 + b_{s,2} \cdot n_2} = 0.6$$

3 -
Crushed
aggregate
+ plastic:

$$b_{s,3} := 0.5 \left(\frac{1 + 3 \cdot n_3}{1 - n_3^2} \right) + \sqrt{\left[0.5 \left(\frac{1 + 3 \cdot n_3}{1 - n_3^2} \right) \right]^2 + \frac{2}{(1 - n_3^2)}} = 2.381$$

$$\alpha_{b,3} := \frac{1 + b_{s,3} \cdot n_3}{2 + b_{s,3} \cdot n_3} = 0.58$$

Using formulations for stabilized cracking

$$l_{es} = \frac{L}{2} \quad \text{transmission length is equal to half the slab length}$$

$$\varepsilon_{c,max} := \frac{0.6f_{ctm}}{E_{c,ef}} = 1.942 \times 10^{-4} \quad \begin{array}{l} \text{(assuming maximum concrete strain)} \\ \text{(reducing the tensile strength with 40\% for a member} \\ \text{subjected to sustained loading)} \end{array}$$

$$\varepsilon_{cs} := 4.025 \cdot 10^{-4} \quad \text{(shrinkage strain for 50 years)}$$

$$s_{cs}(l_{es}) := -\varepsilon_{cs} \cdot l_{es} \quad \text{(end displacement from free shrinkage)}$$

Equations

Neglecting the effect from steel in Equation (10) of Tue & König (1991) gives:

$$\begin{array}{l} \text{End displacement due to} \\ \text{friction:} \end{array} \quad s_c = l_{es} \cdot \alpha_b \cdot \varepsilon_{c,max}$$

Considering end displacement to be the sum of end free end displacement and end displacement due to friction

$$\text{End displacement:} \quad d = s_{cs} + s_c$$

Average frictional bond stress according to Equation (14) of Tue & König (1991) gives:

$$\tau_m = C \cdot \frac{\left(\frac{d}{\text{mm}}\right)^n}{1 + b_s \cdot n}$$

From the average frictional bond stress the normal force (maximum) in the non moving point can be calculated according to:

$$N = \tau_{m,1} \cdot l_{es} \cdot b$$

From this expression the concrete stress can be calculated according to:

$$\sigma_c = \frac{N}{b \cdot h}$$

(this stress can then be compared with the concrete tensile strength)

Applying equations to stress functions

1 -
Sand:

$$s_{c.1}(l_{es}) := l_{es} \cdot \alpha_{b.1} \cdot \varepsilon_{c.max}$$

$$d_1(l_{es}) := s_{cs}(l_{es}) + s_{c.1}(l_{es})$$

$$\tau_{m.1}(l_{es}) := C_1 \cdot \frac{\left(\left| \frac{d_1(l_{es})}{mm} \right| \right)^{n_1}}{1 + b_{s.1} \cdot n_1} \text{ kPa}$$

$$N_1(l_{es}) := \tau_{m.1}(l_{es}) \cdot l_{es} \cdot b$$

$$\sigma_{c.1}(l_{es}) := \frac{N_1(l_{es})}{b \cdot h}$$

2 -
Crushed
aggregate:

$$s_{c.2}(l_{es}) := l_{es} \cdot \alpha_{b.2} \cdot \varepsilon_{c.max}$$

$$d_2(l_{es}) := s_{cs}(l_{es}) + s_{c.2}(l_{es})$$

$$\tau_{m.2}(l_{es}) := C_2 \cdot \frac{\left(\left| \frac{d_2(l_{es})}{mm} \right| \right)^{n_2}}{1 + b_{s.2} \cdot n_2} \text{ kPa}$$

$$N_2(l_{es}) := \tau_{m.2}(l_{es}) \cdot l_{es} \cdot b$$

$$\sigma_{c.2}(l_{es}) := \frac{N_2(l_{es})}{b \cdot h}$$

3 -
Crushed
aggregate
+ plastic:

$$s_{c.3}(l_{es}) := l_{es} \cdot \alpha_{b.3} \cdot \varepsilon_{c.max}$$

$$d_3(l_{es}) := s_{cs}(l_{es}) + s_{c.3}(l_{es})$$

$$\tau_{m.3}(l_{es}) := C_3 \cdot \frac{\left(\left| \frac{d_3(l_{es})}{mm} \right| \right)^{n_3}}{1 + b_{s.3} \cdot n_3} \text{ kPa}$$

$$N_3(l_{es}) := \tau_{m.3}(l_{es}) \cdot l_{es} \cdot b$$

$$\sigma_{c.3}(l_{es}) := \frac{N_3(l_{es})}{b \cdot h}$$

Calculating intersection between maximum concrete stress and f_{ctm} , the variable is maximum slab length

guess := 50m

$$L_{1,max} := 2 \text{root}[(\sigma_{c,1}(\text{guess}) - 0.6f_{ctm}), \text{guess}] = 63.035 \text{ m} \quad \text{red line}$$

$$L_{2,max} := 2 \text{root}[(\sigma_{c,2}(\text{guess}) - 0.6f_{ctm}), \text{guess}] = 55.244 \text{ m} \quad \text{blue line}$$

$$L_{3,max} := 2 \text{root}[(\sigma_{c,3}(\text{guess}) - 0.6f_{ctm}), \text{guess}] = 85.647 \text{ m} \quad \text{green line}$$

Calculating end slip for each studied case, for max length. Comparison with end slip that are needed for maximum friction

$$s_{\text{end},1,max} := d_1(L_{1,max} \cdot 0.5) = -8.859 \text{ mm} \quad u_{\text{max},1} \cdot \text{mm} \leq s_{\text{end},1,max} = 0$$

$$s_{\text{end},2,max} := d_2(L_{2,max} \cdot 0.5) = -7.898 \text{ mm} \quad u_{\text{max},2} \cdot \text{mm} \leq s_{\text{end},2,max} = 0$$

$$s_{\text{end},3,max} := d_3(L_{3,max} \cdot 0.5) = -12.412 \text{ mm} \quad u_{\text{max},3} \cdot \text{mm} \leq s_{\text{end},3,max} = 0$$

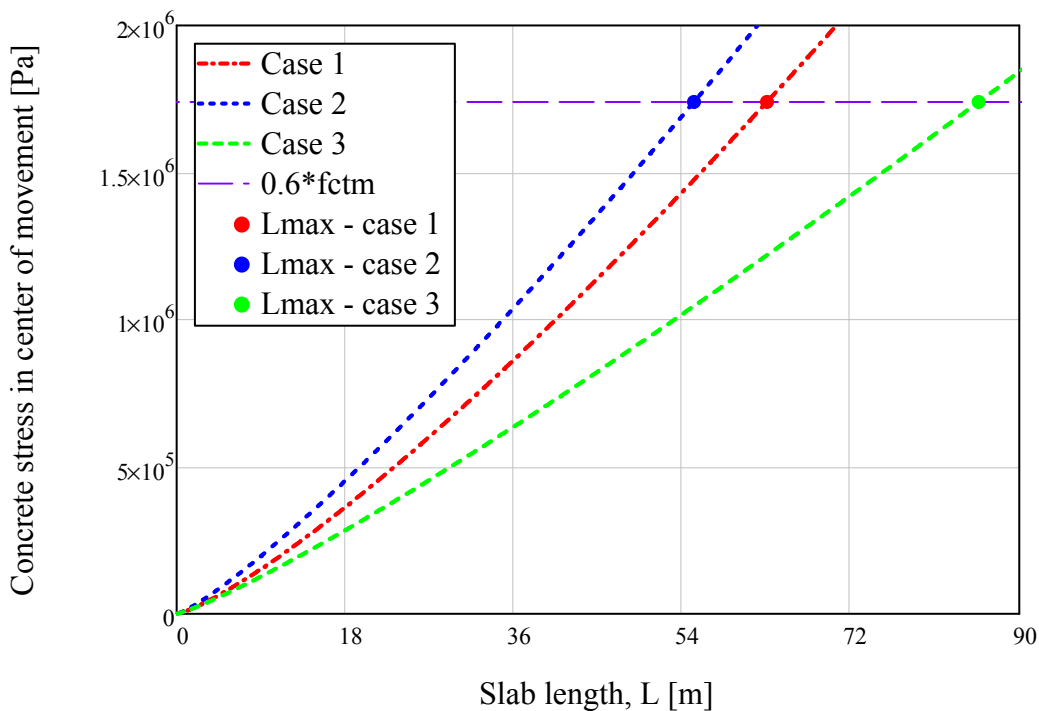
Calculating what end slip free shrinkage would give, to compare with above values

$$s_{cs}(L_{1,max} \cdot 0.5) = -12.686 \text{ mm}$$

$$s_{cs}(L_{2,max} \cdot 0.5) = -11.118 \text{ mm} \quad \text{seems relevant...}$$

$$s_{cs}(L_{3,max} \cdot 0.5) = -17.236 \text{ mm}$$

Plotting total slab length L against maximum concrete stress in non moving point (slab centre). The total slab length will be $l_{es} \cdot 2 = L$



Calculation according to Petersons (1992) to compare with the Analytical model:

$$\gamma_c := 24 \frac{\text{kN}}{\text{m}^3} \quad (\text{Unit weight of concrete})$$

$$q := 3 \cdot \gamma_c \cdot 250\text{mm} = 18 \cdot \frac{\text{kN}}{\text{m}}$$

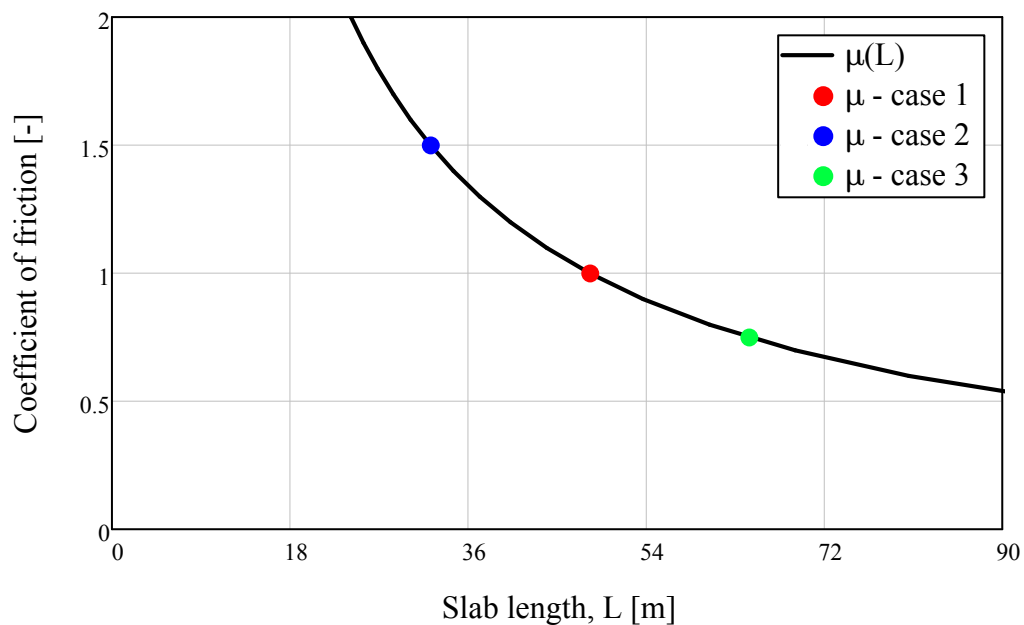
$$cc_{\text{joints}}(\mu) := \frac{2 \cdot h \cdot 0.6 f_{ctm}}{\mu \cdot q}$$

$$\mu_{\text{max.1}} := 1.0$$

$$\mu_{\text{max.2}} := 1.5 \quad (\text{Maximum coefficients of friction from tests according to Petterson (1998)})$$

$$\mu_{\text{max.3}} := 0.75$$

Joint spacing plot according to Petersons (1992), using Pettersons (1998) friction coefficients



Solving intersection, Joint spacing lengths

$$cc_{\text{joints}}(\mu_{\text{max.1}}) = 48.333 \text{ m}$$

$$cc_{\text{joints}}(\mu_{\text{max.2}}) = 32.222 \text{ m}$$

$$cc_{\text{joints}}(\mu_{\text{max.3}}) = 64.444 \text{ m}$$

Conversion of test curves into friction curves

$$SW := \gamma_c \cdot 200\text{mm} = 4.8 \cdot \text{kPa} \quad (\text{Self weight load})$$

$$A_{\text{slab}} := A_{\text{test}} \cdot \text{m}^2 = 0.96 \text{ m}^2 \quad (\text{Area of test slab})$$

$$N_{\text{load}} := 3 \cdot SW \cdot A_{\text{slab}} = 13.824 \cdot \text{kN} \quad (\text{Load on test slab})$$

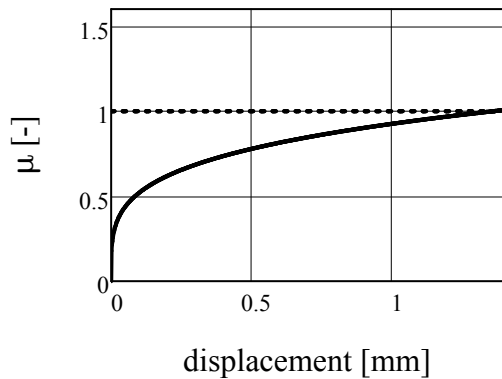
1 -
Sand:

$$F_1(u) := 1000 \cdot 12.8 \cdot (u)^{0.25} \quad \mu_1(u) := \frac{F_1(u)}{N_{\text{load}}}$$

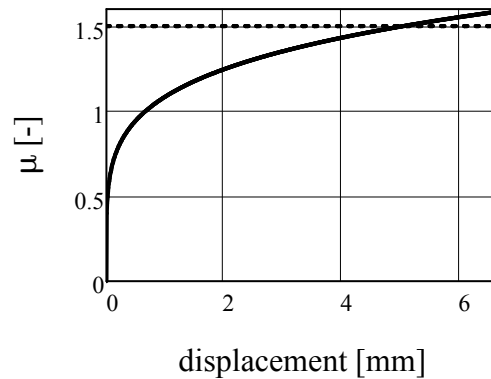
2 -
Crushed
aggregate:

$$F_2(u) := 1000 \cdot 15 \cdot (u)^{0.20} \quad \mu_2(u) := \frac{F_2(u)}{N_{\text{load}}}$$

Case 1



Case 2



3 -
Crushed
aggregate
+ plastic:

$$F_3(u) := 1000 \cdot 9 \cdot (u)^{0.16} \quad \mu_3(u) := \frac{F_3(u)}{N_{\text{load}}}$$

Case 3

